

The HIV-1 entry inhibition capabilities of Isoflavones



UNIVERSITEIT VAN PRETORIA
UNIVERSITY OF PRETORIA
YUNIBESITHI YA PRETORIA



Dissertation

Steven Raubenheimer

17029326

Supervisor: Dr Ntombenhle Gama

Submitted in fulfilment of the requirements for the degree, MSc Biochemistry, in the faculty
of Natural and Agricultural Sciences

University of Pretoria

2023/05/22

DECLARATION OF ORIGINALITY

I, the undersigned, declare that the dissertation, which I hereby submit for the degree, MSc Biochemistry, at the University of Pretoria, is my own work and has not previously been submitted by me for a degree at this or any other tertiary institution.

Full names of student: Steven Gregory Raubenheimer

Student number: 17029326

Date submitted: 22/05/2023

The topic of work: The HIV-1 entry inhibition capabilities of Isoflavones

Signature: 

Supervisor: Dr Ntombenhle Gama

Acknowledgements

I would like to bestow gratitude to the following individuals and organisations for their respective contributions and support during the completion of this study:

- My supervisor, Dr Ntombenhle Gama, for allowing me to work in such an interesting field of research and exercise creative control over the study. Also, thank you Dr Gama for creating an accepting research laboratory.
- The CSIR for the HIV plasmids needed for the research.
- Sandra van Wyngaardt and Sonya September for the guidance given in terms of GLP and maintaining the equipment.
- The Chemistry department, specifically, Phaladi Kunyane and Dr Selepe for the Isoflavones provided.
- My father, Johann Raubenheimer, for his support during my entire education.
- My friends Jaime de Carvalho and Precious-Pearl Hlalele for kindling my creative nature.
- The generator behind the NAS building for its year-long work.
- The University of Pretoria for the opportunity to perform the research.
- God, just God.

Table of Contents

Acknowledgements	3
Table of Contents	4
Figures	7
Tables	8
List of common abbreviations	9
1 Abstract	11
2 Introduction	12
2.1 The Human Immunodeficiency Virus	12
2.2 Mode of replication	14
2.3 Current therapeutics	15
2.4 Novel potential drug targets	16
2.4.1 The HIV Capsid	16
2.4.2 Viral RNA	18
2.5 HIV-1 entry inhibition	19
2.5.1 Non-specific viral attachment	19
2.5.2 The CD4 receptor	20
2.5.3 The Gp120 receptor	20
2.5.4 Gp41	23
2.5.5 Chemokine co-receptors	24
2.6 Isoflavones	26
2.6.1 Isoflavones in medical research.....	27
2.6.2 Documented Anti-HIV-1 activity of Flavonoids.	29
2.7 Microbicides	32
2.8 Computational drug discovery	33
2.8.1 Molecular Docking	34

2.8.2	Fragment-based drug design	34
2.8.3	Drug-likeness	35
2.9	Hypothesis	37
2.10	Aim.....	37
2.11	Objectives.....	37
3	Materials and methods	38
3.1	Dissolving the synthesised compounds	38
3.2	The production of HIV-1 pseudotyped viruses.....	39
3.3	Titering virus to determine the TCID₅₀.....	42
3.4	The effect of the Isoflavones on cellular viability	43
3.5	HIV-1 Inhibition: Luciferase assay.....	43
3.6	Time-of-addition studies	44
3.7	Molecular docking	44
3.8	Fragment-based drug redesign to increase binding affinity	45
3.9	Drug-likeness	46
3.10	Determination of the IC₅₀ and CC₅₀ values.....	47
3.11	Statistical analysis.....	47
4	Results	48
4.1.1	Titering virus to determine the TCID ₅₀	49
4.1.2	The effect of the Isoflavones on cell viability.....	50
4.1.3	Luciferase reporter assay inhibition.....	52
4.1.4	Time-of-addition assay	54
4.1.5	Docking scores and ligand interactions	55
4.1.6	Fragment-based drug design.....	60
4.1.7	Drug-likeness	63
5	Discussion.....	65
5.1	The effect of the Isoflavones on cellular viability	65

5.2	Viral inhibition	66
5.3	Gp120 antagonism.....	68
5.4	Isoflavone-mediated luciferase inhibition	70
5.5	Fragment-based drug design	71
5.6	Drug-likeness	72
6	Conclusion	74
7	Future research	75
8	Appendix	76
	Appendix 1: Tabulation of Myricetin docking method validation	76
	Appendix 2: Reed-Muench calculation for TCID₅₀.....	76
	Appendix 3: Solvent toxicity	77
	Appendix 4: Ligand interactions of the isoflavones without significant activity	78
	Appendix 5: Docking with other anti-HIV target proteins	80
	Appendix 6: Paired student t-test	81
9	References.....	82

Figures

Figure 1: The basic structure of HIV	12
Figure 2: The estimated spread of HIV infections globally.....	14
Figure 3: Common model of HIV replication cycle	15
Figure 4: Anti-capsid compounds	18
Figure 5: The peptidic compound, CGP 64222	19
Figure 6: Structure of gp120	21
Figure 7: Structure of Fostemsavir.....	22
Figure 8: Fostemsavir binding into the CD4 binding region of Gp120	23
Figure 9: Pre-hairpin and hairpin structure of pg41.....	24
Figure 10: Structure of Enfuvirtide.....	24
Figure 11: Structure of CXCR4	25
Figure 12: Structure of Maraviroc	26
Figure 13: Polyphenols and their different structural classifications.....	27
Figure 14: Structures of two common Isoflavones and one common form of oestrogen.	27
Figure 15: Structure of Quercetin	30
Figure 16: The structure of Glycyrrhizin.....	31
Figure 17: Structure of Myricetin	32
Figure 18: Fragment-based drug design.....	46
Figure 19: Overview of the SwissADME BOILED-Egg model.....	47
Figure 20: UV visualised agarose gel with loaded extracted viral DNA.	48
Figure 21: The effect of the Isoflavones on cell viability (24 h)	50
Figure 22: The effect of the Isoflavones on cell viability (48 h)..	51
Figure 23: Luciferase reporter assay.....	53
Figure 24: TOA results.	55
Figure 25: Visualisation of the entry inhibiting Isoflavones in the gp120 binding pocket.....	58
Figure 26: Biochemical interactions in the gp120 binding pocket	59
Figure 27: Docking of B and C in the CD4 entryway of gp120	60
Figure 28: Redesigned isoflavone derivatives	61
Figure 29: Docked derivatives in gp120 binding pocket	63

All figures were used with permission, or they were free from copyright.

Tables

Table 1: Structures of the synthesised Isoflavones	38
Table 2: Details of the pseudovirus plasmids.	40
Table 3: Extracted plasmid quantification and purity analysis using spectrophotometry	49
Table 4: TCID ₅₀ assay for virus titer	49
Table 5: Generated CC ₅₀ values	51
Table 6: Generated IC ₅₀ values.	54
Table 7: Docking scores generated using different HIV-1 entry proteins	57
Table 8: Drug-likeness of the isoflavones and derivatives.	64
Table A 1: Docking method validation.	76
Table A 2: Calculation of infection rate.....	76
Table A 3: Docking scores in other anti-HIV target proteins.	80
Table A 4: p-values from the paired student t-test.	81

List of common abbreviations

AIDS	Acquired Immunodeficiency Syndrome
ARVs	Antiretrovirals
Backbone	Backbone Δ Env
BBB	Blood-Brain Barrier
BOILED-Egg	Brain Or IntestinaL Estimate
cDNA	Complimentary DNA
CD4	Cluster of Differentiation 4
DMSO	Dimethyl Sulfoxide
Env	Envelop plasmid
FBDD	Fragment-based drug design
FDA	The United States Food and Drug Administration
GIT	Gastrointestinal Tract
GM	Growth Media
GPCRs	G-Protein Coupled Receptors
HIV	Human Immunodeficiency Virus
IG	Integrase
MVC	Maraviroc
NRTI	Nucleoside Reverse Transcriptase Inhibitor
NNRTI	Non-Nucleoside Reverse Transcriptase Inhibitor
PBS	Phosphate-Buffered Saline
PBMCs	Peripheral Blood Mononuclear Cells
PDB	Protein Data Bank
RO5	Rule of 5
RLU	Relative Luminescence
RT	Reverse Transcriptase
SBDD	Structure-based drug design
SD	Standard Deviation
SEM	Standard Error of the Mean
TAT	Trans-Activator of Transcription
TAR	Transactivation Response

TCID ₅₀	Tissue Culture Infectious Dose 50
VSW	Virtual Screening Workflow
WHO	World Health Organisation
QSAR	Quantitative Structure Activity-Relationship

1 Abstract

The availability of treatment for HIV infection has resulted in a drastic increase in the life expectancy of infected individuals. However, the current therapeutics fall short in many areas. A considerable 60% of treated individuals will show minor cognitive disorders due to infection, immune reconstruction inflammatory syndrome occurs in a high number of individuals of African descent as a treatment side-effect, and treatment resistance occurs commonly both with long-term infected individuals and newly infected individuals. This all highlights the need for continued research into combating the HIV pandemic.

This research investigated the anti-HIV activity of five novel Isoflavones. Isoflavones and similar compounds have been extensively researched for their ability to hinder HIV reproduction through multiple routes of antagonism in the HIV life cycle but with little research in HIV entry inhibition.

In this study, the anti-HIV activity of the isoflavones was quantified through the generation of IC_{50} values using a luciferase reporter assay. Evidence for potential entry-inhibiting activity was generated through time-of-addition studies and the potential drug targets were hypothesised using computational docking studies.

All the Isoflavones were shown to inhibit HIV replication in the lower micromolar regions with IC_{50} values ranging from 6.2 to 10.6 μ M. Two of the isoflavones, **B** and **C**, were shown to possess significant entry inhibitory activity of HIV-1 through time-of-addition studies (0.041 and 0.007, respectively). Docking studies illustrate the potential for these compounds to act through gp120 antagonism and provide the framework for future drug development using these compounds as gp120 anchoring regions.

2 Introduction

2.1 The Human Immunodeficiency Virus

The Human Immunodeficiency Virus (HIV), of the Lentivirus genus, is the virus behind the HIV pandemic which has plagued the planet for the past four decades [42, 12, 13]. It selectively targets blood cells in possession of the Cluster of Differentiation 4 (CD4) receptor, which includes macrophages, helper T-cells, and dendritic cells, resulting in declining immune system function [43]. Eventually, the virus slowly dilapidates the immune system beyond a point at which the natural protection from opportunistic infections is not effective and the likelihood of developing certain cancers increases [71]. This phase of infection is known as Acquired Immunodeficiency Syndrome (AIDS) [43]. Without proper treatment, the life expectancy of an infected individual is 2 to 15 years [44], with the most common cause of death being non-Hodgkin's lymphoma in developed countries [72] and Tuberculosis related meningitis in South Africa [109].

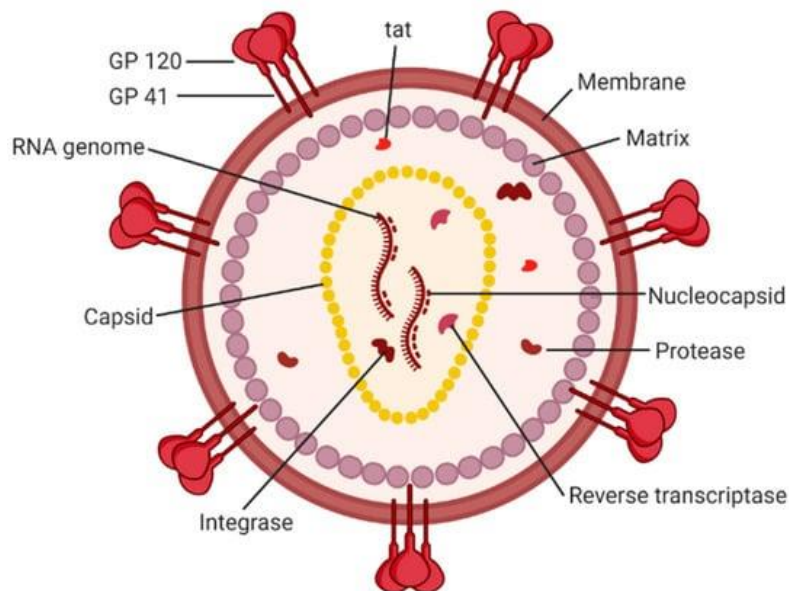


Figure 1: The basic structure of HIV. The simplified illustration of HIV consists of two sense RNA strands, viral proteins, and the envelope lipid membrane [177].

HIV is an enveloped virus in possession of a 9.2 to 9.8 kb genome in the form of two identical sense RNA strands as seen in **Figure 1** [6]. The virus can be broken up into two types: type 1 and type 2 (HIV-1, HIV-2) [6]. These two types arise from differences in their genomes, with HIV-1 coding for the regulatory protein Vpu (Virus protein unique) while HIV-2 codes for Vpx (Virus protein x) [6]. HIV-1 has proven to be the most pathogenic and most common of

the two types [44, 7]. Both types can be further classified, with HIV-1 consisting of groups M, N, O and P and HIV-2 consisting of groups A to H [44], with HIV-1 group M acting as the main driving force behind the global HIV pandemic [7].

HIV is thought to have come into creation through the species barrier crossing of the Simian Immunodeficiency Virus (SIV) [14, 42]. HIV was first identified in 1983, specifically HIV-1, by a research team in Paris that worked under the guidance of Luc Montagnier. In 2008 Luc Montagnier and Françoise Barré-Sinoussi received a Nobel Prize for their world-benefiting scientific discovery [10]. The term AIDS was coined before the discovery of the causative viral agent—HIV—after reasonable suspicion that a new disease was on the incline after two reports [12, 13] published in 1981 noted the sudden increase in patients suffering from rare (at the time) diseases often associated with immunosuppression, such as Pneumocystis Pneumonia and Kaposi Sarcoma [11].

HIV is very much deserving of the title Pandemic, as this virus can be found in all four corners of the world. However, the burden on society differs greatly between developed and developing countries [7], with South Africa carrying the greatest load of infections, as seen in **Figure 2**, with about 5,2 million individuals currently receiving antiretrovirals (ARVs) in 2020. This is a worryingly large number when it is contrasted with the total number of 26 million individuals receiving ARV therapy globally or the 28 thousand receiving treatment in the first world country, Australia [8].



Figure 2: The estimated spread of HIV infections globally. Approximately 36.7 million were infected with HIV worldwide, with the greatest prevalence in Southern and Eastern Africa. [https://www.unaids.org/sites/default/files/media_asset/UNAIDS_2017_core-epidemiology-slides_en.pdf.]

2.2 Mode of replication

HIV enters the human body through unprotected sexual intercourse or the transfer of infected bodily fluids occurring commonly through the transfusion of infected blood, the sharing of needles, natural birth, or the surgical transplantation of infected organs [6]. Once the virus is in the bloodstream of the host, it marks the beginning of the HIV replication cycle, visualised in **Figure 3**. The virus targets the CD4 receptor of certain immune cells, using what is commonly referred to as the spike complex or envelope (env) complex. The env complex, consists of a heterodimeric unit of a surface homotrimer, gp120, and a transmembrane homotrimer, gp41 [46]. The virus binds to the CD4 receptor through the gp120 region of the env complex, after which, membrane fusion occurs, using the gp41 region of the env complex. As a result of the membrane fusion event viral enzymes and genetic material enter the cytoplasm of the host cell under the protection of the viral capsid [18]. The capsid then uncoats in a somewhat organised fashion [18] as the two viral sense RNA strands are converted into complementary DNA (cDNA) by the viral Reverse Transcriptase (RT). In addition to the RNA and DNA template-dependent polymerase activity, the enzyme also possesses RNase H activity which degrades the viral RNA strands post-transcription [73]. The produced cDNA is then integrated into the host's genome using viral Integrase (IN) [74]; this may mark the

establishment of a viral reservoir that enables the continual seeding of the virus [70]. After integration occurs, the host cell's transcription and translation cycles result in the synthesis of new viral genetic material and viral proteins needed for the creation of the viral prodigy. The viral proteins and sense RNA strands then gather at the membrane of the host cell where viral receptor proteins are inserted and the budding of new virions into the extracellular space occurs [14]. These inactive viruses are activated through a process called 'maturation' which involves the cleaving of large viral proteins into smaller functional units using the viral Protease (PR) [70, 110]. These processes are essential points of research as they all serve as possible targets for therapeutic intervention.

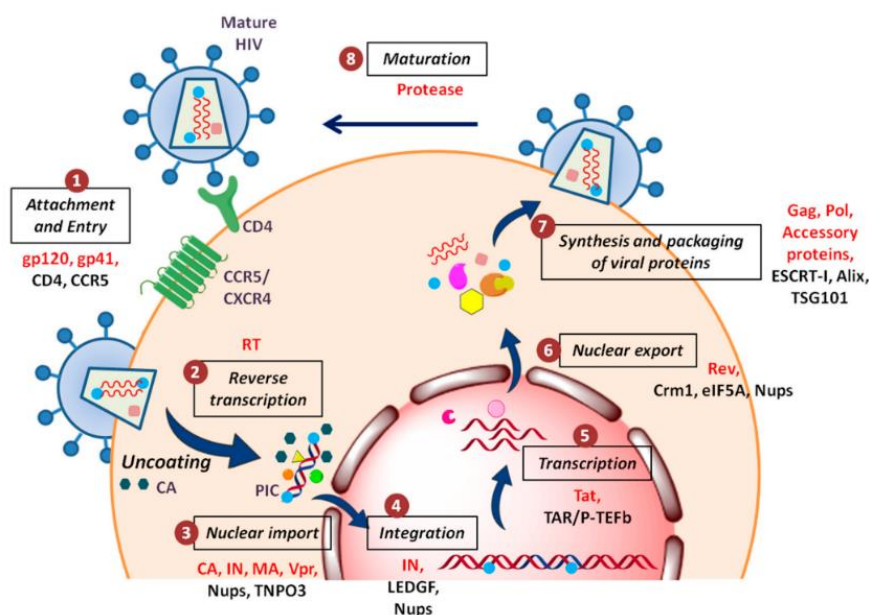


Figure 3: Common model of HIV replication cycle. The model illustrates the main steps in HIV replication, from the entry of the virus using the Env complex to the replication and insertion of the cDNA to the packaging of the newly synthesised viral proteins and sense RNA which ultimately leave the cell as new virions [14].

2.3 Current therapeutics

Through the study of the biological processes of HIV replication, researchers have been able to determine key points that can be targeted using chemotherapy. Compounds with activity against HIV are termed Antiretrovirals (ARVs), and currently, there are more than 30 United States Food and Drug Administration (FDA) approved ARVs. These can be categorised into six categories, namely: Non-nucleoside Reverse Transcriptase Inhibitors (NNRTIs), Nucleoside Reverse Transcriptase Inhibitors (NRTIs), Entry Inhibitors, Fusion Inhibitors, Integrase inhibitors (INI), and Protease Inhibitors (PI) [14]. Both NNRTIs and NRTIs prevent the formation of cDNA by inhibiting RT through binding to the orthosteric or allosteric binding site [44]. Entry inhibitors currently work by binding to the envelope complex and preventing

the conformational changes needed for successful entry initiation [65]. Fusion inhibitors act after the Env glycoprotein complex and the CD4 receptor have interacted and have undergone the conformational changes that signal entry initiation. These inhibitors prevent the fusion of the two membranes which ultimately denies the entry of the viral machinery needed for replication into the host cell [44]. Protease inhibitors act by hindering the catalytic activity of the viral protease which cleaves larger viral proteins into smaller active proteins, thus preventing the successful assembly of new active virions [44].

Despite the impressive arsenal of ARVs currently available, further research into discovering new ARVs is essential as the emergence of drug-resistant viral strains has become a major cause for concern [6]. There is not a single ARV available that HIV is not able to build resistance against [16] but some are less likely than others to induce resistance [15]. Resistance can occur in many ways, namely: transmitted drug resistance, and according to the World Health Organisation (WHO) 26% of newly-infected individuals starting first-line treatment are already in possession of a resistant strain of HIV [15]. The second way is through acquired drug resistance, which occurs when adherence to the treatment regime falls below 100% compliance; with one study reporting that even individuals who were 80 to 95 % compliant were twice as likely to develop treatment resistance than individuals who were ≥ 95 % compliant [16,17]. This has become a great motivation for the discovery of new drug targets within the viral life cycle.

In the USA, a country privileged enough to offer not only extensive preventative measures but also therapeutic ones, there is a large HIV burden of around 50,000 infected individuals per year who experience resistance to first-line therapy [113]. The individuals then fall into dependence on the second-line regime, which introduces the entry inhibitor, Maraviroc. [113] A drug, which by nature, is more susceptible to resistance as discussed in section 2.5.5.

2.4 Novel potential drug targets

As researchers continue to explore drug development for HIV, they are also delving deeper into the underlying physiology of the virus. Recent years have brought new discoveries in the form of novel drug targets, which offer the potential for the development of innovative therapeutics with unique mechanisms of action. Such novel drug targets are discussed below.

2.4.1 The HIV Capsid

The viral capsid consists of repeating hexameric and pentameric units of capsid proteins that form a conical-shaped structure that houses the replication machinery of the virus [18]. The

HIV capsid has commonly been depicted as the ‘delivery package’ carrying the viral replication machinery [47] which until recently, has been found to be an incorrect description. Numerous depictions of the viral replication cycle, such as **Figure 3** above, depict the idea that once the fully intact viral capsid containing the viral replication machinery enters the host cell, it disassembles fully, and reverse transcription and integration then occur without further input from the capsid. It is now known that specific intracellular interactions of the capsid are necessary for the virus to progress through the replication and infection cycle [18, 47]. It is known that the HI viral capsid interacts with multiple host cellular proteins including nucleoporins (Nup) 153 and 358, Cyclophilin A and Cleavage and Polyadenylation Splicing Factor 6 (CPSF6) [47]. Both the Nup 153 and CPSF6 proteins have been found to target the same site between two hexameric capsid units [47]. The proteins only bind strongly when the units are associated indicating that HIV only benefits when the capsid is either partially or fully assembled [47]. Through studies involving mutations at the Nup 153/CPSF6 binding site, the binding of these proteins is thought to assist in nuclear migration. Both Pfizer and Boehringer-Ingelheim have discovered anti-capsid compounds: PF74 and BI-2 [48, 49], as seen in **Figure 4** below. Both these compounds competitively bind to the Nup 153/CPSF6 binding site and thus likely inhibit the migration of the capsid/cDNA complex into the nucleus of the host cell preventing integration [47,48].

The importance of the stability profile of the capsid in terms of HIV replication is supported by research that compared the effects of varying capsid stabilities (low-level to high-level) on reverse transcription and integration products [18]. It was found that if the capsid is severely destabilised, reverse transcription is mostly hindered. Extreme stabilisation (does not dissociate into its monomeric units as easily) on the other hand also hinders integration [18].

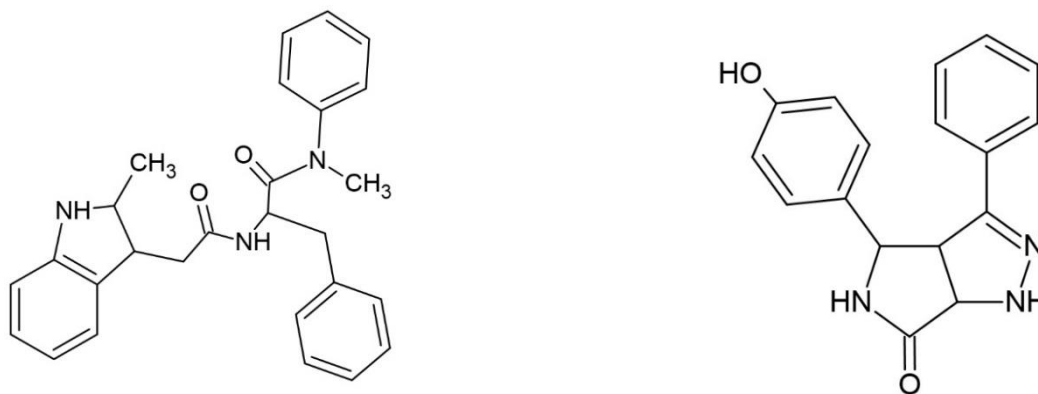


Figure 4: Anti-capsid compounds. These are two anti-HIV compounds currently in clinical trials which both target the Nup 153/CPSF6 binding site on the HIV capsid. The one on the left, PF-74, was developed by Pfizer and the one on the right, BI-2, was developed by Boehringer-Ingelheim. From: **Lamorte** [49].

2.4.2 Viral RNA

Unlike DNA, which simply serves to store genetic information, RNA has a range of functions: from the transfer and storage of genetic material to directing enzymes, and even enzymatic activity [50]. These different physiological roles are mainly due to differing structural confirmations; RNA can adopt a wide range of structural conformations such as hairpin loops, double-stranded regions that create stems and turns, and even pseudoknots [50]. HI-viral RNA is no exception and does indeed achieve a unique structural confirmation, not only because of the structural range of RNA naturally but also because the two strands of RNA transported to the new budding virions in the infection cycle unite and form a single three-dimensional structure [19]. This is an interesting and promising find given that the cornerstone of medical research is to take advantage of the structural differences between pathogens and the host.

Currently, there is a proteinaceous compound that inhibits the interaction between the Tat protein and a highly conserved region on HI-viral RNA: the TAR (Transactivation Response) element (**Figure 5**). The TAR is a loop-stem element consisting of 59 residues on the 5' end of the HI-viral RNA. The Tat/TAR interaction is necessary to ensure efficient viral reverse transcription, without this interaction the process is sluggish and tends to produce incomplete transcripts [50], which is on par with the previously described action of Tat in increasing the polymerase's elongation capacity [51]. The compound, CGP64222, competitively competes with Tat for binding to TAR, suppressing the effectiveness of viral replication [51].

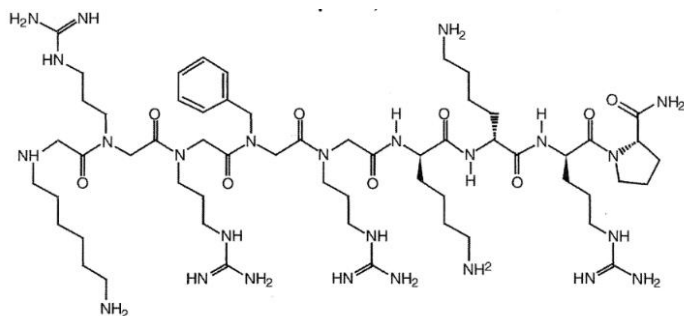


Figure 5: The peptidic compound, CGP 64222. CGP 64222 is capable of halting HIV activity at the nanomolar range by inhibiting the transactivation process [51].

Following the numerous ways in which HIV inhibition can be achieved, this study focused on the discovery of novel HIV entry inhibitors.

2.5 HIV-1 entry inhibition

The entry of the replication machinery needed for HIV to produce viral progeny is a multistep process [63]. The viral Env complex, which targets the CD4 immune cells, consists of three identical gp120 surface units attached non-covalently to three identical gp41 transmembrane units [46]. This complex first attaches to the immune cell via non-specific viral-cellular interactions [65], which then allows for the gp120 Env unit to attach to the cellular CD4 receptor. After the interaction of gp120 and CD4, a series of conformational changes and co-receptor binding (CCR5 or CXCR4) allow for viral entry [63, 65].

2.5.1 Non-specific viral attachment

As stated above, the first step in HIV entry occurs when the virus binds to the immune cell via non-specific interactions [63, 65]. These interactions include the associations of the positively charged regions of gp120 Env unit with negatively charged cell surface regions, which include: Heparin sulphate proteoglycans, $\alpha 4\beta 7$ integrins, Dendritic cell-specific intercellular adhesion molecular 3-grabbing non-integrin (DC-SIGN) and Mannose-binding C-type Lectin Receptors (MCLR) [63, 65]. Compounds that inhibit this step in HIV entry are referred to as attachment inhibitors [65] and they interfere with these non-specific interactions. There is no FDA-approved attachment inhibitor currently, but research has shown soluble anions and sulphated polysaccharides such as Heparin, Dextran Sulphate, and Cyclodextrin Sulphate can block these non-specific interactions [65, 77].

Dextran Sulphate, which is a sulphated polysaccharide, has been shown to inhibit HIV replication [77], however, further research into its entry inhibition capabilities found that at concentrations where dextran sulphate functions as a replication inhibitor, there is insignificant gp120-CD4 receptor binding inhibition, proven through ELISA studies [77]. On performing a second ELISA using gp120 units and monoclonal antibodies, it was found that the binding of certain antibodies was blocked. This provides evidence that Dextran Sulphate has entry inhibition properties [77]. Furthermore, these studies revealed attachment of monoclonal antibodies was blocked by targeting a positively charged region around residues 303 to 338 of the V3 gp120 loop, an essential region for virus-cell attachment [77]. The key proteins involved in the viral entry are further discussed below.

2.5.2 The CD4 receptor

As stated above, CD4⁺ cells are immune cells in possession of the CD4 glycoprotein receptor. The receptor, which is a type 1 membrane protein [54] assists in the recognition of Major Histocompatibility complex II (MHC), leading to the activation of the immune cells [52]. The CD4 receptor consists of four extracellular domains, D1-D4, connected by a short segment that leads to the transmembrane domain. The cytoplasmic region interacts with p65Lck, which is a Src tyrosine kinase [54]. The domains strongly resemble, in both sequence and structure, immunoglobulins [54, 55] and consist of 370 amino acid residues [56]. The receptor is an elongated structure with D1 being the outermost domain [53]. There are two N-linked glycosylated sites, one in D3 and the other in D4 [56].

Using crystallography and site-directed mutagenesis, it has been found that the binding of gp120 to CD4 occurs through the CDR-2-like loop in domain 1 [55]. The binding of CD4 to gp120 results in conformational changes that result in the dissociation of gp120 from gp41, which exposes regions of gp41 that can function as targets for antibody targeting [55].

Ibalizumab which was discovered by **Kuritzkes** [65, 78] is an IgG4 monoclonal antibody that targets the CD4 receptor, and it results in the decrease of HIV-1 RNA viral loads and a subsequent increase in CD4⁺ cells [78]. The compound functions by binding to the D2 domain of CD4 and prevents conformational changes of the receptor, leading to inhibited viral entry [65].

2.5.3 The Gp120 receptor

There are five variable regions within gp120, denoted V1-V5, which have been revealed through sequence analysis studies of different viral strains [79]. The first regions, V1-V4, form

disulphide-stabilised loops, resulting in a total of seven highly conserved disulphide bonds between regions [79]. It is widely accepted that the interaction of the CD4 receptor with the gp120 unit causes the V3 loop to project outward, allowing for it to interact with a co-receptor [80]. It has been noted that the co-receptor tropism of the HIV strain (CCR5 or CXCR4 or both) is mostly dictated by the sequence of the V3 loop, as mutational studies have revealed that the tropism of a strain can be changed through site-directed mutagenesis [79].

Gp120 contains two domains: an inner and an outer domain as seen in **Figure 6** below. Between the two of these, there are 25 strands involved in the β -sheet formation, ten loop-forming regions (5 of which are variable) and five α -helices [79]. The ‘bridging sheet’, which is involved in CD4 binding, consists of 4 antiparallel β -strands: strands 2, 3, 20, and 21, with strands 2 and 3 forming between the V1/V2 neck [79]. It has also been hypothesized that α -helix 3 and β -strand 15 are required for CD4 binding [79].

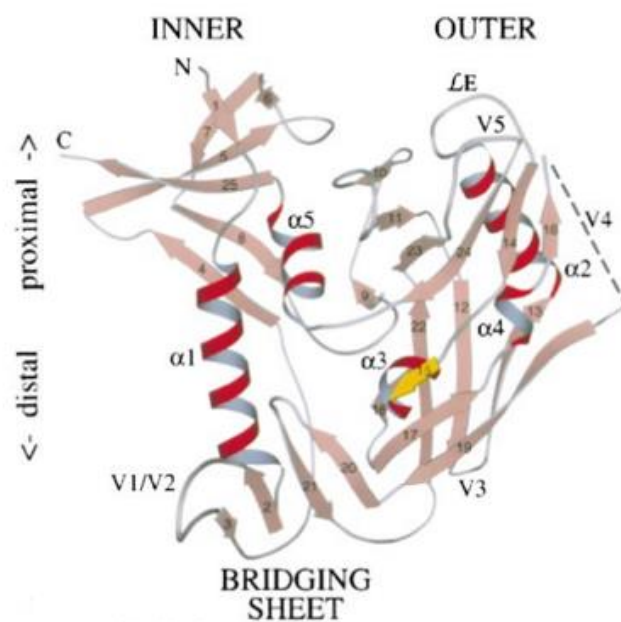


Figure 6: Structure of gp120. The above illustration of gp120 indicates the two domains of the protein: the inner and outer domains. There are five variable regions (V1-V5) each comprising a loop stabilised by disulphide bonds. There are also five α -helices and 25 β -strands. V3 is essential for co-receptor binding and the bridging sheet is involved in CD4 binding [79].

At first glance, the heavily glycosylated gp120 unit would serve as the ideal target for vaccine development, however, the glycosylation sites are extremely variable which results in effective immune responses shortly becoming ineffective—this is the main reason there has been no successful HIV vaccine trial thus far [81].

A gp120 antagonist was approved in 2020, Fostemsavir [113] (**Figure 7**). The drug is available for heavily treatment-experienced individuals unable to take other medically preferred ARVs due to safety concerns or ARV resistance [113, 114]. Fostemsavir can cause a serious adverse reaction, Immune Reconstruction Syndrome, in 3% of individuals [115]. Fostemsavir is a prodrug of Temsavir, under the chemical classification of phosphoxymethyl agents. Fostemsavir can be seen in **Figure 7**; the compound was altered to improve the antiviral and pharmacokinetic activities of the agent [113].

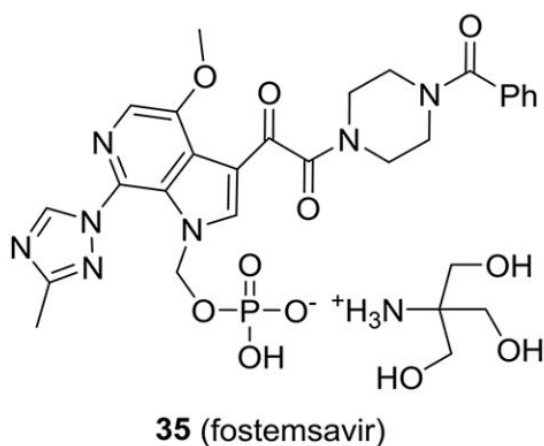


Figure 7: Structure of Fostemsavir. Fostemsavir is the compound initially shown to act as a Gp120 antagonist. The pro-drug Temsavir is the marketed, FDA-approved, structure as it has increased oral bioavailability [113].

As can be seen in **Figure 8**, Fostemsavir blocks CD4 binding by insertion of the benzamide moiety in the area occupied by W427 in the gp120 open state. This forces W427 and β 20-21 into regions the CD4 receptor would nestle into upon binding, thus preventing viral attachment [113].

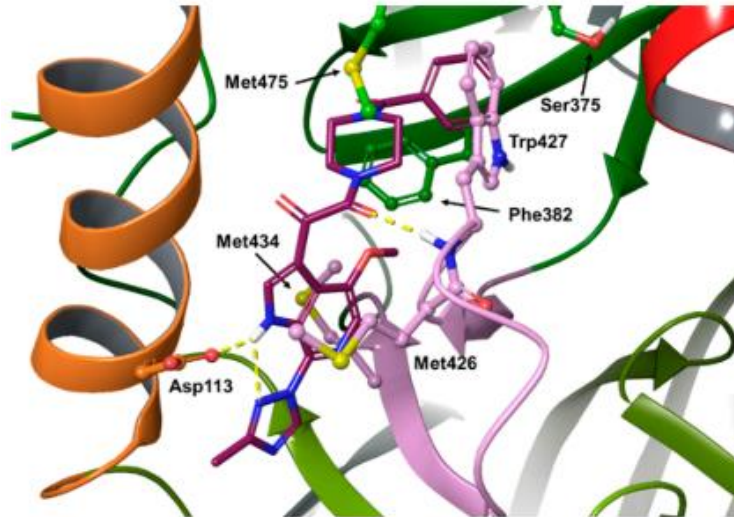


Figure 8: Fostemsavir binding into the CD4 binding region of Gp120. The figure depicts the binding of Fostemsavir under the β 20-21 regions of the CD4 receptor [113].

2.5.4 Gp41

This is the unit of the Env complex that is responsible for the fusion of the viral envelope with the immune cell membrane [83]. The N-terminal of the gp41 unit is referred to as the Fusion Peptide, which is a hydrophobic glycine-rich section that protrudes forward into the host membrane after the CD4/Gp120 interaction forms [84]. Following this insertion event, the gp41 has now adopted the pre-hairpin structure which is conformationally stable and holds for a relatively long period [84]. The pre-hairpin contains two, 4-3 heptad repeat regions containing hydrophobic residues, as seen in **Figure 9** below. Repeat 1 is found on the N-terminal side after residue 36 and repeat 2 is found on the C-terminal side before residue 34 [83, 84]. After the pre-hairpin transitions into the hairpin structure, six helices form comprising the two heptad repeats in a core structure known as the N36/C34 complex as seen in **Figure 9** below [84]. The helices from the N-terminal region of the gp41 unit form the centre helices while those from the C-terminal region form the outer helices, with the different helices interacting mainly through hydrophobic residues [84]. The formation of the N36/C34 complex brings the envelope and cell membrane into proximity, which allows for the fusion of the two [84].

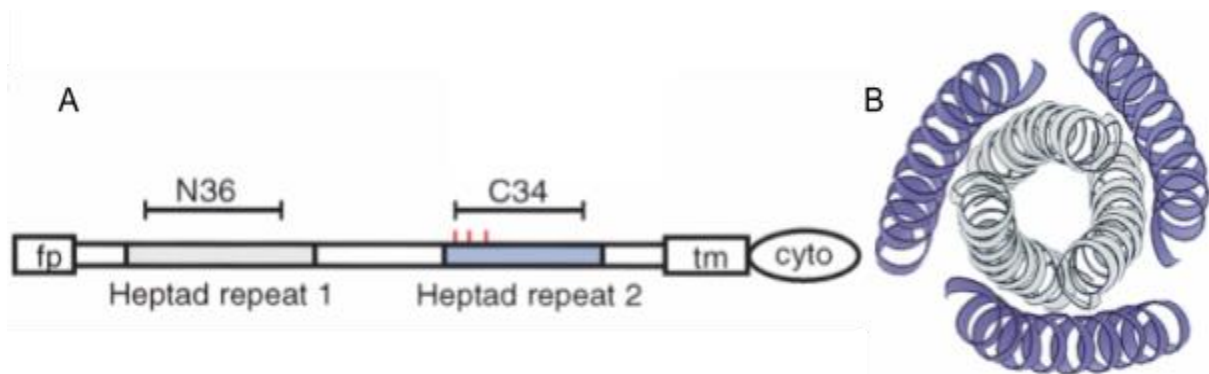


Figure 9: Pre-hairpin and hairpin structure of gp41. Section A (left) represents the pre-hairpin, elongated structure of gp41 right after CD4/gp120 binding. Gp41 contains two heptad repeats, a fusion insertion section (fp), a transmembrane region and a cytosolic region. Section B (right) represents the hairpin structure, more specifically, the N36/C34 core formed from hydrophobic interactions between the heptad regions [94].

There is currently one FDA-approved drug which targets the gp41 structures needed for fusion to occur: Enfuvirtide [85]. Enfuvirtide, **Figure 10**, is a proteinaceous compound made of 36 amino acids that mimic the residues found in Heptad repeat 2. This association of Enfuvirtide with this region inhibits the formation of the hairpin structure, thus preventing fusion [85].

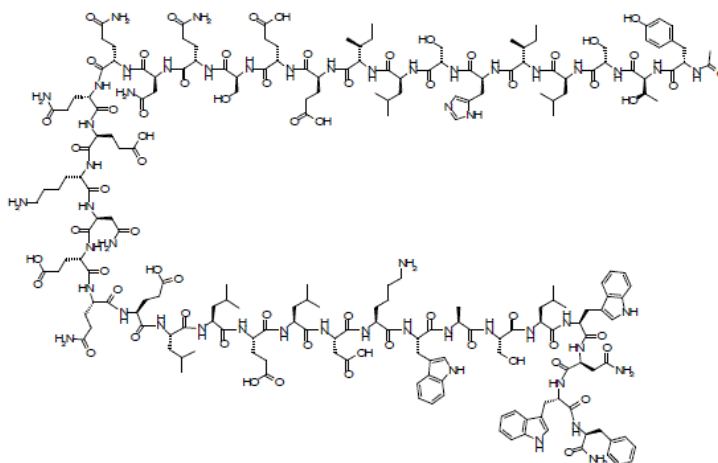


Figure 10: Structure of Enfuvirtide. The polypeptide, Enfuvirtide, is the only gp41 antagonist, acting on the fusion protein by mimicking the amino acid residues on gp41 [85].

2.5.5 Chemokine co-receptors

There are two CD4⁺ cell-related co-receptors that HIV can utilise in the process of cellular infection: CCR5 and CXCR4. Depending on the strain, HIV can utilise only one of them, strain R5 uses the CCR5 co-receptor while strain X4 uses the CXCR4 co-receptor, or both of them (strain R5X4) [86, 87]. Both of these co-receptors are structurally related G-Protein Coupled Receptors (GPCRs), however, there are some minor differences, one being that CXCR4 has 21 phosphorylation sites and CCR5 has seven [88]. Both the co-receptors contain seven transmembrane α -helices connected by three extracellular and three intracellular loops [86], as

shown in **Figure 11** below. Structural studies looking into these two chemokine receptors have proven difficult as GPCRs are notoriously difficult to crystallise owing to their large hydrophobic transmembrane region [88].

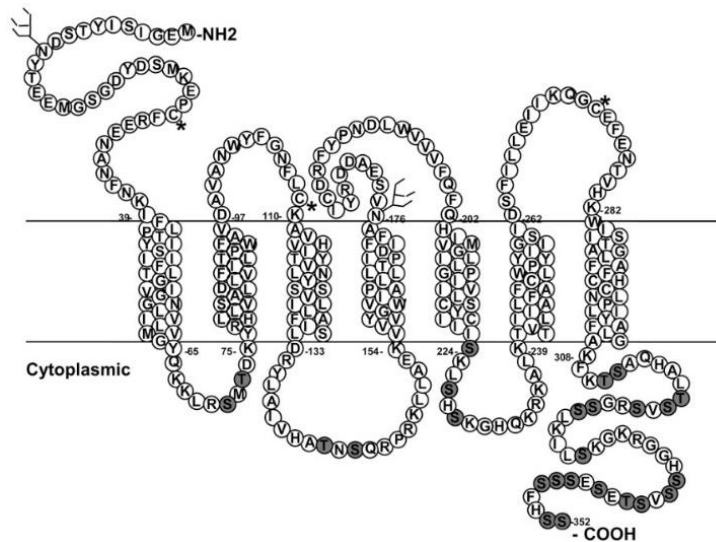


Figure 11: Structure of CXCR4. Both CXCR4 and CCR5 are GPCR-like proteins. They both contain seven transmembrane regions with three extracellular and intracellular loops [88].

There is only one FDA-approved drug thus far that acts as a co-receptor antagonist: Maraviroc (MVC). This compound is only functional against R5 strains [86, 87]. It is believed that compounds that would display activity against the CXCR4 co-receptor could potentially be extremely toxic, as previous research has noted that mice without the CXCR4 co-receptor die *in utero* due to cardiovascular problems. However, mice and even people, with defective CCR5 co-receptors develop fully [88].

MVC prevents the activation of the gp41 unit by inhibiting the binding of the V3 loop of gp120 to the CCR5 co-receptor [65, 87]. MVC binds to a hydrophobic cavity created from the transmembrane α -helices 2, 3, 6 and 7 [65, 87]. Studies determining the essential residues responsible for CCR5-mediated activation of the forthcoming fusion event found that the drug binds to two of the essential residues: Y37 and W248, as seen in **Figure 12** below [86]. It has previously been described that the specific distribution of charges and steric hindrance is important for MVCs activity [86].

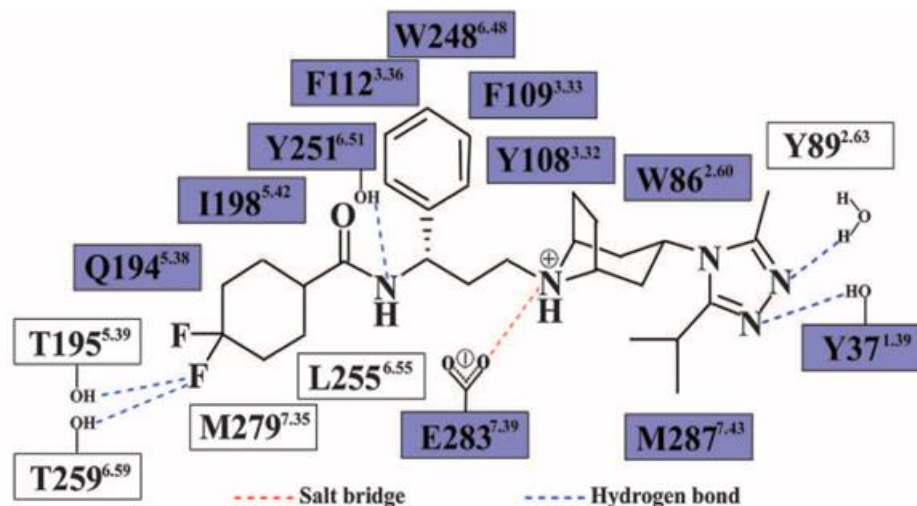


Figure 12: Structure of Maraviroc. Above is an illustration of MVC, the residues it interacts with and the nature of the interactions. Most of the interactions are hydrogen bonds with one being an ionic bond (red dotted line). The hydrogen bonds (dotted blue lines) with Y37 and W248 are deemed essential for inhibition [86].

This study investigated novel isoflavones for the potential inhibition of HIV, specifically through HIV entry inhibition.

2.6 Isoflavones

Isoflavones are phenolic compounds that belong to a group of naturally occurring secondary plant metabolites known as flavonoids [21]. Phytoestrogens which are non-steroidal, oestrogen-like plant compounds can be divided into flavonoids and non-flavonoids with flavonoids including isoflavones, coumestans and prenylflavonoids and non-flavonoids including lignans [21]. There are more than 8000 described phenolic compounds [29] and these are classified according to the degree of oxidation and unsaturation in the C ring, as well as the way the C and B rings are connected (**Figure 13**) [69].

Structural characterisation of the flavonoids notes the two aromatic carbon rings (ring A and B) linked together by a three-carbon bridge (ring C) [170]. The A ring is derived from the malonic acid pathway while the B ring is derived from the shikimic acid biosynthesis pathway [170].

Isoflavones, and their category, offer considerable diversity. They are further categorised as coumaronochromones, rotenoids, pterocarpanes, 3-aryl coumarins and coumestans [170].

High concentrations of these compounds naturally occur in soybeans, tofu and legumes [22]. Their biological activity in plants ranges from predator protection, antimicrobial activity, reproduction, and germination [29].

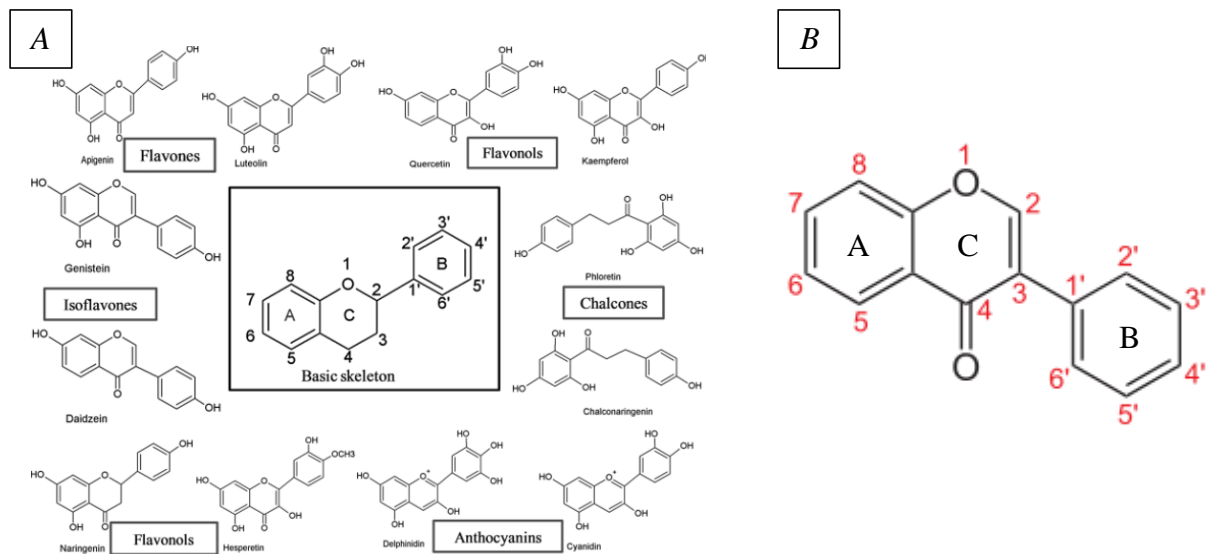


Figure 13: Polyphenols and their different structural classifications. In the centre of A (left) is the basic structure ring structure of a flavonoid. Isoflavones, section B, consist of a B ring bonded to the C-ring via residues 3 and 1' [69].

Some common Isoflavones, in both research and dietary availability, include Daidzein and Genistein [22] (**Figure 14**) which can be compared to oestradiol, the most common form of oestrogen in women of childbearing age [24].

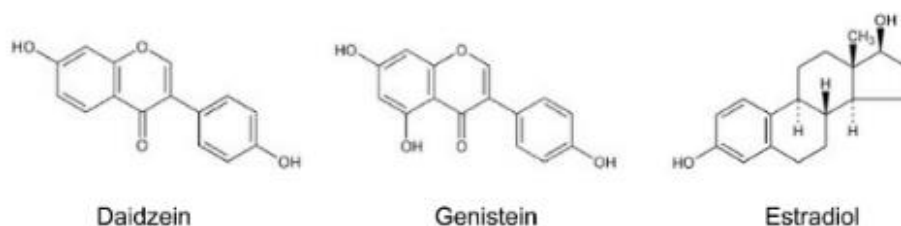


Figure 14: Structures of two common Isoflavones and one common form of oestrogen. Daidzein and Genistein are regularly found in research and plant extract. They differ by an A ring hydroxyl group. Oestradiol is the most common form of oestrogen in women of childbearing age, and it strongly resembles the common isoflavone structure [22].

2.6.1 Isoflavones in medical research

There currently are extensive research programs looking at the various potential health benefits of Isoflavones and these include investigating their effects on cardiovascular diseases,

osteoporosis, thyroid dysfunctions, endocrine diseases, and cancer, as well as their anti-oxidant activity [21].

Endocrinology

Isoflavones have been extensively studied in terms of their biological impact on human health with the most obvious arising from properties derived from their structure—their oestrogenic properties. In the human body, there are two types of oestrogen receptors: Oestrogen Receptor Alpha ($ER\alpha$) and Oestrogen Receptor Beta ($ER\beta$), both of which serve as targets for Isoflavones [21]. Different locations in the human body favour one type of receptor over another and it has been found that phytoestrogens seem to have higher binding affinities for $ER\beta$ than $ER\alpha$ [25]. When a phytoestrogen binds to an ER it can either act agonistically, antagonistically or simply competitively inhibit the binding of more dangerous forms of oestrogen [22]. Due to oestrogen being a steroidal hormone, it can easily diffuse in and out of cells [25, 26, 27], which plays important functions in the development and maintenance of sexual characteristics in both males and females [25,27]. Their site of receptor binding occurs intranuclearly and results in the modulation of transcription of certain genes [25, 26]. Even though oestrogen is primarily thought of as a sex hormone, it plays several biological roles such as:

- The stimulation of high-density lipoprotein and triglycerides in adipose tissue.
- The reduction of bone resorption and increase in bone mineralisation and formation in adults.
- The increase in collagen formation, blood flow and thickness in the skin.
- The regulation of proteins such as those involved in the coagulation cascade.
- The increase in insulin expression in beta cells in the pancreas.

All these effects serve as areas of research for the medicinal use of oestrogen [27].

Cancer research

Isoflavones have been involved in several cancer-related research topics with expected promise in these research areas originating from the fact that countries with a high daily intake of Isoflavones (Asia: 25-50mg/day) experienced a lower occurrence of certain cancers than countries where the daily intake is much lower (America: < 2mg/day) [21]. Although this may not be a cause-and-effect relationship, this difference is likely attributed to the extremely different diets between the two regions.

Yanagihara [75] found that Biochanin A and Genistein (**Figure 14**) caused both cell growth inhibition and cell death in cancer cell lines originating from the gastrointestinal tract at concentrations of $\geq 10 \mu\text{g/ml}$ [75]. The mechanism of cytotoxic activity was attributed to the induction of apoptosis as made evident by the presence of fragmented nucleic acid [75]. Other researchers have also confirmed cell death due to apoptosis from the introduction of Isoflavones [75].

Anti-inflammatory research

Isoflavones have been found to inhibit the expression of pro-inflammatory cytokines $\text{TNF-}\alpha$, $\text{IL-1}\beta$, IL-6 , and IL-12 through the modulation of transcription of these inflammatory molecules, especially in macrophages [22]. Certain inflammatory molecules, such as IL-6 and $\text{TNF-}\alpha$, can also be expressed in the presence of high concentrations of certain compounds such as lipopolysaccharides (LPS), and Genistein has been found to prevent this [22].

2.6.2 Documented Anti-HIV-1 activity of Flavonoids.

To expand the range of pertinent research, all documented instances of anti-HIV activity associated with flavonoids have been incorporated, rather than limiting focus solely to research centred on isoflavones, owing to the structural similarities between them. As noted, flavonoids demonstrate a wide-range of anti-HIV activity, with no single flavonoid class demonstrating higher activity than another.

HIV Protease inhibition

When it comes to HIV protease-inhibiting activity there is evidence of potential activity, however, it is somewhat unclear how potent the activity is. One study in 1994 found that out of a whole panel of Flavonoids, Quercetin (**figure 15**) produced the best IC_{50} value of $58.8 \mu\text{M}$ while another study conducted in 2007 found that Quercetin produced an IC_{50} value of $>100 \mu\text{M}$ [116, 117]. Considering that the papers found different values, what is important to note is there is definite activity, the potency is just up for debate. Quercetin has been found to inhibit other types of proteases, such as bacterial protease, specifically the bacteria that causes Shigellosis [121], and other viral proteases such as the protease from SARS-Cov-2 [122].

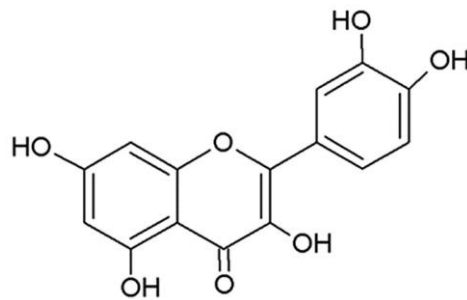


Figure 15: Structure of Quercetin. Quercetin has proven to inhibit three types of pathogenic proteases, two of them viral [116].

HIV Reverse Transcriptase inhibition

Even though it is the most therapeutically targeted HIV enzyme, reverse transcriptase still serves as an ideal target to develop future ARVs: as 14 of the current drugs have the potential to develop severe side effects and have well-known mechanisms of resistance [123]. A study from 2014 found that Myricetin (**Figure 17**) was able to significantly reduce the activity of RT when compared to the negative control [118]. Myricetin produced a maximum inhibition value at 100 μ M resulting in 49% RT inhibition [118].

HIV Integrase inhibition

One of the most crucial steps in the HIV life cycle is indeed the integration step, by which the viral genome is cemented into the human genome: potentially solidifying lifelong HIV infection [70]. This insertion is achieved by the enzyme Integrase. Integrase has three enzymatic functions which achieve viral-genome-host-genome integration: cleavage, insertion and disintegration [131, 74]. Cleavage serves to process the 3' termini of the viral genome through cleavage of the terminal dinucleotide [131, 74]. Insertion, which involves the insertion of the genome into the host genome through the cutting of the host genome and attachment of the 5' end of the cut and the attachment of the altered 3' viral-genome terminus [131, 74]. Disintegration follows the insertion step simply in reversal [131,74].

Fesen [131] studied the effects of multiple flavonoids on the inhibition of the cleavage and insertion catalytic functions of integrase and found potent flavonoids with a range of IC_{50} values from 0.1-97.8 μ M [131]. The authors reported increases in activity for subsequent increases in the hydroxylation of the compounds [131].

HIV Entry inhibition

Interestingly, there is strong evidence to suggest that isoflavones pose as suitable entry inhibitors [63]. *Pueraria lobata*, known commonly as Kudzu, is a plant used to suppress the

desire to consume alcohol (antidipsotropic). It has been used both traditionally in Asian culture and in research—which has shown that the isoflavones Daidzein and Daidzin account for the antidipsotropic effects [64].

A previous study [63] used Kudzu root extract to determine if there were potentially any compounds in the extract which would inhibit HIV entry. They made use of a cell line that contains the LacZ reporter gene which responds to the initial expression of the Tat protein via the 5'LTR region of the HIV genome [63]. The root extract comprised 33% crude root and 67% of ethanol/glycerol solvent; they proved the ethanol and glycerol had no entry-inhibiting capabilities, verifying that the results seen were indeed due to compounds present in the Kudzu root extract. The inhibition seen was proven to be due to denying the very initial step in attachment, the binding of the virus to cell surface heparin sulphate, proteoglycans, $\alpha 4\beta 7$ integrins, DC-SIGN or MCLR [63]. Although the specific compound that carries the anti-HIV activity was not identified, the authors ruled out proteinaceous inhibition as they heated the extract and still observed activity. None of the known Isoflavones found in the extract showed individual inhibition, suggesting possible synergistic effects. Ultimately, there is reason to believe the active compound is an undiscovered isoflavone or some sort of steroidal/polyphenolic compound. This assumption is supported by other studies which have found that similar molecules can inhibit non-specific viral attachment [66, 65]. Glycyrrhizin, for example, as seen in **Figure 16** below, is a triterpenoid saponin (glycosylated steroidal molecule) extracted from liquorice root [66] that has been found to prevent non-specific HIV cellular attachment [67].

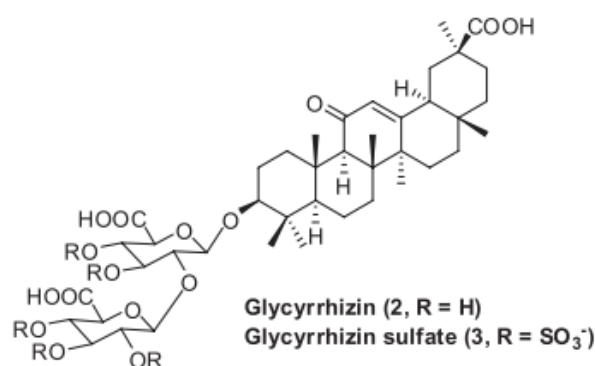


Figure 16: The structure of Glycyrrhizin. Glycyrrhizin is a glycosylated steroidal molecule extracted from Liquorice root [65].

As discussed above, Isoflavones fall under a larger category known as Flavonoids, and one group like Isoflavones are Flavonols. Research conducted on the potential anti-HIV activity of

three Flavonols reported that one of them, Myricetin, possessed entry-inhibiting activity (**Figure 17**) with an IC_{50} value of $20.43 \mu\text{M}$ in TZM-bl cells [68]. The mechanism of inhibition for this compound still needs to be determined, however.

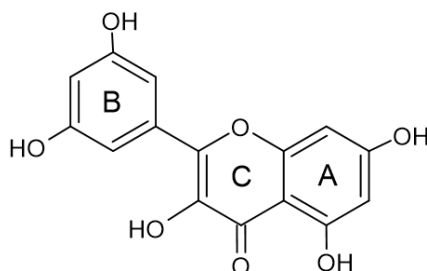


Figure 17: Structure of Myricetin. Myricetin is a Flavanol with strong anti-oxidant properties. It is commonly found in fruits and vegetables and has previously been shown to possess anti-HIV activity [68].

Mahmood [143] published information regarding Myricetin as a possible entry inhibitor and the researchers found that myricetin seemed to be a gp120 antagonist as it prevented the binding of 2 out of 4 gp120 antibodies [143]. The effectiveness against the antibodies at $10 \mu\text{g/ml}$ seemed to be either perfectly effective or completely ineffective, creating a possible map of where the flavanol may potentially antagonise the protein.

2.7 Microbicides

Microbicides are products formulated to prevent the transmission of HIV through the application of the product in mucosal tissues of the vagina and rectum [145]. The products differ from other prevention strategies such as making use of physical contraception as it requires no consent from the other partner. It has been documented that most of the women who are infected with HIV in sub-Saharan Africa, contract it from their only sexual partner [146]. This highlights the need to empower female individuals to offer themselves protection without consent [146].

Microbicides can potentially exist as vaginal rings, gel formulations, suppositories, films or foam. There are no current FDA-approved options, however, the WHO and South African Health Products Regulatory Agency (SAHPRA) recommend the use of the dapivirine ring, which is a vaginal ring that slowly releases Dapivirine into the vaginal mucosal tissue for 28 days [147]. It is not a perfect prevention option as the range of the efficacy of the ring is 27 to 35%. [147].

For entry inhibitors to make plausible microbicidal agents, they need to have an extremely small window of time to be active before the virus crosses the complete barrier of the vaginal

lumen [144]. This small window of time is because the entry stage in viral replication is relatively quick when compared to the 8 h window needed for the creation of integrative viral DNA into the human genome. Research has also shown, using labelled viruses, that the virus can travel past the vaginal epithelial layers without infecting CD4-presenting cells. Once they transverse the layer the virus then infects T-cells and Langerhans cells [144]. This all shows a very narrow window for when an entry inhibitor can act.

Isoflavones are suitable candidates for the production of microbicides as they are small molecules capable of interacting with one or several HIV infection stages, they are stable under biological environments, they can transverse epithelial tissue, potentially affordable to design [144, 146].

2.8 Computational drug discovery

Modern-day drug discovery involves the usage of multiple computational techniques to elucidate the mechanism of action of compounds tested *in vitro*, to design compounds with increased activity of interest and to pre-emptively provide criteria to exclude certain compounds to avoid failed drug trials [190]. Several drugs approved for disease treatment, have been discovered through *in silico* research, such as Sunitinib (gastrointestinal cancer) and Crizotinib (lung cancer) [191]. Additionally, the first FDA-approved protease inhibitors (Saquinavir and Amprenavir) for HIV-1 were developed through the efforts of computational drug discovery in the early 1900s, which greatly improved the lifesaving HIV treatment regime for the time [190].

There is a range of computational techniques which can be utilised in drug discovery, but for this study docking was utilised to hypothesise a mechanism of action, fragment-based drug discovery (FBDD) was implemented to construct new compounds with increased activity, and bioavailability testing utilising known exclusionary criteria were used to highlight which new compounds would pose as the best candidates for future drug research.

2.8.1 Molecular Docking

Computational docking utilising the positioning of compounds in known or hypothesised allosteric or orthosteric binding sites of proteins is becoming more popular in drug discovery [190]. From these generated biochemical computational models, researchers can provide explanations for known *in vitro* activity to narrow down on the biological targets responsible for the documented activity, such as the mechanism of action seen in a cytotoxic assay e.g. ATP synthase inhibition. The models can also be used when the protein target is known, but the mechanism of action in the protein remains unclear [190].

Molecular docking requires the structural information of drug targets, acquired experimentally by nuclear magnetic resonance or X-ray crystallography [192]. This 3D information can be used to identify compounds with a high binding affinity through molecular docking algorithms, which predict energetically favourable orientations through electrostatic and Van der Waals interactions [193].

Considering the plethora of structural research that has gone into characterising the drug targets of HIV, molecular docking is indeed a beneficial tool that can be used to cheaply elucidate a mechanism of action for compounds with *in vitro* HIV entry-inhibiting capabilities [190].

2.8.2 Fragment-based drug design

FBDD is similar in methodology to structure-based drug design (SBDD) which is the process of utilising three-dimensional information generated from an active compound in the active site and making strategic structural changes to improve biological activity [179]. New compounds are often designed from well-described fragments from known active compounds in an attempt to create a new compound with increased activity [152, 155]. FBDD has yielded FDA-approved drugs such as Pexidarlinib, Vemurafexib, Venefoclox and Erdafitinib [183].

FBDD is an ideal method for increasing the activity of the isoflavones in this study as although flavonoids have demonstrated broad *in vitro* activity against HIV-1 with a strong indication of potential entry inhibiting activity, none of the activity noted has been in the nanomolar range, which is where all FDA-approved anti-HIV compounds display activity for HIV entry inhibition [152]. It is still believed that the isoflavones will reveal a novel class of entry-inhibiting structures.

2.8.3 Drug-likeness

Drug-likeness is a method of hypothesising which active compounds can be used successfully as therapeutics based on certain chemical features [184]. The goal of describing the drug-likeness of active compounds is reducing the number of compounds that enter and then ultimately fail clinical trials [184]. In this study, the two rule sets used to describe drug-likeness were Lipinski's rule of five (RO5) and the Ghose Filter [184]. These two rule sets were chosen due to popularity, success rate and the different parameters measured in each.

Lipinski's RO5 was first described by Christopher Lipinski in 1997 [185] after they noted that most orally active compounds adhere to five simple principles:

1. Has a molecular weight of ≤ 500 g/mol
2. Has an octanol/water partition coefficient ($ClogP$) ≤ 5
3. Has ≤ 5 hydrogen bond donors
4. Has ≤ 10 hydrogen bond acceptors
5. No more than two of the above rules can be violated.

Lipinski's RO5 is still used today as a means of measuring drug-likeness as it is satisfied by 85.4% of oral drugs on the market [184].

The second rule set is the Ghose filter, which originated after it was discovered that 80% of active compounds on the market meet the following chemical criteria [184]:

1. AlogP value between -0,4 and 5,6
2. A molecular weight between 160 and 480 g/mol
3. A molar refractivity between 40 and 130
4. A total count of 20 to 70 atoms

The same parameters measured in the above rule sets can also be used to determine which compounds are computationally expected to easily cross the gastrointestinal tract (GIT) and the blood-brain barrier; i.e. describe bioavailability. A major problem with the current regime of HIV treatment is the lack of blood-brain barrier (BBB) permeability, and therefore it is important to not only find drugs that can easily enter the bloodstream after oral consumption, but that can also reduce the viral strain infection inflicts in the brain [165, 175].

Concluding from the literature review, it is evident that isoflavones not only have a place in HIV drug discovery but need to expand into entry inhibition research where the research has

lacked. Biologically, isoflavones satisfy the need for the discovery of suitable microbicide candidates, and BBB-permeable retrovirals.

2.9 Hypothesis

Based on the literature reviewed, the hypothesis of the study was:

H₁: Isoflavones will exhibit significant viral entry inhibition ($P < 0.05$).

H₀: Isoflavones will not exhibit significant viral entry inhibition ($P < 0.05$).

2.10 Aim

This study aimed to investigate the HIV-1 entry inhibitory capabilities of five novel Isoflavones.

2.11 Objectives

The objectives of the study were to:

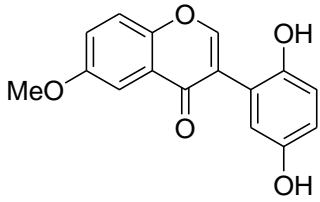
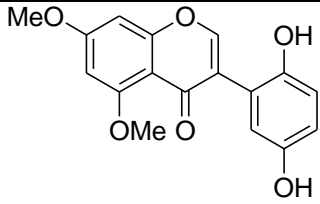
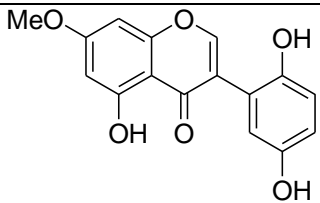
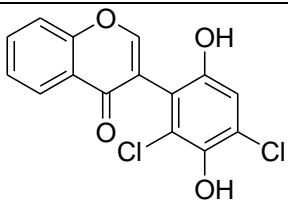
- Determine the CC₅₀ values of the Isoflavones using TZM-bl cells at 24 and 48 h.
- Produce and extract HIV envelope and backbone plasmids on a large scale, using DH5 α and Stbl2 cells, respectively.
- Transform HEK293 T-cells with produced plasmids to create pseudo viruses.
- Determine the IC₅₀ of the isoflavones using a luciferase reporter assay.
- Perform time-of-addition studies with the isoflavones using a luciferase reporter assay.
- Performing docking studies of active compounds to hypothesise the mechanism of action.

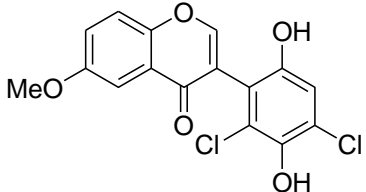
3 Materials and methods

3.1 Dissolving the synthesised compounds

The isoflavones used in this study, illustrated in **Table 1**, were synthesised by the chemistry department at the University of Pretoria by Phaladi Kunyane under the supervision of Dr M.A Selepe, with the method of synthesis available under the publication title “Synthesis of Isoflavones by Tandem Demethylation and Ring-opening/Cyclization of Methoxybenzoylbenzofurans” [170]. The Isoflavones differ in methoxylation, hydroxylation and chlorination of the general Isoflavone backbone (**Figure 13**). The isoflavones share the characteristic in-ring oxygen and double-bonded oxygen on the C ring and contain the unique double hydroxylation on the B ring, at 2' and 5'. The compounds are novel as they have not been described in any previous research.

Table 1: Structures of the synthesised Isoflavones. The structures of the synthesised Isoflavones are depicted alongside their assigned single-letter notation (A to E) compound codes and IUPAC names.

Compound Codes	IUPAC names	Structure	Single-letter notation
PK-87C3	3-(2,5-dihydroxyphenyl)-6-methoxy-4 <i>H</i> -1-benzopyran-4-one		A
PK-110	3-(2,5-dihydroxyphenyl)-5,7-dimethoxy-4 <i>H</i> -1-benzopyran-4-one		B
PK-118C2	3-(2,5-dihydroxyphenyl)-5-hydroxy-7-methoxy-4 <i>H</i> -1-benzopyran-4-one		C
PK-149C2	3-(2,4-dichloro-3,6-dihydroxyphenyl)-4 <i>H</i> -1-benzopyran-4-one		D

PK-144C3	3-(2,4-dichloro-3,6-dihydroxyphenyl)-6-methoxy-4 <i>H</i> -1-benzopyran-4-one		E
----------	---	--	----------

The five synthesised novel Isoflavones were all dissolved in 400 μ l of DMSO. The quantities provided for A-E respectively were: 2,98, 2,56, 2,86, 2,81, and 2,89 mg. The testing concentrations were influenced by achieving the maximum number of replicates from the samples whilst maintaining a maximum concentration of 1% (v/v) DMSO in the first wells with the highest compound concentrations: to avoid cytotoxic effects from the DMSO. The given parameters yielded aliquots of 400 μ M. The aliquots were stored at -20°C until needed.

3.2 The production of HIV-1 pseudo typed viruses

Table 2, describes the two plasmids used to create the HIV-1 pseudo typed viruses, with the Env plasmid only containing the coding sequences for the HIV envelope complex and the Δ Env plasmid containing the entire HIV genome with the exception of the region coding for the Env complex.

Table 2: Details of the pseudo virus plasmids. pTZ19U and pcDNA3.1 vectors were utilised in this study with their respective HIV genome composition.

Plasmid	Description	GenBank accession no.	Size (bp)
Envelope plasmid (Env)	Consists of the Env genome (Cap210, subtype C) integrated into a pTZ19U vector (Allows for Ampicillin resistance selection)	DQ435683	8729
Backbone with missing envelope region (Δ Env)	Consists of the HIV- 1 genome with a removed Env region integrated into a pcDNA3.1 vector (Allows for Ampicillin resistance selection)	L02317	14788

The two viral plasmids needed to make HIV-1 pseudo viruses, Δ Env and Env plasmid were amplified through bacterial transformation and propagation, using Stbl2 (Max Efficiency Stbl2 Competent Cells; Thermo Fisher Scientific, Massachusetts, USA) and DH5 α cell lines, respectively. The cell lines were made competent using the CaCl₂ method in which the cells were grown normally in either TB (Stbl2) or LB (DH5 α) media. **Luria-Bertani (LB) medium:** Contained 1% (w/v) Peptone, 0.5% (w/v) yeast extract, 1% (w/v) NaCl and made to the final volume using dH₂O. **Terrific Broth (TB):** Contained 1.2% (w/v) Peptone, 2.4% (w/v) yeast extract, 0.23% (w/v) KH₂PO₄ and 1.25% (w/v) K₂HPO₄ with a final pH of 7.2. Made to the final volume using dH₂O.

The cells were grown to an OD₆₀₀ reading of 0.4 to 0.5 from an overnight culture grown. The cells were then pelleted at 8500 x g for 10 min at 4 °C, resuspended in sterile 0.1 M CaCl₂ and kept on ice for 30 min, after which a second identical pelleting event was carried out. The pellet was resuspended in a CaCl₂-Glycerol solution (75% (v/v) 0.1 M CaCl₂: 15% Glycerol) and stored at -80°C.

The glycerol stock was then used to heat shock the cells with the preferred plasmids: Δ Env for Stbl2 and Env plasmid for DH5 α . The cells were transformed with the plasmids by heat shocking the glycerol stock for 45 seconds at 42°C. Streaked LB agar-ampicillin plates (Contained 1.5% (w/v) bacto-agar, 98.5% (v/v) LB medium and 10 mg/mL ampicillin) were used to select the plasmids of interest.

Plasmid-yielding colonies, growing in the presence of ampicillin, were grown overnight in Erlenmeyer flasks using 30 mL of LB or TB media. The plasmids were extracted using either the silica-column extraction kit (Gene Jet: Thermo Fisher Scientific, Massachusetts, USA) or the ethanol exclusion technique. The cells with the plasmid of interest were pelleted at 8500 rpm for 10 min at 4 °C. The cells were then resuspended with 250 µL resuspension buffer (GeneJet) and benched for five min at room temperature. Thereafter, the cells were lysed using 250 µL alkaline Lysis buffer (GeneJet) for five min. The cell lysis was halted using 350 µL of Neutralisation buffer (GeneJet). The cellular debris was pelleted at 13 000 rpm for five min and the supernatant was either transferred to a silica gel column or a microcentrifuge tube, both of which received 500 µL wash buffer (GeneJet) and then spun at 13 000 rpm for five min. The flow-through of the silica gel column was discarded as was the supernatant of the microcentrifuge tube; this step was repeated for both methods. The DNA trapped in the silica-gel column was eluted with 50 µL Elution buffer (GeneJet) and a final 13000 rpm centrifugation was done. The final pellet for the ethanol exclusion technique was resuspended with 100 µL elution buffer and both extracts were analysed using a NanoDrop 2000 spectrophotometer (Thermo Fischer Scientific: USA, Massachusetts) to quantify the extracted DNA and to determine the purities.

The extracted DNA was visually analysed by performing a restriction enzyme digest and viewing the cleaved products on a 1% agarose gel in comparison with a 1kb ladder. The restriction enzyme digest made use of a kit from New England BioLabs (Ipswich, MA, USA) that contained the BamH1-HF restriction enzyme which performs a double-strand digest on both vectors at only one location. The double digest reaction was initiated by adding 1000 ng of the isolated plasmid in a solution containing 1 X NEBuffer and 400 units/mL BamH1-HF. The final volume was reached using dddH₂O and the reaction continued for 15 min at 37 °C, after which it was halted by the addition of loading dye to a final 1 X concentration. Both cleaved and uncleaved plasmid products were loaded onto a 1% (w/v) agarose gel that contained 5 µL SafeView (Applied Biological Materials Inc: Canada, BC, Richmond) and viewed using UV-light in a Gel Doc XR+ (Bio-Rad: USA, California).

Once the plasmids were extracted, 5 µg of the Env plasmid was mixed with 10 µg of the Backbone plasmid in 300 µL plain Dulbecco's Modified Eagle's Medium (DMEM, high glucose which contains 4500 mg/L glucose, phenol red, and L-glutamine, Sigma-Aldrich, MO, USA). A volume of 120 µL PolyFect or TurboFect transfection reagent was added to the plasmid solution and gently vortexed for 10 seconds. The solution was then incubated at room

temperature for 10 minutes. A volume of 1,5 mL **Growth media** was then added to the transfection solution (GM, DMEM was supplemented with 3.7 g sodium hydrogen carbonate [Merck: Darmstadt, Germany], sodium pyruvate to a final concentration of 1.1 mM [Cytivia: Illinois, USA], HEPES to a final concentration of 25 mM [Carl Roth: Karlsruhe, Germany] and Gentamycin to a final concentration of 0.025 ng/ μ L [final volume of 1L, pH 7.2] with 10% FBS). The transfection solution was then added to a T75 culture flask containing HEK-293 T-cells in the log phase of growth at 10% confluency with 10 mL GM. The cells were grown at **standard incubation settings** (37°C, 5% CO₂, and 90% humidity in an incubator [Plymouth, MA, USA]). After 8 h the GM was removed, and an additional 20 mL GM was added. The culture was incubated for 36 h at standard incubation settings. The culture media was then extracted and filtered with a 0,45 μ m syringe filter (Pall Acrodisc: USA, New York, Port Washington). The filtrate was then analysed using a TCID₅₀ assay to quantify the produced pseudo virus.

3.3 Determining the virus TCID₅₀

To quantify the extracted virus, a luciferase TCID₅₀ assay was incorporated using a luciferase reporter cell line, TZM-bl cells. The TCID₅₀ assay quantifies extracted virus in terms of luciferase activity in comparison to the background value, and it was first described by Reed and Muench [124]. The assay was prepared as previously described by **Montefiori** [180]. The assay was initiated by adding 100 μ L GM to all the wells of three rows in a clear 96-well plate. A volume of 25 μ L thawed-extracted viral solution was added to the first wells in column 1 of the assay. A serial five-fold dilution series was carried out to the 6th column with the final 25 μ L discarded; the wells in the 7th column serve as a background control, as they contain no virus. A mixture of 100 000 TZM-bl cells/mL was prepared and 100 μ L was added to all the wells in the assay. The plate was incubated for 48 h at standard incubation settings.

The BrightGlo reagent (Promega: Madison, WI, USA) was prepared according to the manufacturer's guidelines by mixing the Luciferase substrate mixture with the BrightGlo buffer solution. The reagent was aliquoted and stored at -20°C.

After 48 hours, 100 μ L of media was removed from all the wells and an equal volume of BrightGlo reagent was added. The lysis reaction continued for two min at room temperature, after which, 150 μ L of the lysed solution was transferred to the corresponding wells in a white 96-well plate (Costar: Corning, NY, USA). The luminescence was analysed using a SpectraMax Paradigm Multi-Mode Microplate Reader (SpectraMax Paradigm: San Jose, CA,

USA). The results were then analysed to acquire the TCID₅₀ value using the Reed-Muench method [125] as performed by **Lei** [187].

3.4 The effect of the Isoflavones on cellular viability

Before the isoflavones could be tested for virus inhibition in TZM-bl cells, the cytotoxic effects of the isoflavones on TZM-bl cells needed to be determined. The cytotoxic effects were quantified using an MTT assay, which followed three phases, namely: plating, treating, and MTT product quantification, as described by **Xia** [35].

Plating: TZM-bl cells were thawed in thawing media in a T75 culture flask. Once the cells reached the log stage of growth, they were cultured in GM. The cells were then trypsinised and counted using the Trypan Blue Exclusion technique. Cells were then seeded in clear 96-well plates at a concentration of 2.3×10^4 cells/well in 100 μ L media in GM. The plates all received a water ridge to reduce volume loss through evaporation; the water ridge consisted of 100 μ L of dddH₂O. The cells were then incubated overnight at standard incubating conditions.

Treating: The next day, the cells were analysed microscopically to roughly confirm equal seeding, particularly amongst the first and final wells. In a separate 96-well plate, the compound preparations were prepared in growth media utilising a double dilution series. The compound preparations were transferred to the corresponding wells in the cultured plate. The concentrations tested ranged from 200 μ M to 6 μ M. The plates were then incubated for either 24 or 48 hours.

MTT product quantification: GM from all the wells was removed and the cells were washed once with Phosphate-Buffered Saline (PBS), with the final volume of plain media in the wells being 100 μ L. PBS-dissolved MTT solution (50 mg/ml) was then added to each well resulting in a final concentration of 0.5 mg/ml. The plates were then incubated for two hours at standard incubation settings. After the incubation period, all the media was removed and 100 μ L DMSO was added to all the wells to rupture the cells and dissolve the crystals. The plates were then read in a spectrometer at 570 nm (SpectraMax Paradigm: San Jose, CA, USA), and the results were normalised against a background control and the viabilities determined from a set of untreated cells.

3.5 HIV-1 Inhibition: Luciferase assay

Following the method set by **Martinez** [68], in a 96-well plate, a double dilution series was carried out in 100 μ L GM in triplicate for each compound from a starting concentration twice

that of the desired concentration. In the 100 μL compound solution, 50 μL of cell solution (100 000 cells/mL) was added. Dextran Sulphate was used as the positive control for viral entry inhibition at 20 μM [77]. Following, 50 μL of the thawed viral solution was added, resulting in a final TCID₅₀ of 400. The final isoflavone concentrations ranged from 25 μM to 3 μM . The plates were then incubated for 48 hours, after which 150 μL of the well solution was removed and 50 μL of premade BrightGlo solution (Stored at -20°C) was added to the wells. A two-minute incubation period followed to allow for complete lysis of the cells. The wells were resuspended and the lysed contents were transferred to a white plate and read in a microplate reader. The luminescence was quantified as relative luminescence units (RLU).

3.6 Time-of-addition studies

The luciferase reporter assay eloquently displays whether a compound displays notable anti-HIV-1 activity, however, it is not specific for the discovery of entry inhibitors. Any activity seen in the assay can be due to entry inhibition, reverse transcriptase inhibition and integrase inhibition: all the viral proteins involved before the integration of the viral genome into the host genome, resulting in luciferase expression [113]. To clarify which point of the assay the inhibition in luciferase production was occurring, time-of-addition (TOA) studies were performed as it has been well documented when and where the HIV cycle occurs [132]. The cells were plated as in 3.6 in a 96-well plate and infected with pseudo virus (400 TCID₅₀). After 90 min, significant viral entry would have taken place [132], and the compounds were added at 25 μM , a concentration higher than all generated IC₅₀ values and lower than all generated CC₅₀ values, at 0- and 90-min post-infection. The control, Nevirapine, an NNRTI, was added at 20 μM [133]. Comparing the results of Nevirapine at 0- and 90-min post-infection, it is expected that there will be no drop-in activity seen, this will indicate that only the entry stage of the life cycle has been avoided and not any other replication step post-entry.

3.7 Molecular docking

Docking scores were generated for the isoflavones in regions entry inhibitors and anti-HIV compounds active against viral replication are known to bind, in an attempt to hypothesise on a possible mechanism of action. The docking software used was Maestro version 12,8 (Schrödinger, New York City, USA).

Using the LigPrep feature of Maestro 3D structures of the isoflavones were created at a pH of 7.2 ± 0.2 to generate the potential ionisation states of each compound at physiological pH, using Epik.

The crystal structures of the proteins of interest were downloaded from the Protein Data Bank (PDB) archives. The ID codes for the proteins involved in the viral entry were 1RZJ, 5U7O (Gp120), 4MBS (CCR5) and 2KP8 (Gp41). The ID codes for the HIV proteins involved in replication were 1EP4, 3V4I (RT) and 1QS4, 5KRS (IG).

The proteins were then prepped using the Protein Prep Wizard task of Maestro. Water molecules were deleted beyond 3\AA , bond orders were assigned, metals were deleted, and missing residues and loops were added using the prime function. The proteins were minimised and optimised with the OPLS4 force field and PROPKA, respectively. The receptor grid was then generated using the Receptor Grid Generation Tool. The van der Waals radius scaling factor was set to 1,0 with a positive charge cut-off set at 0,25.

Utilising the generated receptor grid file, docking studies were performed using the Virtual Screening Workflow (VSW) tool. Epik states penalties were utilised for Extreme Precision (XP) docking. The ligands were docked flexibly and had a van der Waals radius scaling factor of 0,25 with a partial charge cut-off of 0,15.

For 1RZJ, a crystal structure of gp120 docked with the target receptor CD4, chain L (antibody 17b light chain) chain H (antibody 17b heavy chain) were deleted. All the residues on chain C (CD4) were deleted except Ser-42, Phe-43 and Leu-44 as these dock into the gp120, Phe-43 binding cavity [153], and they were used for receptor grid generation.

The method used for docking was validated following the procedure by **Okesola** [150] whereby Myricetin was docked (**Appendix 1**).

3.8 Fragment-based drug redesign to increase binding affinity

Once the hypothesised mechanism of entry inhibition of these compounds had been described, the compounds were redesigned according to the binding site in an attempt to increase binding affinity. The compounds were redesigned by adding residues from the known gp120 inhibitor, Fostemsavir, making this form of drug design, FBDD, as it attempts to increase the affinity of the isoflavones through the addition of known gp120-active residues: to essentially increase fit and essential target interactions [181]. These residues were added strategically by superimposing the docked structures of the active entry-inhibiting isoflavones, **B** and **C**, with

Fostemsavir (BMS-626529) in gp120 (PDB: 5U7O). A representation of the methodology of FBDD can be seen in **Figure 18** [181]. The new compounds were docked into the cavity and the structures which yielded greater docking scores than the scores of the original isoflavones were kept.

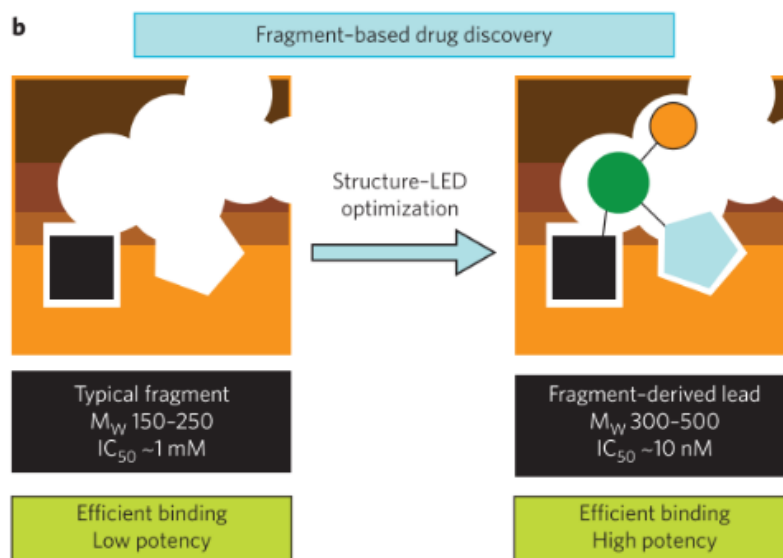


Figure 18: Fragment-based drug design. Illustrated is the computational method of adding known active residues, for a certain biological target, to increase potency and activity [181].

3.9 Drug-likeness

In this study, the two rule sets used to describe drug-likeness were determined using SwissADME; the rule sets were Lipinski's rule of five (RO5) and the Ghose Filter [184]. These two rule sets were chosen due to popularity, success rate and the different parameters measured in each.

SwissADME was then also used to determine which compounds are computationally expected to easily cross the gastrointestinal tract (GIT) and the blood-brain barrier; i.e. describe bioavailability. SwissADME speculates which compounds will be able to cross the GIT and BBB using a BOILED-Egg (Brain Or IntestinaL Estimate) model unique to the SwissADME platform [136, 186]. The BOILED-Egg model has mapped out where on a graph of lipophilicity (WlogP) vs polarity (tPSA/A²) known BBB and GIT permeable molecules appear (**Figure 19**). Using this data, the BOILED-Egg model estimates the bioavailability of novel compounds.

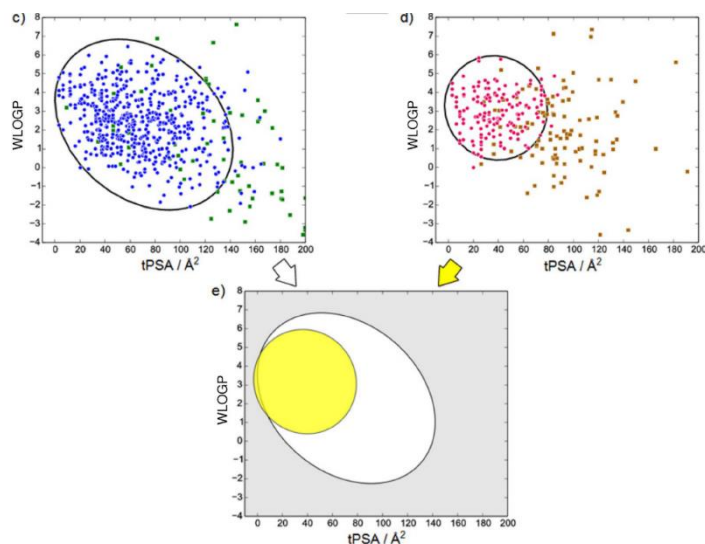


Figure 19: Overview of the SwissADME BOILED-Egg model. The figure with the white and yellow ellipses below indicates the BOILED-Egg model, with the white region indicating good GIT absorption and the yellow region indicating good BBB permeability. All the graphs are of WlogP (lipophilicity) vs tPSA / Å² (polarity). The blue and green dots indicate regions of good and poor GIT absorption, respectively. The magenta and brown dots indicate regions of good and poor BBB permeability, respectively [186].

3.10 Determination of the IC₅₀ and CC₅₀ values

The IC₅₀ and CC₅₀ values were generated using GraphPad Prism 5 (GraphPad: San Diego, CA, USA) using non-linear regression from three repeats. The software was also used to calculate the Standard Error of the Mean (SEM).

3.11 Statistical analysis

For the TOA studies, the analysis of whether the difference between the means of the two post-infection points (0 and 90 min) are significantly different with $P < 0.05$ was performed with the computer programme JMP, using a student-paired t-test.

4 Results

The management of HIV infection remains a health challenge, and this study investigated the effects of novel isoflavones for their HIV entry inhibition activity. This was done utilising a pseudo typed virus. The production of the HIV-1 pseudo typed virus started with the amplification of the Δ Env plasmid and the Env plasmid in Stlb2 and DH5 α cells, respectively.

The extracted plasmids from the silica-gel column or through the ethanol precipitation method were visualised in a 1% agarose gel under UV light as seen in **Figure 20**, after which a spectrophotometer was used to quantify the extracted DNA and elucidate the purity, which can be seen in **Table 3**.

The relative placements of the bands in relation to the 1 kb ladder show the expected results for a shorter band for the Env plasmid (8729 kb) and a larger band for the Backbone Δ Env (1478 kb) plasmid. It is clear from the results that lane 1 shows the greatest yield for extracted plasmid through the ethanol extraction method.

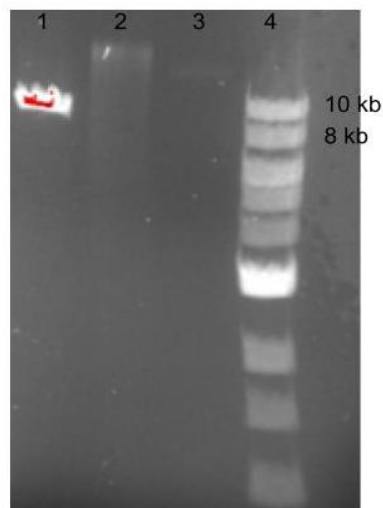


Figure 20: UV visualised agarose gel with loaded extracted viral DNA. The 1% agarose gel consists of four wells labelled at the top 1 to 4. Well 1: Extracted Env plasmid (ethanol extraction method). Well 2: Extracted backbone (Silica-Column method). Well 3: Extracted backbone (Silica-Column method) Well 4: Contains 1 kb ladder. All wells show expected plasmid sizes. The red marking in lane 1 indicates a high concentration of DNA analysed, as determined by the imaging software. The DNA was analysed using Image Lab 3.0 (Bio-Rad).

The visualised bands also indicate that the ethanol extraction method seems to be the better method for extracting the most plasmid, as lane 1 has a much visibly higher yield than lanes 2 and 3, which both utilised the silica-column extraction method. These results are further corroborated by the plasmid quantification results tabulated in **Table 3**.

Table 3: Extracted plasmid quantification and purity analysis using spectrophotometry. The plasmids were quantified in a NanoDrop 200 Spectrophotometer. Their relative purities are described with the 260/280 and 230/280 ratios, which relate to RNA and protein contamination, respectively. Any purity rating over 1.8 is considered pure. **1** is the Env plasmid in green (ethanol exclusion method). **2** is the Backbone (Silica-gel method). **3** is the backbone plasmid (silica-gel method).

Extract	1	2	3
[ng/ μ L]	3924.6	263.3	206.3
260/280	1.85	1.88	1.99
230/280	2.35	2.35	2.78

From the above, it is clear the ethanol extraction method yielded the highest concentration of extracted plasmid. The plasmid extracted from the ethanol exclusion technique was used to transfect HEK-293 T-cells to produce pseudo virus. The extracts from the pseudo virus production were then used to perform the TCID₅₀ assay as seen in **Table 4**.

4.1.1 Determining the virus TCID₅₀

A TCID₅₀ assay was performed by utilising the TZM-bl luciferase reporter assay with the media from the cultured HEK293 T-cells, after 48 hours with the transfection reagent and the amplified viral plasmids. The TCID₅₀ assay quantified the amount of virus in the dilutions in RLU (Relative Luminescence), as seen in **Table 4**.

Table 4: TCID₅₀ assay for virus titre. The extracted virus received a five-fold dilution series until column 6. The RLU values are indicated, with the reactions described as positive if they are above 2.5 times the mean control value (28.5) and negative if they are below.

Log of virus dilution	-1	-2	-3	-4	-5	-6
Row 1	21526	6128	2011	720	383	19
Row 2	20647	6730	1858	352	191	38
Row 3	24118	6262	1548	555	116	19
Positive reactions (%)	100	100	100	100	100	33.33

The values were then used to work out the dilution needed to achieve a TCID₅₀ value of 400 using the Reed-Muench method, with results above the mean background value (28,5 RLU) deemed as positive for an infection and those below deemed as negative for infection [68]. The calculations can be seen in **Appendix 2**. The transfection reaction for the production of pseudo virus was indeed as successful as dilutions up to 5⁻⁵ produced 100% positive reactions; indicating a high viral load from the extracts. Since this is simply to quantify the viral load produced, the results cannot be compared to those previously published as they will differ. The

production of the virus is simply deemed a success when compared to the background (negative control).

4.1.2 The effect of the Isoflavones on cell viability

Before testing the isoflavones for their anti-HIV activity, their effects on the viability of TZM-bl cells were investigated using an MTT assay to quantify viability at 24 h (Figure 21) and 48 h (Figure 22) post-cell exposure.

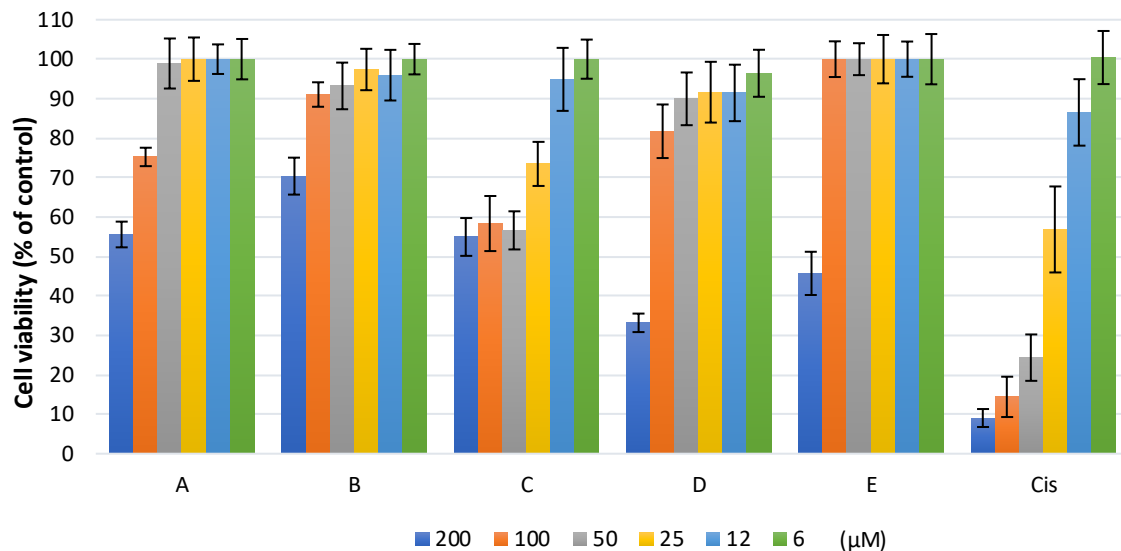


Figure 21: The effect of the Isoflavones on cell viability (24 h). The results indicate the viability of TZM-bl cells after exposure to the Isoflavones for 24 h, using an MTT assay. The positive control is Cisplatin with a CC_{50} value of 20 μ M. The legend on the right indicates the range of concentrations tested (200 μ M to 6 μ M). The error bars indicate the SEM for $n = 3$.

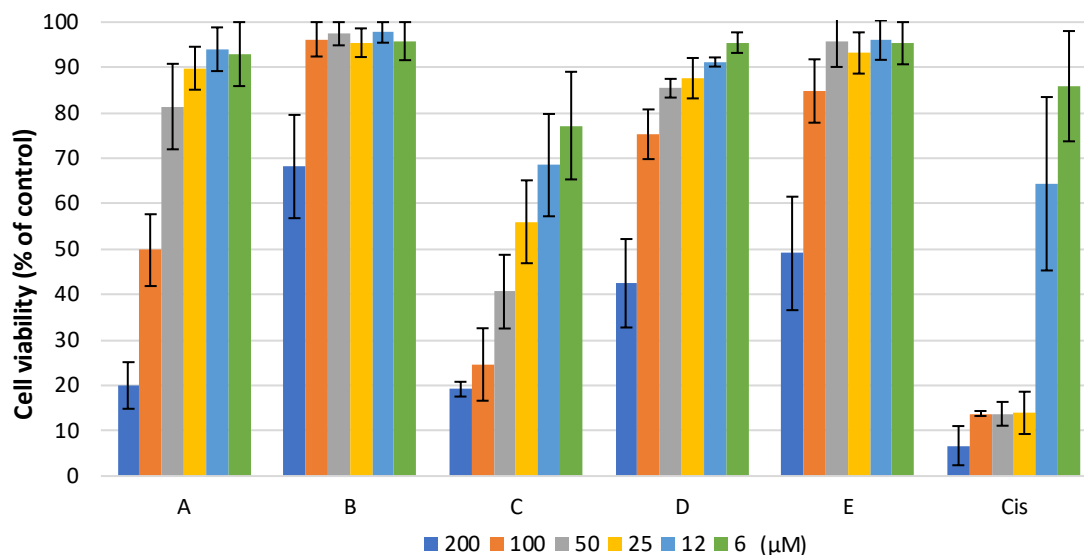


Figure 22: The effect of the Isoflavones on cell viability (48 h). The results indicate the viability of TZM-bl cells after exposure to the Isoflavones for 48 h, using an MTT assay. The positive control is Cisplatin with a CC_{50} value of 14.1 μM . The legend on the right indicates the range of concentrations tested (200 μM to 6 μM). The error bars indicate the SEM for $n = 3$.

The above dose-response curves were used to calculate the CC_{50} values for each compound. These were generated using non-linear regression on GraphPad Prism 5 and displayed in μM . Cisplatin is the antineoplastic positive control. **Table 5** represents the calculated CC_{50} values.

Table 5: Generated CC_{50} values. The CC_{50} values are rounded to the first decimal place, depicted alongside the SEM ($n = 3$) value. CC_{50} values that were above the concentration range tested were reported as $>200 \mu\text{M}$.

Compound		A	B	C	D	E	Cisplatin
$CC_{50} \pm$ SEM [μM]	24 H	>200	>200	>200	158.8 ± 1.1	195.6 ± 1.2	17.3 ± 1.7
	48 H	99.4 ± 1.1	>200	30.9 ± 1.2	182.8 ± 1.2	198.6 ± 1.1	14.8 ± 1.3

The combination of the dose-response curves and tabulated CC_{50} results indicates exceptionally well that no single compound stands out as a potential antineoplastic, relative to Cisplatin, within the 24 h treatment period. Only the chlorinated Isoflavones, **D** and **E**, reduced viability past 50%. According to the graphs, the lowest viability at 24 h is achieved by **D**, however, the comparable CC_{50} results (159 μM and 196 μM , respectively) suggest that **D** and **E** are the most cytotoxic Isoflavones in the group of five tested in this study. This is no longer the case after looking at the 48-h post-treatment results generated as there appears to be a time-dependent decrease in cellular viability.

Both **D** and **E** show no signs of major increases in toxicity from 24 h to 48 h with their CC_{50} values decreasing by 24 and 3 μ M, respectively, at 48-h.

The cytotoxic profile of **A** and **C** changes drastically after 48 h post-Isoflavone treatment, as depicted in **Figure 22** and **Table 5**. **A** and **C** had not even managed to pass the 50% viability point at 24 h post-treatment, but after an additional 24 h, the compounds both managed to reduce cellular viability by around 80% for the highest concentration tested. **C** demonstrates that it is the most cytotoxic isoflavone, with a CC_{50} value of 48-h comparable to both the 24 h and 48 h Cisplatin CC_{50} values. The positive control for toxicity, Cisplatin, behaved as expected as it produced a 24 h CC_{50} value that aligns with previous research (Cisplatin: CC_{50} = 20.0 μ M [119]). Analysing the results from 24 h and 48 h post-Isoflavone treatment, **B** appears to be the most ideal compound to display anti-HIV activity as it shows the least cytotoxic effect.

The results were further strengthened by evaluating the cytotoxicity of the solvent used to dissolve the Isoflavones: DMSO. The cytotoxicity of the max concentration DMSO (1% v/v) used to dissolve the isoflavones was tested at 48 hours. The results indicated no deviation from 100% viability with a standard deviation value of 4% (**Appendix 3**). **Forman** [126] studied the cytotoxic effect of several compound solvents on the HeLa cell lineage [126]. The researchers described that the cytotoxic effects of DMSO are not prevalent at concentrations lower than 2% (v/v), however many researchers favour keeping the DMSO concentration at 0.1% as it avoids not only toxic effects but unwanted cellular metabolic changes [126].

4.1.3 Luciferase reporter assay inhibition

The anti-HIV activity of the Isoflavones was quantified based on the susceptibility of TZM-bl cells to HIV-1 infection. After the virus enters the cells and undergoes transcription and translation to produce the viral protein, TAT, the cells produce firefly luciferase in response to tat-induced transcriptional activation. The light-producing reaction of luciferase in the presence of luciferin was then quantified with and without the isoflavones to calculate the decrease in luciferase activity which can be used to evaluate the anti-HIV activity. The reporter assay results depicted graphically in **Figure 23**, illustrate the percentage reduction in luciferase activity against the control.

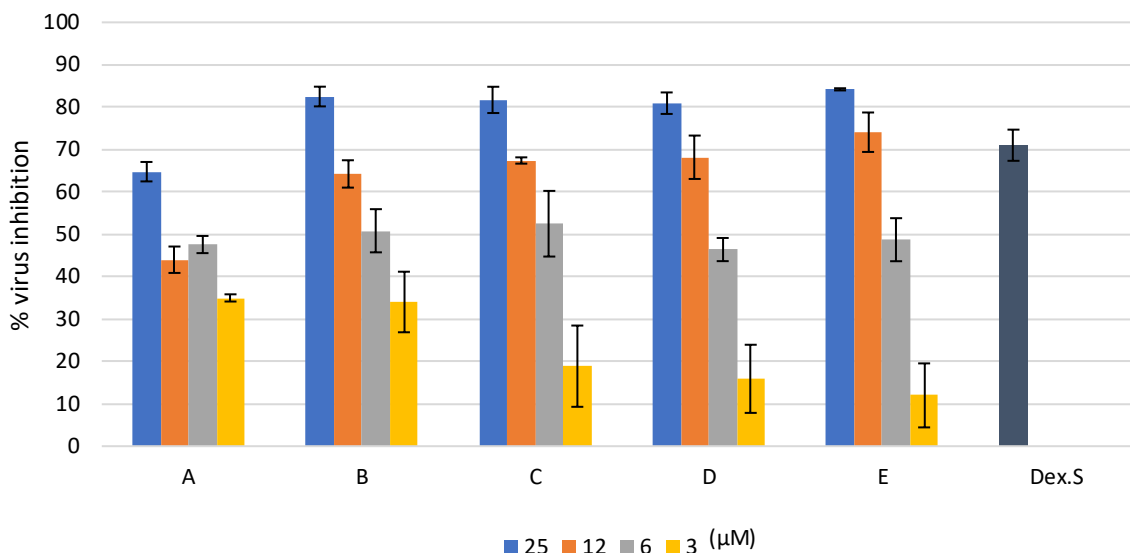


Figure 23: Luciferase reporter assay. The reduction in luciferase activity from 100% according to the concentrations tested (25-3 μM) for the five isoflavones is shown. Error bars represent SEM for n = 3. The positive control for entry inhibition is Dextran Sulphate, tested at 20 μM.

The results demonstrate notable anti-HIV activity from all the isoflavones with the range in maximum inhibition seen at the highest concentration tested, 25 μM, being 64 to 82%. **A** achieved the lowest maximum inhibition while **B** to **E** achieved around 82% inhibition ($\pm 2\%$), at the highest concentration tested.

The calculated IC_{50} values shown in **Table 6** demonstrate that although **A** may appear initially to be outperformed by the other Isoflavones, it produced an impressive, albeit the highest, IC_{50} value of 10.6 μM. **B**, the least toxic Isoflavone, produced the lowest IC_{50} value of 6.2 μM. **Table 6** depicts the IC_{50} values alongside the residues that differentiate the Isoflavones into unique compounds. Although this study did not have the benefit of a large library of closely related Isoflavones, conclusions can still be made from the placement of certain residues, namely the methoxy, hydroxyl and chlorine groups. The chlorinated Isoflavones, **D** and **E**, possessed symmetrically placed chlorine groups on 4' and 6'. These groups appear to convey no noteworthy benefit, as **E** and **A** differ structurally only in the chlorine groups, and the IC_{50} values differ by 3.2 μM.

Table 6: Generated IC₅₀ values. The generated IC₅₀ values are listed alongside the residues that make each isoflavone unique from the general backbone structure. MeOH residues are listed in blue, the OH group is listed in orange and the Cl groups are listed in green. The IC₅₀ values are listed alongside SEM values from triplicate repeats.

Isoflavone	5	6	7	2'	6'	IC ₅₀ ± SEM (µM)
A	H	MeOH	H	H	H	10.6 ± 1.1
B	MeOH	H	MeOH	H	H	6.2 ± 1.0
C	OH	H	MeOH	H	H	7.1 ± 1.1
D	H	H	H	Cl	Cl	7.8 ± 1.5
E	H	MeOH	H	Cl	Cl	7.2 ± 1.0

4.1.4 Time-of-addition assay

The TOA studies involved the addition of the compounds at the highest concentration tested for the Luciferase reporter inhibition assay studies, 25 µM, 90 min after the interaction of the pseudo virus with the cells. The results displayed graphically in **Figure 24**, demonstrate the % luciferase inhibition witnessed after adding the isoflavones 90 min later in comparison to the addition of the isoflavones immediately after viral treatment of the TZM-bl cells. Each isoflavone loses activity at the 90 min post-infection interval, however, only **B** and **C** showed a significant difference between the 0 and 90 min post-infection points ($P < 0.05$, **Appendix 6**). **A** lost the least amount of activity (3.2%), strongly indicating that although **A** possesses notable anti-HIV activity, none of it is due to HIV-1 entry inhibition. **B**, which is the most potent of the anti-HIV acting isoflavones in the study, has also shown the greatest reduction in anti-HIV activity after 90 min post viral infection, with a decrease in activity by 37.8%; **C** had a reduction of 20.4%.

Nevirapine, which is an NNRTI, was added 0 and 90 min post viral infection. This served as the positive control showing a high level of viral inhibition. This high level of anti-HIV activity from Nevirapine validates this assay as one which can provide evidence of entry inhibition as it has been shown it is still indeed possible to strongly inhibit HIV-1 at this point. Nevirapine generated a high inhibition value (72%) at 90 min post-infection and lost no observable activity when compared to the 0 min infection results, indicating the loss of activity seen in these compounds occurs before the reverse transcriptase step. It was expected that at 20 µM Nevirapine would have induced 100% inhibition. It is possible that with the high prevalence of NNRTI resistance in South Africa, 18.9% in 2017, the plasmids were isolated from an individual with a resistance to the control [176].

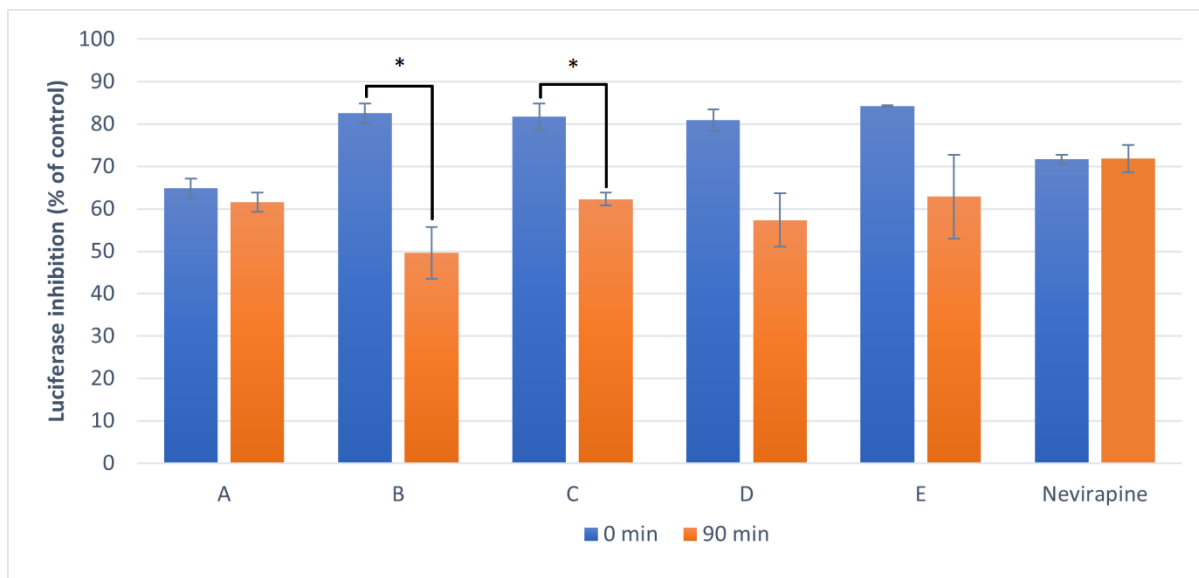


Figure 24: TOA results. The TOA results show the % reduction in Luciferase activity at 0 (blue) and 90 min (orange) post-viral infection when treated with the Isoflavones; each at a concentration of 25 μ M. The error bars represent the SEM (n =3) with the asterisks indicating a significant difference between the means of the two groups ($P < 0.05$) The control was Nevirapine, tested at a concentration of 20 μ M.

4.1.5 Docking scores and ligand interactions

After proving these compounds act as entry inhibitors, the next step was to hypothesise where their mechanism of entry-inhibiting activity lies. This was achieved through the generation of docking scores in known antagonistic binding sites of the proteins involved in viral entry. Once the scores were collected, as seen in **Table 7**, the same docking software was used to visually depict the most energetically likely binding of the isoflavones in the active sites. This visual data was then used to hypothesise on the biochemical activity in the binding pockets. Only the ligand interactions for **B** and **C** are displayed as these are the only Isoflavones that show signs of significant entry-inhibiting activity from the TOA results. The ligand interactions for **A**, **D** and **E** are shown in **Appendix 4**.

All the Isoflavones were docked into the binding sites within the receptor proteins to make distinctions between the binding scores and the observed activity. **Table 7** shows that the best docking scores were achieved in the hydrophobic Gp120 binding pocket (PDB: 5U7O), by all the Isoflavones. As stated by the Schrodinger website, docking scores of -8 to -9 kcal/mol may indicate ‘very good’ scoring when dealing with small binding pockets, or hydrophobic binding pockets [154], which the gp120 binding pocket can be classified as [152]. After rejecting all docking scores above -8 kcal/mol, the compounds all show favourability for the gp120

hydrophobic binding pocket. The worst docking scores were achieved when docking against the gp41 fusion protein.

With the co-receptors, only CCR5 was utilised as there is no data on the co-receptor tropism on the subtype C-Cap210 variant used in this study. The viral genetic material was isolated from a South African infection and most infections in South Africa involve R5 tropism [157], therefore it is assumed to be R5 tropic.

With the docking into the crystallised CCR5 protein, the results are not as promising as the gp120 docking results, as they fall above -8 kcal/mol, however, the data set is the second best in terms of docking scores, with **A** producing the highest docking score of -6.224 kcal/mol.

Table 7: Docking scores generated using different HIV-1 entry proteins. The docking scores (kcal/mol) generated are listed alongside the receptor protein they were docked in for the generation of the binding scores. The values in red represent the values regarded as poor docking scores as they are above -8 kcal/mol while the areas in blue indicate the docking scores of the antagonists of the respective active sites.

PDB code	Compound	Docking score (kcal/mol)
Gp120		
5U7O	A	-8.821
	B	-8.613
	C	-10.392
	D	-9.112
	E	-8.943
	Fostemsavir	-6.507
1RZJ	A	-3.116
	B	-4.004
	C	-4.861
	D	-3.306
	E	-3.580
	CD4	-4.797
CCR5		
4MBS	A	-6.224
	B	-5.146
	C	-5.541
	D	-5.699
	E	-4.329
	Maraviroc	-9.239
Gp41		
2KP8	A	-1.867
	B	-4.568
	C	-3.327
	D	-2.690
	E	-2.989
	XIG	-1.525

It was assumed that with such similar structures and IC₅₀ values amongst the isoflavones, the isoflavones would dock similarly into the binding proteins, however, in **Figure 25**, which shows the docking of **B** and **C** into the hydrophobic binding cavity, the isoflavone backbone with **B** and **C** adopts opposite polarities in the pocket. With **B**, the double-ring (A + C) region interacts with the entrance of the cavity, while with **C** the single B-ring region interacts with

the entrance of the cavity. This shows that the general hydrophobic nature of the isoflavones confers **B** and **C** entrance into the cavity, but it can be seen in **Figure 26** that the residues that they share: the 2' and 5' OH groups show no indication of similar activity in the binding pocket.

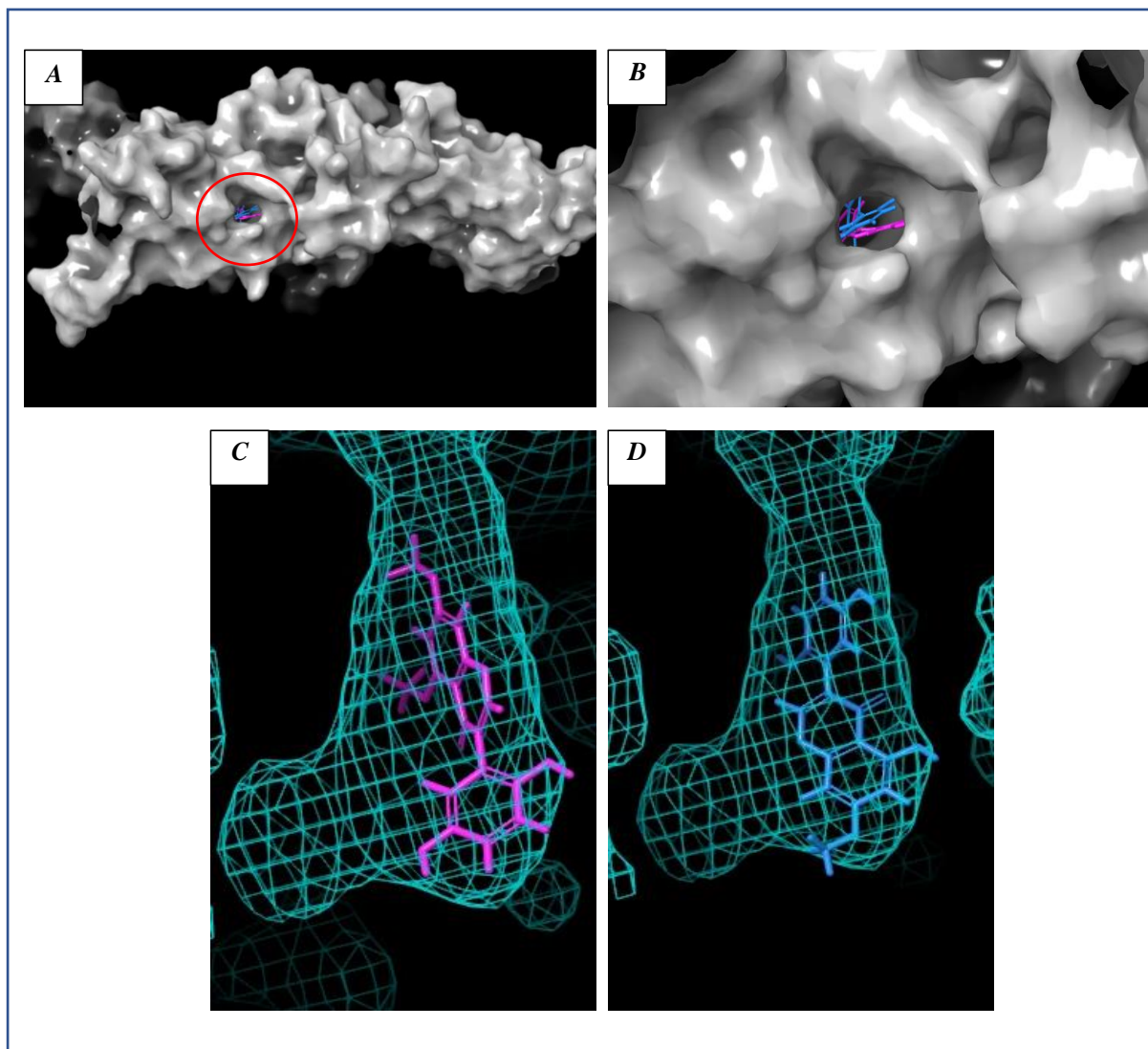


Figure 25: Visualisation of the entry inhibiting Isoflavones in the gp120 binding pocket. **A** shows the complete gp120 protein with the docked isoflavones highlighted by the red circle, in the hydrophobic binding cavity. **B** is the enlarged version of the docked isoflavones in the solid protein structure. **C** and **D** provide visual information on the orientations of the isoflavones deep in the hydrophobic binding pocket, with the protein displayed as a blue mesh. Isoflavone **B** is in magenta and compound **C** is in blue. Compounds **B** and **C** adopt opposite orientations in the binding cavity with respect to the isoflavone backbone structure. With isoflavone **B** the double-ring structure interacts with the entrance of the hydrophobic cavity and with isoflavone **C** the single-ring section interacts with the entrance of the cavity. PDB: 5U7O.

Figure 26 also indicates, that the nature of the hydrophobic pocket around the isoflavones is mostly a non-polar region (indicated in a green band), with some polar areas (indicated in blue) and a charged area (indicated in red) around the charged amino acid, Glu 370.

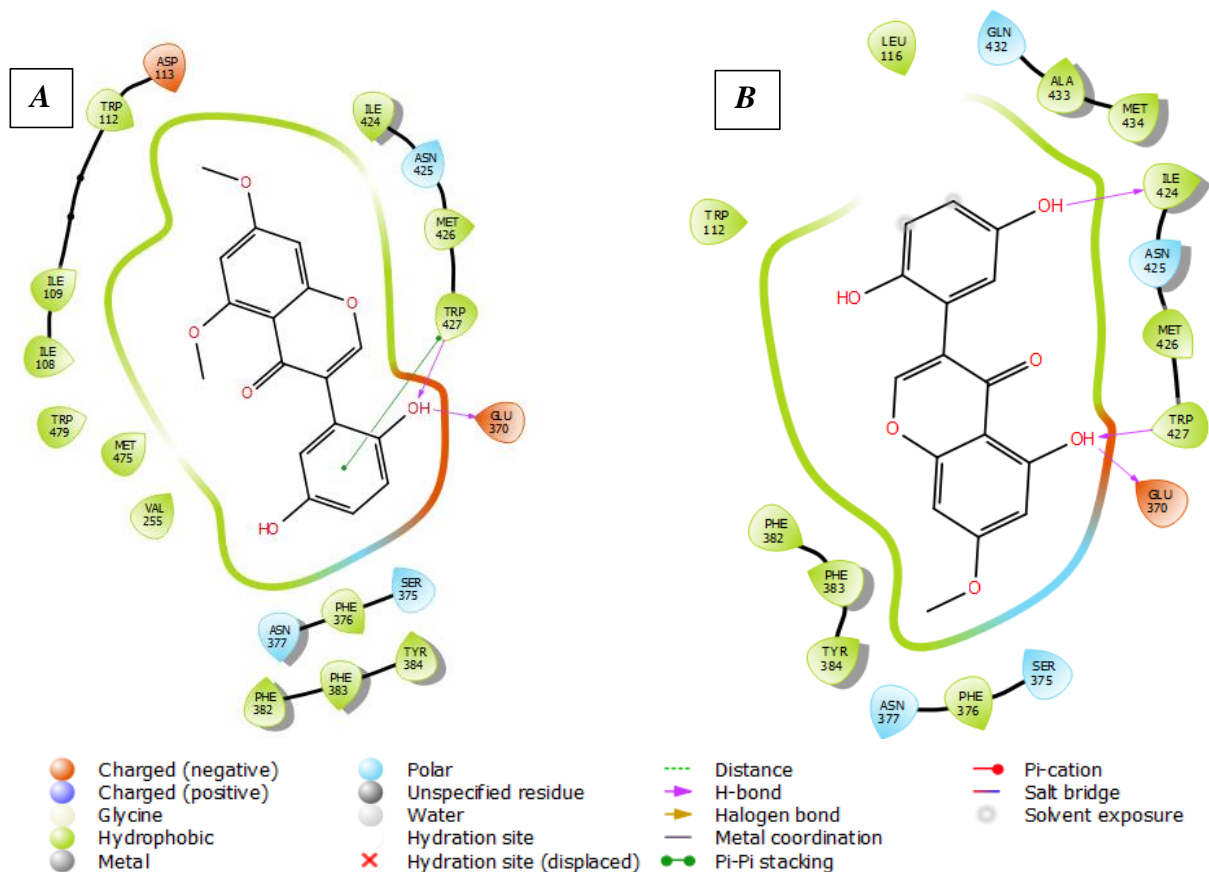


Figure 26: Biochemical interactions in the gp120 binding pocket. *A* illustrates the suggested biochemical interactions of isoflavone **B** in the binding pocket, while *B* illustrates the interactions of isoflavone **C** with the binding pocket. The type of interactions seen is mostly hydrophobic, hydrogen bonding and pi-pi stacking. The Trp 427 and Glu 370 region dictates the region nearest the opening of the cavity.

Another Gp120 binding simulation was computed (PDB: 1RZJ) which docks the isoflavones in the CD4 entryway, which naturally interacts with the immune cell CD4 residue, Phe 43 (**Figure 27**). Interactions of drugs in this area are a proposed method of gp120 antagonism as it would prevent CD4 binding [155]. The Isoflavones did not dock as well in the CD4 entryway, which was expected as the literature describes this area as a hydrophilic region [152], which would not be ideal for the lipophilic isoflavones.

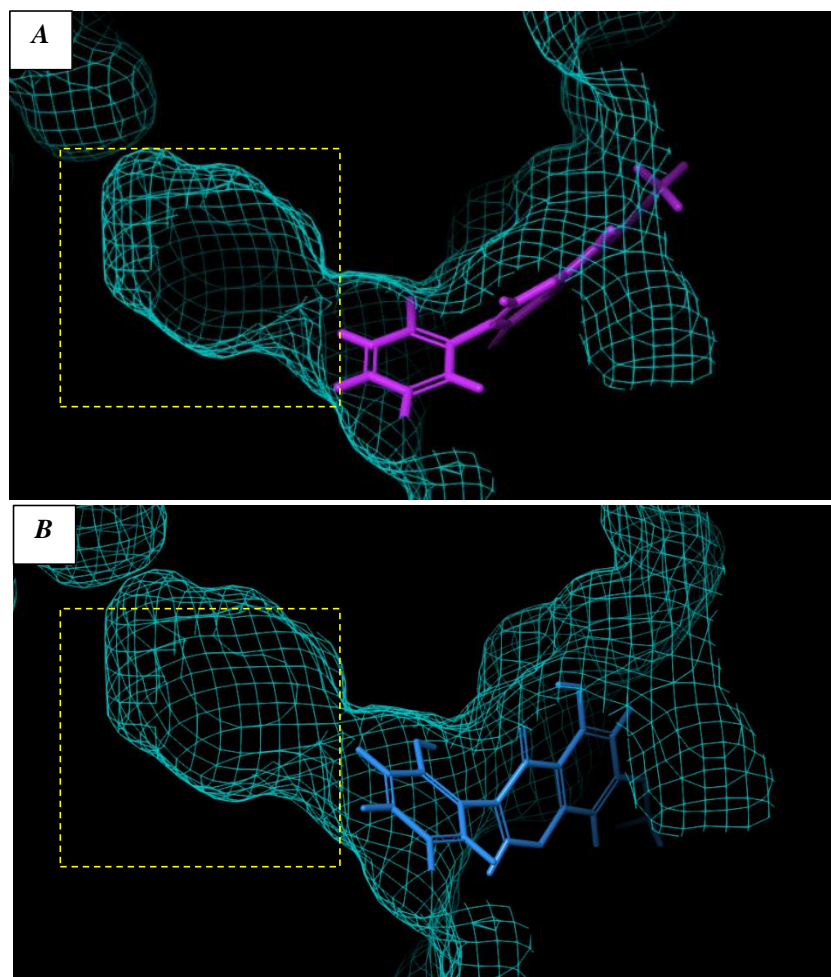


Figure 27: Docking of B and C in the CD4 entryway of gp120. A depicts isoflavone **B** (magenta) position in the entranceway of the binding pocket, while B depicts isoflavone **C** (blue) in the entranceway. The yellow dotted square isolates the deep hydrophobic binding pocket of the gp120 protein where the approved gp120 inhibitor, Fostemsavir, binds. PDB: 1RZJ.

4.1.6 Fragment-based drug design

The isoflavones with proven entry-inhibiting activity, **B** and **C**, were used for the creation of new compounds to increase activity and hopefully yield derivatives with activity in the nanomolar region. Each isoflavone yielded two new compounds with improved docking scores when fragments from the FDA-approved gp120 antagonist, Fostemsavir, were attached to the isoflavones. The isoflavone **B** derivatives are labelled **B1** and **B2**, while the isoflavone **C** derivatives are labelled **C1** and **C2**, as seen in **Figure 28**.

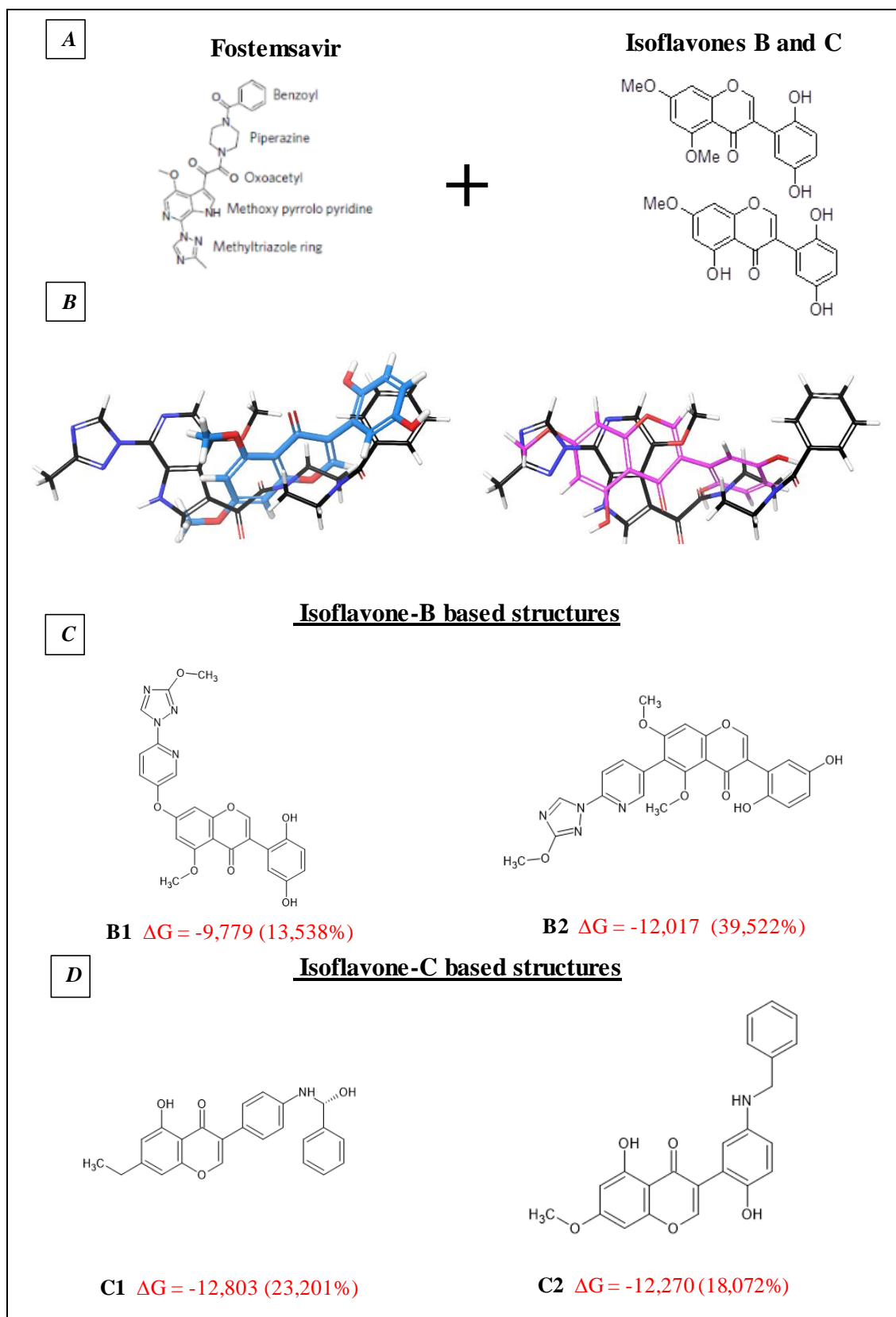


Figure 28: Redesigned isoflavone derivatives. Section 1 depicts the chemical segments of Fostemsavir and the active Isoflavones **B** and **C**. Section 2 is a depiction of the fragment-based compound design where docking was used to visualise the plausible active Temsavir sides chains that could be used to elongate the isoflavones (PDB:5U7O). Sections 3 and 4 display the new structures that generated docking scores higher than the original isoflavone docking scores. The docking scores are displayed in **red** in kcal/mol with the percent increase in binding affinity from the original docking score illustrated in brackets.

In section 2 of **Figure 28**, a representation of the FBDD methodology is presented with the structures of isoflavones **B** and **C** superimposed with Fostemsavir. This provides a clear indication of which fragments of Fostemsavir can be added to the isoflavones while ensuring that they maintain the same positions as seen on Fostemsavir docked in gp120. This resulted in the addition of the methoxy pyrrole-pyridine and the methyltriazole-ring fragments of Fostemsavir (section 1 **Figure 28**) to **B**. Similarly, the piperazine and benzoyl fragments of Fostemsavir (section 1) were added to **C**.

The decrease in docking scores, which ranges from 13.538 to 38.522% (**Figure 28**), serves as a computational indication that the affinity of the compounds for the gp120 hydrophobic pocket has been increased [183].

The nature of FBDD involves strategically adding fragments to the original docked compounds, therefore the derivatives expected to have activity in the gp120 binding pocket are those that maintained exact or similar positioning of the isoflavone moiety to the originally docked isoflavones. The alignment of the isoflavone moieties in the new derivatives to the original isoflavones is an indication that these fragments will contribute to the unique activity the isoflavones have in the gp120 binding cavity. The only two new derivatives to match up with the original isoflavone positioning in gp120 are **B2** and **C2** as seen in **Figure 29** (Sections 2 and 4). The other derivatives adopt unique positionings with the isoflavone moieties in the cavity, which were not predicted through FBDD (**Figure 29** Sections 1 and 3).

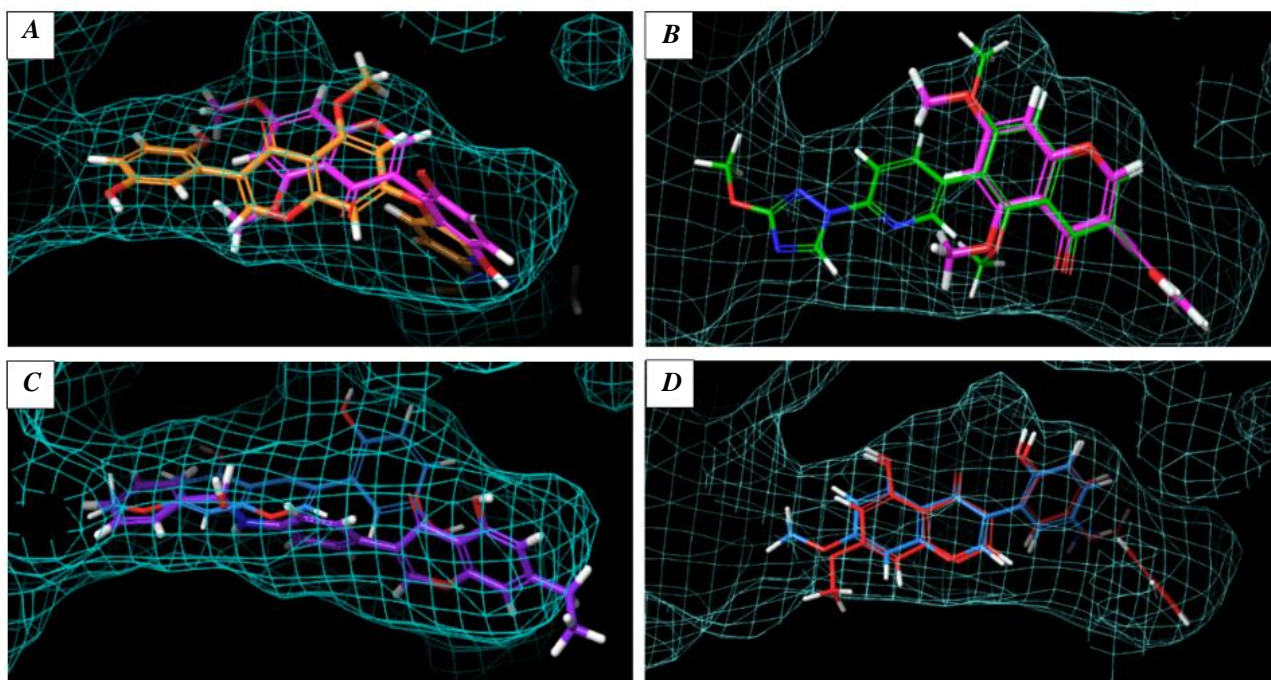


Figure 29: Docked derivatives in gp120 binding pocket. A and B of the above figure visualise Isoflavone **B** (magenta) superimposed in gp120 with **B1** (orange) and **B2** respectively (green). C and D visualise Isoflavone **C** (blue) with **C1** (purple) and **C2** (red) in gp120, respectively. **B2** and **C2** are the derivative compounds that share the same positioning of the original isoflavones with the isoflavone moieties.

4.1.7 Drug-likeness

The drug-likeness of the isoflavones and the derivatives were assessed using the free web tool, SwissADME [136]. The drug-likeness of the compounds (isoflavones and the derivatives) was described using two common rule sets (RO5 and the Ghose filter) and the BOILED-Egg model which estimated BBB permeability and GIT absorption. The results are tabulated in **Table 8**.

All the isoflavones and derivatives appear to be ideal oral drug candidates, according to the RO5, with **B1** and **B2** each having a single violation of both having 10 or more nitrogens and/or oxygens (N or O) i.e. possession of 10 or more hydrogen bond acceptors. When further filtering using the Ghose filter, **B2** is no longer a viable drug candidate as there is a single violation with the molecular weight (488.45 g/mol) being greater than the max of 480 g/mol. The single violation of the RO5 in **B1** and **B2** is a violation shared with the FDA-approved gp120 inhibitor, Fostemsavir, which also has too many hydrogen bond acceptors. Fostemsavir, like **B2**, also is deemed unfit for oral drug use by the Ghose filter, however, for different reasons: Fostemsavir has a molecular refractivity greater than 130 while **B2** has a molecular weight greater than 480.

Despite Fostemsavir's Ghose filter violation, it is still reported by SwissADME to be GIT permeable (**Table 8**).

In terms of bioavailability only one of the compounds, **D**, is expected to cross the BBB with all the compounds, except **B1** and **B2**, scoring high likelihoods of GIT permeability. These results suggest **D** is the most drug-like compound and **B2** is the least.

Table 8: Drug-likeness of the isoflavones and derivatives. The results presented are of the compounds from the drug-likeness rules sets, Lipinski and Ghose, and the BIOLED-Egg bioavailability testing, using SwissADME. The descriptions listed in red are negative results. Fostemsavir serves as an FDA-approved gp120 antagonist control.

	Rule sets		Bioavailability	
	Lipinski	Ghose	BBB permeant	GIT absorption
A	Yes	Yes	No	High
B	Yes	Yes	No	High
C	Yes	Yes	No	High
D	Yes	Yes	Yes	High
E	Yes	Yes	No	High
Fostemsavir	Yes. 1 violation NorO \geq 10	No. MR >130	No	High
B1	Yes. 1 violation NorO \geq 10	Yes	No	Low
B2	Yes. 1 violation NorO \geq 10	No. MW>480	No	Low
C1	Yes	Yes	No	High
C2	Yes	Yes	No	High

5 Discussion

The study provided evidence that these novel isoflavones are HIV antagonists with two of them capable of HIV entry inhibition at concentrations non-toxic to human cells. From these novel isoflavones, new compounds were designed that mimic known potent gp120 antagonists.

5.1 The effect of the Isoflavones on cellular viability

The viability studies were carried out with an MTT assay, with the results for both the 24 and 48 h assays illustrating an ideal set of values a researcher hopes to achieve when looking for compounds with anti-HIV activity: they do not appear toxic at low micromolar concentrations. The set methodology amongst drug discovery research appears to mostly describe the cytotoxic values of compounds in a 24 h period, however, since the luciferase reporter assay requires 48 h worth of treatment with the compounds, it was argued that the cytotoxic analysis would have to be tested at the 48-h mark. All the research referenced for this study whereby the researchers tested the anti-HIV activity of compounds using the TZM-bl luciferase reporter assay, reports the cytotoxic analysis on the TZM-bl cell line at the 24 h post-compound-exposure mark [68, 197, 199]. The results from this study show this is indeed an incomplete methodology as at the 48-h mark, **A** and **C** showed increases in cytotoxicity. This becomes significant as the CC_{50} simply reports on the concentration whereby a 50% reduction in cell viability is achieved. The degree of overlap between the concentration ranges of anti-HIV activity and the cytotoxic activity influences the accuracy of the anti-HIV test results as the reporter assay measures the decrease in luciferase activity: which can be achieved through either inhibiting HIV activity or by killing the cells.

Yanagihara [75] tested the anti-proliferative activity of several isoflavones against 12 human immortal cell lines. Since Isoflavones share a simple backbone structure and simply differ in the side chain functional groups, these findings were used to make predictions on the expected results of these compounds due to shared side chains. The predictions stated that **C** would be the most cytotoxic isoflavone due to the presence of a C5 hydroxyl group and **B** would be the least due to the presence of a C7 methoxy group [75]. Which was the outcome of the results produced with **C** being the most cytotoxic and **B** being the least.

Isoflavones are described as phytoestrogens, meaning they are plant-derived compounds often reported with oestrogen-receptor binding activity. This activity often accounts for the induction of programmed cell death [167]. Yanagihara [75] reported that the group of tested isoflavones did not induce cell death through oestrogen-dependent pathways, while Chen [167] found that

in the HeLa cell line, apoptosis was triggered through the oestrogen-receptor-mediated PI3K/Akt-NF- κ B pathway [167]. Since the TZM-bl cell lines are a HeLa lineage derivative this may also explain the possible mechanism of cell death associated with **C**. The National Cancer Institute defines a pure compound as a cytotoxic agent if it has produced a CC_{50} value of ≤ 4 $\mu\text{g/mL}$ within 48-72 h [189]. None of the isoflavones meets this criterion with isoflavone **C** producing the lowest CC_{50} value of 9.2 $\mu\text{g/mL}$. The death seen in **C** is noted as it may indicate estrogenic activity which would present a potential hazard in oral medications as it can produce side effects such as clotting [21].

Apart from estrogenic activity, the reduction of cell viability may be due to targeted anti-cancer activity. Zhang [166] reported that cell death from isoflavones appears to be cell type-specific as Biochanin A, Genistein and Daidzein displayed anti-carcinogenic effects against colon cancer cell lines with differing apoptotic effects that are thought to be attributed to differing p53 status in the cell lines [166]. It was reported that cells showed greater arrest in the G2/M checkpoint in p53^{+/+} cells than in p53^{-/-} cells [166].

Although the guidelines provided by the National Institute of Cancer indicate these isoflavones are not cytotoxic, it is worth noting that the reduction in cell viability represented in the results simply suggests the possibility the isoflavones will exhibit less cytotoxicity amongst non-carcinogenic cells. This further incentivises future drug research of these isoflavones as one of the main goals of drug discovery is to find compounds with a high toxic concentration and a low active concentration [194].

The results from the cytotoxic studies allowed for the progression of the study as the compounds could be tested at concentrations non-toxic to TZM-bl cells at 48 h.

5.2 Viral inhibition

The viral inhibition from the isoflavones was described using results from the luciferase reporter assay, the TOA studies and the molecular docking studies.

The isoflavones were investigated for their anti-HIV activity using a luciferase reporter assay, utilising TZM-bl cells. In the presence of the HIV-1 pseudo typed virus, the viral TAT protein induces the production of luciferase, which produces a quantifiable light-producing reaction. Any decrease in this reaction observed when adding the isoflavones to the luciferase assay would indicate anti-HIV activity. The results show noteworthy anti-HIV activity with IC_{50}

values ranging from 6.2 to 10.6 μM [132]. Based on the literature, flavonoids are active against a wide range of HIV target sites and inhibition at any or all of these target sites contributes to the IC_{50} values produced. To specifically determine the entry-inhibiting activity of these compounds, the possible inhibition at other target sites needs to be excluded. This is routinely done by incorporating additional enzyme-specific assays involving reverse transcriptase or integrase, which quantify the end products of the relevant enzymatic reactions. In this research, the entry-inhibiting capabilities were studied through TOA studies which take advantage of the well-documented replication cycle of HIV with a 24 h infection cycle [158]. It is known that entry inhibitors lose entry-inhibiting activity at around 2 h post-infection as all the virus has entered the cells [158]. For the TOA assay, the compounds were added 90 min post-infection. Any decrease seen in the results would prove entry-inhibiting activity from these isoflavones.

It was observed that **A** lost no significant amount of anti-HIV activity as there was a difference in inhibition of 3.2%. The other isoflavones all showed a much greater loss in viral inhibition with the range being 21.3-37.8%. **B** was the most active entry inhibitor as it lost the greatest amount of activity (37.8%). **B** and **C** are the only isoflavones to show a significant difference in luciferase activity from the TOA assays for $P < 0.05$. It is possible that with a further 30 min increase in post-treatment addition of **B** inhibition closer to 50% may be observed. Increasing the time of post-infection treatment may also see **D** and **E** fall into the area of significant difference in terms of entry-inhibiting activity. The control for the experiment was the reverse transcriptase inhibitor, Nevirapine. The control showed no decrease in activity for both the 0- and 90-min post-infection stages, indicating that the decrease observed is due to HIV replication events that occur before reverse transcription, which according to the HIV life cycle, is HIV entry and fusion [14].

The TOA studies prove that **B**, **C**, **D** and **E** have HIV-1 entry-inhibiting capabilities, with significant activity in **B** and **C**. It can also be seen that **B**, **C**, **D** and **E** act elsewhere in the HIV replication cycle, which is to be expected from flavonoids given their myriad of reported HIV activity in the literature review.

Since the research into flavonoids as HIV entry inhibitors is limited, the IC_{50} values produced from the TZM-bl luciferase reporter assay were compared to the IC_{50} generated in other research projects utilising the same cell line. This would allow for a relative comparison of the activity these novel isoflavones present against HIV. Pasetto [68] reported a range of IC_{50} values of 20.43 to 346.75 μM , with Myricetin showing the highest activity. Cole [197] reported

a low IC_{50} of 4,4 μ M for a novel flavonoid structure. These results show that the novel isoflavones in this study compete well with other flavonoid structures deemed fit for future drug research [68, 197].

After proving anti-HIV activity and then entry-inhibiting activity, the mechanism of entry-inhibition was hypothesised through molecular docking. The docking sought to evaluate if the entry inhibition was due to gp120, CCR5, or gp41 inhibition. The CXCR4 co-receptor was not studied as there is no data on the co-receptor tropism on the subtype C-Cap210 variant used in this study. It is known that the viral genetic material was isolated from a South African infection and most infections in South Africa involve R5 tropism [157], therefore it is assumed that the viral strain is R5 tropic.

5.3 Gp120 antagonism

The docking scores indicated a high likelihood that all the isoflavones could behave as gp120 antagonists with docking values ranging from -8.613 to -10.392 kcal/mol. The results indicate gp120 antagonism as they are the lowest scoring values produced from all the entry targets, and the values are lower than -8 kcal/mol (a target provided by the Schrodinger website [152]). Results produced by **Mahmood** [143] prove gp120 binding of the common flavonoid, Myricetin. They analysed the ability of Myricetin to block the binding of gp120 binding antibodies to gp120. The published results show above 90% inhibition against two of the gp120 antibodies at 10 μ g/ml [143]. It cannot be proven that these antibodies bind to the hydrophobic binding pocket used to dock the isoflavones in, as information on the antibodies cannot be found, however, it does prove there is a strong binding of Myricetin to the gp120 protein at biologically relevant locations. It was therefore assumed from the docking results and the literature cited that these isoflavones behave as gp120 antagonists to prevent HIV-1 entry into cells. This would introduce isoflavones as a potential novel class of gp120 antagonists.

As **B** and **C** are the top two most potent inhibitors, the ligand interaction results for **B** and **C** were the only ones displayed. When only looking at the TOA results demonstrating the entry inhibiting activity of the compounds, it was considered that structurally, the similar activity must be due to the shared MeOH group at carbon number 7 of both compounds. The ligand interactions suggest that these regions of the compounds do not occupy the same position in the hydrophobic cavity of gp120 and therefore it cannot contribute to their similar antagonistic activity.

A had no arguable drop-in activity from the TOA studies. This benefits the research as it provides insight into what residues are counteractive for entry inhibition, such as the 6 MeOH group. **A** and **E** both possess the 6 MeOH group, however, **E** shows a much greater decrease in entry-inhibiting activity than **A** (21.3% vs 3.2%). This suggests that the di-chlorinated B ring of **E** contributes to an increase in entry-inhibiting activity. This hypothesis on the di-chlorinated B ring increasing entry inhibiting activity is backed by the fact the **D** (di-chlorinated) produced similar results for the TOA studies. This is supported by the docking results, as the chlorine groups appear to force the 6 MeOH closer to the hydrophilic entryway the CD4 receptor would enter, possibly deterring the binding of the natural ligand (CD4) through steric hindrance. It may be possible to achieve this mechanism of action with a single chlorine group on the 4' region. This hypothesis was not tested, however, as **D** and **E** showed no significance in the reduction of entry inhibition and were therefore not used to design new derivatives. Only **B** and **C** were used to design new derivatives with **B** making the most ideal candidate for further drug development studies as it showed the least toxicity, highest anti-HIV activity and greatest entry-inhibiting capabilities.

The isoflavones were docked in an alternative gp120 region: The entrance to the hydrophobic binding pocket (1RZJ), where CD4 binds. This region is described as being more hydrophilic and the binding of antagonists here is hypothesised to prevent the binding of the Phe 43 residue of CD4 [170]. The docking score shows the compounds do not dock well in the entranceway, which supports the notion the region is hydrophilic with the isoflavones being largely hydrophobic as indicated by the docking results showing the isoflavones mostly interact with the gp120 cavity through hydrophilic interactions. Although 1RZJ is at a different location in the gp120 protein, the docking of Fostemsavir shows that even though the compound executes antagonism in the hydrophobic pocket, there are regions that interact with the CD4 entryway. Therefore, the poor docking of the isoflavones in 1RZJ and the fact they do not interact with the entryway when bound to the hydrophobic binding cavity, proves these compounds need to be designed with regions that are more hydrophilic that can interact with the entryway, to increase potency [156]. This would deter the passage of Phe 43 from the CD4 receptor into the cavity, preventing gp120 activation [156]. Previous research into designing gp120 antagonists has shown that the goal of creating a potent gp120 antagonist that can challenge the current FDA-approved gp120 antagonist, Fostemsavir, is to produce a molecule that can comfortably sit in the highly hydrophobic binding pocket and interact, to some extent, with the hydrophilic entryway [152, 153]. The gp120 antagonist would also need to bind near Trp 427 and possess

donor regions that can form hydrogen bonds with Trp 427 and Asp 368 [152, 153]. In this study, all the isoflavones, besides **E**, bound to Trp 427. Binding to Trp 427 is hypothesised to function antagonistically by displacing the gp120 β 20-21 strands into regions the CD4 receptor would normally occupy, thus preventing CD4 binding.

All the compounds that have been found to bind into the gp120 hydrophobic binding cavity differ greatly in size [155, 156]. It appears that the cavity can accommodate a wide range of inhibitors in terms of size, and this has been noted in research with the cavity being described as ‘exhibiting significant plasticity’ [155, 156]. The entry-inhibiting isoflavones **B** and **C** (with IC_{50} values of 6.2 and 10.6 μ M, respectively) all bind to Trp 427 but are not as potent as Fostemsavir in entry inhibition ($CC_{50} = 100$ nM [113]). The isoflavones may not be as potent as other gp120 antagonists due to the small size of the compounds in the large flexible gp120 cavity, preventing strong, permanent interactions with essential residues such as Trp 427. The difference in the size of the isoflavones compared to Fostemsavir is noted in the FBDD studies where the isoflavones are superimposed on the gp120 antagonist, showing Fostemsavir has a much greater span of the hydrophobic binding pocket. Research published on other gp120 antagonists also replicated this large span of Fostemsavir in the binding pocket with regions dedicated to interacting with the hydrophilic entryway and the deep hydrophobic binding pocket [152, 153]. Increasing the size of the compounds may stabilise the compounds in the binding cavity to maintain the essential amino acid interactions, thus hypothetically overcoming the plasticity of the pocket and thus the reasoning for the FBDD.

5.4 Isoflavone-mediated luciferase inhibition

The anti-HIV activity and TOA both quantified the viral inhibition due to the decrease in firefly luminescence compared to the controls [168]. It has been documented that this enzyme is open to compound antagonism and can therefore potentially give false positive results [168]. **Kenda** [168] reported the inhibitory capabilities of certain isoflavones against firefly luciferase. Inhibition could be seen at concentrations as low as 1 μ M, with Genistein producing an IC_{50} value of 36.9 μ M [168].

Although the potential luciferase-inhibiting capabilities of these isoflavones were not explored in this study, the TOA studies normalised for luciferase inhibition, meaning the isoflavones are undoubtedly entry-inhibitors. The TOA studies simply show the difference in luminescence produced after compound addition at 90 min post-infection. Any luciferase inhibition would be seen at both the 0 and 90 min points and would not reflect in the difference in luminescence.

So, the difference in activity is due to the delayed addition of the compounds i.e. entry inhibition. Therefore, the aim of the study is proven, however, the IC_{50} results generated may be less impressive due to possible luciferase inhibition. However, the potential firefly luciferase inhibiting capabilities of these compounds can be quantified, in future, by quantifying the activity of the β -galactosidase, which is also expressed in response to the HIV Tat protein in TZM-bl cells [169]. A simple assay utilising only firefly luciferase would also be effective at visualising any possible inhibition. Alternatively, one could utilise *in silico* methods by performing quantitative-structure activity relationship (QSAR) studies to hypothesise the potential for these compounds to inhibit firefly luciferase: a method performed by **Kenda** [168] which was found to produce results that corroborate with the *in vitro* results.

5.5 Fragment-based drug design

The goal of FBDD was to increase the docking scores of the isoflavones to produce compounds with increased activity and to increase the site specificity of the isoflavones for the gp120 hydrophobic cavity. Isoflavones, and flavonoids, can make excellent drug candidates but they often lack site specificity. Flavonoids are extremely bioactive compounds that have been found to bind to several human proteins, such as oestrogen receptors [22] and kinases [171]. Increasing site specificity through FBDD will hopefully reduce any toxicity of these isoflavones due to non-target interactions such as oestrogen receptor antagonism.

The isoflavones were docked simultaneously with Fostemsavir, and residues were added to the isoflavone backbone where active fragments of Fostemsavir could bind to the isoflavones backbone and still maintain their activity. The isoflavones do indeed present as novel chemicals for gp120 antagonism due to their small size, as seen when superimposed with Fostemsavir. The benefit the isoflavones are thought to have for the creation of novel gp120 antagonists is to serve as anchoring molecules in the hydrophobic pocket due to their lipophilic nature and small size. The goal of drug design using these isoflavones was to elongate the structures to have regions that sync up with the more hydrophilic entranceway of the pocket, to hopefully increase beneficial amino acid interactions and to stabilise the isoflavone backbone at the bottom of the cavity for efficient and prolonged Trp 427 binding. This would increase the tendency of the isoflavones to prevent CD4 binding.

Similarly, **Vangal** [182] formed new gp120 antagonists from the manipulation of structures through the addition of active, gp120 antagonising, side chains. The structures yielded IC_{50} values ≤ 29 nM with the docking scores generated for these new structures ranging from -5,863

to - 8,350 kcal/mol. The highest docking score generated for the isoflavone derivatives in this study was -9,779 kcal/mol. This provides possible evidence for the needed presence of isoflavones in gp120 drug design research as it does computationally support the theory they are gp120 targeting molecules due to the low docking scores generated. **Vangala** [152] found that redesigning Fostemsavir through FBDD led to a 92.08% increase in *in vitro* activity for a 4,565% decrease in docking scoring [152]. Based on this it is hypothesised that a subsequent increase in potency will be seen for the new derivatives.

The methodology of FBDD is to make active compounds more shape complementary to the active site. The isoflavones were proven to have entry-inhibiting activity, and from that activity, it was hypothesised that the isoflavones act on the gp120 hydrophobic binding pocket. The FBDD utilised these positionings of **B** and **C** in the pocket to attempt to increase the activity of the isoflavones. It is therefore argued that although all four of the derivatives showed increased docking scores only the derivatives that maintain the original isoflavone positioning is most likely to keep the original gp120 antagonising properties of the isoflavones. These derivatives are **B2** and **C2**. The low docking scores of **B1** and **C1** do however warrant future research into these compounds as gp120 antagonists.

5.6 Drug-likeness

Analysing the physicochemical properties of biologically active compounds allows for the filtering out of compounds with undesirable properties [184]. The *in silico* analyses of the chemical properties of the isoflavones and the derivatives utilised two well-documented filtering techniques; Lipinski's RO5 and the Ghose filter. All the compounds satisfied Lipinski's RO5, however, the Ghose filter highlighted one of the derivatives, **B2**, as unsuitable for drug development due to the large size. Of the four derivatives, that leaves three viable options for future gp120-antagonist drug development after applying the drug-likeness filtering techniques. It is important to note that Lipinski's RO5 and the Ghose filter are not satisfied by all drugs on the market as seen with Fostemsavir, which violates the Ghose filter, much like **B2**. Given the Ghose filter violation of Fostemsavir, **B2** will still be excluded as a potential orally active drug due to the fact the two compounds violate the Ghose filter in two importantly different ways. Fostemsavir violates the Ghose filter by having too large a molar refractivity value. In the original publication that introduced the Ghose filter, **Ghose** [198] stated that compounds that fall into the molar refractivity range of 40 to 130 have better cellular uptake, receptor binding and bioavailability. Fostemsavir can be argued to overcome this rule for a few reasons: The drug does not need to act intracellularly as it is an entry inhibitor. The drug does

not bind to the exterior of a receptor rather it travels into a deep hydrophobic binding pocket which can be attributed to the long design and hydrophilic nature of the molecule. Finally, it has been given a high GIT absorption likelihood from SwissADME due to the molecule's lipophilic nature and small size ($M_w > 480$). **B2** violates the rule due to a high molecular weight ($M_w < 480$), which means the molecule may be too large for cellular migration. As **B2** is intended to act as an entry inhibitor it does not need to cross the cellular membrane to act intracellularly, however, it does need to cross the GIT to be orally active. So, given that SwissADME expects the molecule to have a low GIT absorption, **B2** is not expected to make a good orally active drug.

B1 shows through the results generated from the BOILED-Egg method, that the compound may show poor GIT permeability, which would exclude the compound from being used as an orally active pharmaceutical. Although there are intravenous formulations of anti-HIV compounds available on the market (Enfuvirtide), these formulations tend to yield the lowest compliance. [188].

A big target for creating new derivatives was to create derivatives that could cross the BBB as there is a big need for anti-HIV compounds that can cross into the brain. Many HIV-infected individuals will display HIV-1-associated neurocognitive disorders after many years of treatment, and this is due to the suboptimal therapeutic levels orally active ARVs tend to achieve in the CNS [175]. It was believed the isoflavones and the derivatives would yield high BBB permeability results as flavonoids are believed to easily transverse the blood-brain barrier due to their lipophilicity and interactions with efflux proteins [165]. Studies looking at the *in vitro* analysis of BBB permeability have noted impressive migration across the built cell models [165]. However, none of the derivatives appears to be BBB permeable and only one of the isoflavones, **D**, can cross the BBB. The derivatives may still be able to cross the BBB as flavonoids may enter the brain via interactions with the efflux proteins in the BBB [165]. The BOILED-Egg model does not consider this as the model only looks at the lipophilicity and polarity of the compounds.

From these results, the isoflavone **C** drug derivatives are the most drug-like compounds, which is beneficial as the FBDD results conclude that **C2** will maintain the potential gp120 antagonising activity discovered in this research study, meaning it is the most likely of the derivatives to be an entry-inhibitor.

6 Conclusion

The study aimed to describe the entry-inhibiting capabilities of five novel isoflavones, of which all five were proven to have anti-HIV activity, and two were shown to have significant entry-inhibiting capabilities.

This study successfully proved that flavonoids, specifically isoflavones, have entry-inhibiting capabilities and that isoflavones are a potential novel class of gp120 antagonists. This novel class is believed to present properties needed for new anti-HIV compounds such as BBB permeability. Even though **D** was the only isoflavone to present with BBB permeability from the *in silico* analysis, isoflavones have been shown to migrate the BBB utilising efflux proteins [165]. Considering the long-term effects HIV has on the CNS that the current regime of antiretrovirals cannot treat, it is worth exploring the potential of isoflavone-based drugs to enter the CNS via efflux proteins.

Additionally, this study is the first to draw a distinction between the placement of a 5 OH group on isoflavones and a subsequent increase in cell death. Although none of the isoflavones are by definition cytotoxic (The National Cancer Institute) **C** had the greatest reduction in cellular viability in the cytotoxic studies. Future research into producing drugs from isoflavones can benefit from this discovery to alleviate any cytotoxicity noted.

Based on the above, the null hypothesis, which states that none of the isoflavones will demonstrate significant entry inhibition, was rejected.

7 Future research

There are multiple routes of possible future research studies that can naturally originate from the results of this study, some of which are described below.

The mechanism of action hypothesised in this research of the isoflavones, gp120 antagonism, can be proven using a CD4/gp120 binding ELISA to quantify the reduction of CD4-gp120 binding in the presence of the isoflavones [175]. More importantly, the derivatives produced are concluded to fully be gp120 antagonists and this can be proven with the same assay.

The results from the anti-HIV assay show that all the isoflavones, especially **A** antagonise multiple HIV replication events. The isoflavones were docked in other anti-HIV locations the luciferase reporter assay can detect, and the best scores were for allosteric inhibition on reverse transcriptase (**Appendix 5**), meaning the isoflavones may also act as NNRTIs. The docking scores ranged from – 8.915 to -10.158 kcal/mol, with **C** achieving the lowest docking score. The worst docking scores were achieved for allosteric integrase inhibition. Future research can prove and quantify any reverse transcriptase antagonism. Even though the derivatives were designed to be more site-specific for gp120 antagonism, the isoflavone backbone may still confer additional anti-HIV activity through the suspected RT antagonism, meaning the potential for the dual anti-HIV activity of the derivatives would need to be explored. The dual activity of a single compound would arguably allow for an individual to take one less anti-retroviral which could result in a decrease in the presentation of unwanted side effects [195].

If gp120 antagonism is proven for the isoflavones and the derivatives, more isoflavones and flavonoids should be tested for gp120 binding to increase the library of isoflavone side chains that assist in gp120 antagonism. The pathway set in this research to then design compounds with increased gp120 activity can then be followed.

8 Appendix

Appendix 1: Tabulation of Myricetin docking method validation

To proceed with the docking studies, the method utilised from the literature needed to be validated. The results of the method validation were obtained from using Myricetin for docking in the crystal structure of the human progesterone receptor-binding protein. The results are tabulated in **Table A1**.

Table A 1: Docking method validation. The method for docking the isoflavones into the protein binding sites were validated using the procedure from **Okesola [150]**, utilising the PDB code 1E3K.

The docking score reported in the literature	The docking score achieved
-8.889	-8.916

Appendix 2: Reed-Muench calculation for TCID₅₀

The TCID₅₀ results from **3.13.2** were used to calculate the dilution of stored viral solution needed to achieve a TCID₅₀ of 400 for the luciferase assay inhibition studies (**3.13.4**). The method was used as described by **Lei [187]**.

First, the infection rate (%) was determined as seen in **Table A2**.

Table A 2: Calculation of infection rate. The infection rate was calculated using the cumulative positive (A) units and the cumulative negative (B) units for each dilution of the virus. The blue arrows indicate the direction from which the cumulative units were calculated.

Log of virus dilution	Positive units/ total units	Cumulative positives (A)	Cumulative negatives (B)	Infection rate (A/A+B x 100)
-1	3	15	0	100 %
-2	3	12	0	100 %
-3	3	9	0	100 %
-4	3	7	0	100 %
-5	3	4	0	100 %
-6	1	1	2	33.3 %

Secondly, the dilution where 50% of the reactions are positive and 50% are negative (the 50% endpoint) was identified. Looking at the results in **3.13.2** this lay between dilutions 5 and 6. From this, the proportionate distance (PD) between the two dilutions was calculated, as follows:

$$\begin{aligned}
 PD &= \frac{\% \text{ positive above } 50\% - 50\%}{\% \text{ positive above } 50\% - \% \text{ positive below } 50\%} \\
 &= \frac{100\% - 50\%}{100\% - 33.3\%} \\
 &= 0.75
 \end{aligned}$$

Thirdly, the dilution (ID_{50}) where 50% of the test units would experience infection was calculated.

$$\begin{aligned}
 \log ID_{50} &= \log(\text{dilutin above } 50\%) + PD \times (-\log \text{dilution factor}) \\
 &= -5 + 0.75 \times -0.70 \\
 &= -5.53 \\
 ID_{50} &= 10^{-5.53}
 \end{aligned}$$

Fourthly, the $TCID_{50}/mL$ is calculated by taking the reciprocal of the ID_{50} and dividing it by the volume of media used in the $TCID_{50}$ assay, in mL.

$$\begin{aligned}
 TCID_{50} &= \frac{1}{10^{-5.53}} \div 0.025 \text{ mL} \\
 &= 1.36 \times 10^7 \text{ TCID}_{50}/mL
 \end{aligned}$$

Once the $TCID_{50}$ has been calculated, the volume of viral stock that needs to be added to the viral solution that will be used for the inhibition assay and yield a final concentration of 400 $TCID_{50}$, can be calculated using the simple $C_1V_1 = C_2V_2$ formula. C_1 will equal 1.3×10^7 $TCID_{50}/mL$ and C_2 will equal 400 $TCID_{50}/mL$.

Appendix 3: Solvent toxicity

The toxicity of the compound solvent, DMSO, was tested for cytotoxicity, utilising an MTT assay, at the max concentration of its use (1% v/v) for 48 h, in TZM-bl cells. **Figure A1** shows no decrease in cell viability from 100%. Providing evidence that the compound solvent has no additive cytotoxic effects on the effects the isoflavones have on cellular viability.

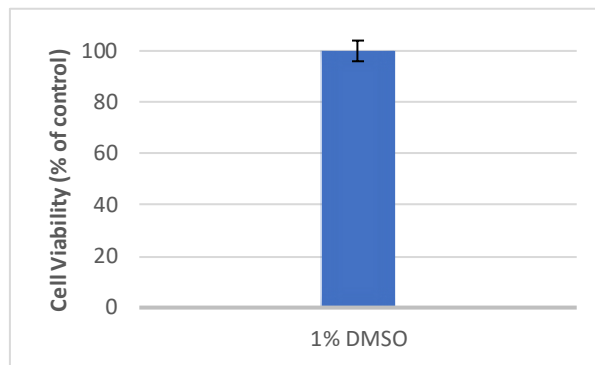


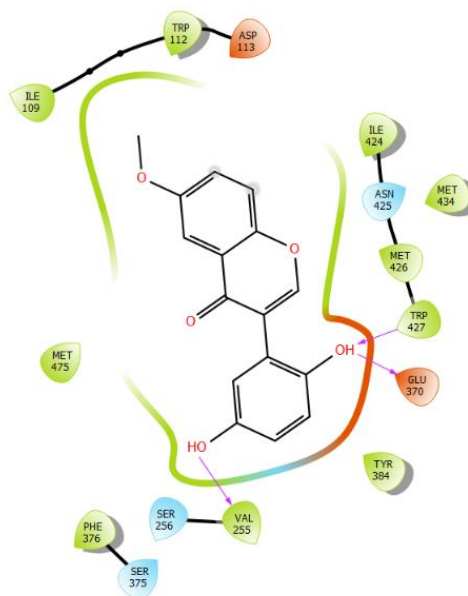
Figure A 1: Viability of cells after 48 h 1% DMSO exposure. The viability of the TZM-bl cells was evaluated in the presence of the compound solvent at the highest concentration (1% v/v) the solvent appears in the cytotoxic studies. The graph represents a single repeat with the error bars representing SD (SD= 4.0).

Appendix 4: Ligand interactions of the isoflavones without significant activity

A, D and E presented without significant reduction ($P < 0.05$) in RLU for the TOA studies.

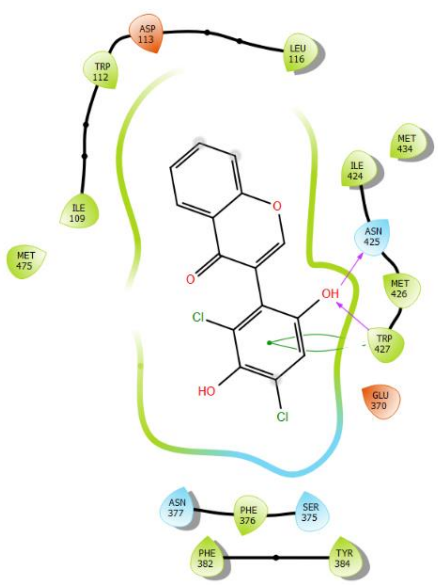
Below are the respective ligand interactions for gp120 (PDB: 5U7O), in **Figure A2**.

A

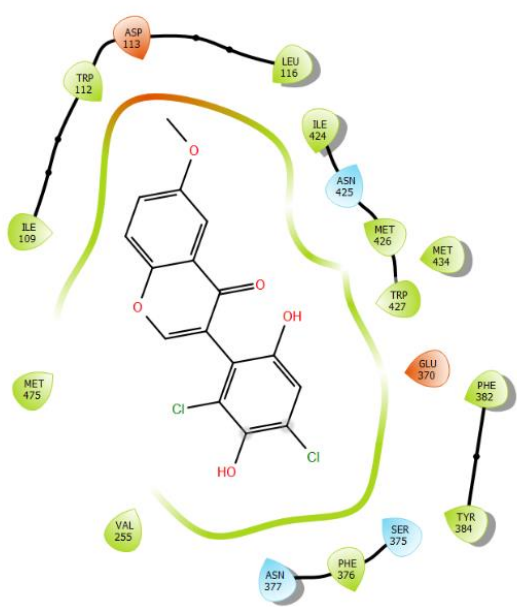


- | | | | |
|--------------------|----------------------------|--------------------|------------------|
| Charged (negative) | Polar | Distance | Pi-cation |
| Charged (positive) | Unspecified residue | H-bond | Salt bridge |
| Glycine | Water | Halogen bond | Solvent exposure |
| Hydrophobic | Hydration site | Metal coordination | |
| Metal | Hydration site (displaced) | Pi-Pi stacking | |

D



E



- | | | | |
|--------------------|----------------------------|--------------------|------------------|
| Charged (negative) | Polar | Distance | Pi-cation |
| Charged (positive) | Unspecified residue | H-bond | Salt bridge |
| Glycine | Water | Halogen bond | Solvent exposure |
| Hydrophobic | Hydration site | Metal coordination | |
| Metal | Hydration site (displaced) | Pi-Pi stacking | |

Figure A 2: Docking results of Isoflavones without significant entry inhibition. The figures of the docking results are organised with the assigned single-letter notation of the isoflavones. **E** is the only isoflavone to cause inhibition without the proposed Trp 427 H-bonding. All isoflavones were docked in the gp120 binding site (PDB: 5U7O).

Appendix 5: Docking with other anti-HIV target proteins

The luciferase reporter assay can identify activity from entry, reverse transcriptase and integrase inhibitors. Since the results from the TOA studies strongly allude to multiple forms of anti-HIV activity, the isoflavones were docked with reverse transcriptase and integrase proteins. The results are displayed in **Table A3**.

Table A 3: Docking scores in other anti-HIV target proteins. The isoflavones were docked in the orthosteric and allosteric binding sites of reverse transcriptase and integrase. The docking scores are displayed in -kcal/mol and the docking scores of the crystallised inhibitors are in [blue](#).

PDB code -inhibition type	Isoflavone	Docking score (kcal/mol)
Reverse Transcriptase		
1EP4 (NNRTI) -allosteric	A	-9.847
	B	-9.440
	C	-10.158
	D	-9.074
	E	-8.915
	S1154	-13.422
3V41 (NRTI) -orthosteric	A	-6.038
	B	-6.088
	C	-6.498
	D	-6.876
	E	-5.624
	AZTP	Did not dock
Integrase		
5KRS -allosteric	A	-3.070
	B	-4.495
	C	-4.462
	D	-1.567
	E	-1.499
	6XI	-3.284
1QS4 -orthosteric	A	-4.273
	B	-4.616
	C	-5.147
	D	-4.216
	E	-4.585
	5-CITEP	-5.176

Appendix 6: Paired student t-test

Table A 4: p-values from the paired student t-test. The means of the two groups, 0- and 90-min post compound addition, were compared to show if the time-of-addition affected the activity of the isoflavones. Significance is noted in red for $p < 0.05$.

Compound	\bar{x}_1 (0 min)	\bar{x}_2 (90 min)	$\bar{x}_1 - \bar{x}_2$	p-value
A	64.77	61.54	3.23	0.246
B	82.50	44.65	37.85	0.041
C	81.71	61.43	20.28	0.007
D	80.93	57.33	23.60	0.074
E	84.20	62.88	21.32	0.169

9 References

1. Platt, E. J., Wehrly, K., Kuhmann, S. E., Chesebro, B., & Kabat, D. (1998). Effects of CCR5 and CD4 Cell Surface Concentrations on Infections by Macrophage-tropic Isolates of Human Immunodeficiency Virus Type 1. *Journal of Virology*, 72(4), 2855–2864. <https://doi.org/10.1128/jvi.72.4.2855-2864.1998>.
2. Pourahmad, J., & Salimi, A. (2015). Isolated human peripheral blood mononuclear cell (PBMC), a cost-effective tool for predicting immunosuppressive effects of drugs and Xenobiotics. *Iranian Journal of Pharmaceutical Research*, 14(4), 679–980. <https://doi.org/10.22037/ijpr.2015.1790>.
3. Bøyum, A. (1968). Isolation of mononuclear cells and granulocytes from human blood. *Scandinavian Journal of Clinical and Laboratory Investigation*, 21, 77–89.
4. Sigma Aldrich. 2021. *A Recommended Standard Method for Isolating Mononuclear Cells*. Available at: <https://www.sigmaaldrich.com/technical-documents/protocols/biology/isolation-of-mononuclear-cells/recommended-standard-method>. [Accessed 25 February 2021].
5. Harding A, Lanese N. The 12 deadliest viruses on Earth. *Livescience.com*. 2020 [cited 25 February 2021]. Available from: <https://www.livescience.com/56598-deadliest-viruses-on-earth>.
6. Seitz, R. (2016). Human Immunodeficiency Virus (HIV). *Transfusion Medicine and Hemotherapy*, 43(3), 203–222. <https://doi.org/10.1159/000445852>.
7. Sharp, P. M., & Hahn, B. H. (2011). Origins of HIV and the AIDS pandemic. *Cold Spring Harbor Perspectives in Medicine*, 1(1). <https://doi.org/10.1101/cshperspect.a006841>.
8. AIDS info | UNAIDS [Internet]. *Aidsinfo.unaids.org*. 2020 [cited 1 March 2021]. Available from: <https://aidsinfo.unaids.org/>
9. F. Barré-Sinoussi, J. C. Chermann, F. Rey, M. T. Nugeyre, S. Chamaret, J. Gruest, C. Dautet, C. Axler-Blin, F. Vézinet-Brun, C. Rouzioux, W. R. and L. M., & Source: (1983). Isolation of T-lymphotropic retrovirus from a patient at risk for AIDS. *Science*, 240.
10. Schmid S. The discovery of HIV-1 [Internet]. *Nature.com*. 2018 [cited 1 March 2021]. Available from: [nature.com/articles/d42859-018-00003-x#:~:text=In%201983%2C%20Luc%20Montagnier's%20team,AIDS\)%2C%20such%20as%20lymphadenopathy](https://www.nature.com/articles/d42859-018-00003-x#:~:text=In%201983%2C%20Luc%20Montagnier's%20team,AIDS)%2C%20such%20as%20lymphadenopathy).
11. Starling S. The levee breaks—initial reports of AIDS [Internet]. *Nature.com*. 2018 [cited 1 March 2021]. Available from: <https://www.nature.com/articles/d42859-018-00002-y>
12. CDC. (1981). Kaposi's Sarcoma and Pneumocystis Pneumonia Among Homosexual Men — New York City and California. *Morbidity and Mortality Weekly Report*, 30(25), 305–316. <https://stacks.cdc.gov/view/cdc/1265/>
13. Gottlieb M. Pneumocystis Pneumonia --- Los Angeles [Internet]. *Cdc.gov*. 1981 [cited 2 March 2021]. Available from: https://www.cdc.gov/mmwr/preview/mmwrhtml/june_5.htm#:~:text=Pneumocystis%20Pneumonia%20%2D%2D%20Los%20Angeles&text=In%20the%20period%20October%201980,Two%20of%20the%20patients%20died.
14. Ekta Shukla, R. C. (2019). Host-HIV-1 Interactome : A Quest for Novel Therapeutic Intervention. *Cells*, 8(1155), 1–24.
15. HIV Drug Resistance. *Who.int*. 2020 [cited 2 March 2021]. Available from: <https://www.who.int/news-room/fact-sheets/detail/hiv-drug->

[resistance#:~:text=HIV%20drug%20resistance%20is%20caused,of%20drug%2Dresistant%20virus%20strains.](#)

16. Pennings, P. S. (2013). HIV drug resistance: Problems and perspectives. *Infectious Disease Reports*, 5(SUPPL.1), 21–25. <https://doi.org/10.4081/idr.2013.s1.e5>.
17. Lima, V. D., Gill, V. S., Yip, B., Hogg, R. S., Montaner, J. S. G., & Harrigan, P. R. (2008). Increased resilience to the development of drug resistance with modern boosted protease inhibitor-based highly active antiretroviral therapy. *Journal of Infectious Diseases*, 198(1), 51–58. <https://doi.org/10.1086/588675>
18. Christensen, D. E., Ganser-Pornillos, B. K., Johnson, J. S., Pornillos, O., & Sundquist, W. I. (2020). Reconstitution and visualization of HIV-1 capsid-dependent replication and integration in vitro. *Science (New York, N.Y.)*, 370(6513). <https://doi.org/10.1126/science.abc8420>.
19. Brown, J. D., Kharytonchyk, S., Chaudry, I., Iyer, A. S., Carter, H., Becker, G., Desai, Y., Glang, L., Choi, S. H., Singh, K., Lopresti, M. W., Orellana, M., Rodriguez, T., Oboh, U., Hijji, J., Ghinger, F. G., Stewart, K., Francis, D., Edwards, B. Summers, M. F. (2020). Structural basis for transcriptional start site control of HIV-1 RNA fate. *Science*, 368(6489), 413–417. <https://doi.org/10.1126/science.aaz7959>
20. Huang, D., Tran, J. T., Olson, A., Vollbrecht, T., Tenuta, M., Guryleva, M. V., Fuller, R. P., Schiffner, T., Abadejos, J. R., Couvrette, L., Blane, T. R., Saye, K., Li, W., Landais, E., Gonzalez-Martin, A., Schief, W., Murrell, B., Burton, D. R., Nemazee, D., & Voss, J. E. (2020). Vaccine elicitation of HIV broadly neutralizing antibodies from engineered B cells. *Nature Communications*, 11(1). <https://doi.org/10.1038/s41467-020-19650-8>.
21. Křížová, L., Dadáková, K., Kašparovská, J., & Kašparovský, T. (2019). Isoflavones. *Molecules*, 24(6). <https://doi.org/10.3390/molecules24061076>
22. Yu, J., Bi, X., Yu, B., & Chen, D. (2016). Isoflavones: Anti-inflammatory benefit and possible caveats. *Nutrients*, 8(6), 1–16. <https://doi.org/10.3390/nu806036>.
23. Setchell, K. D. R., & Cassidy, A. (1999). Dietary isoflavones: Biological effects and relevance to human health. *Journal of Nutrition*, 129(3 SUPPL.), 758–767. <https://doi.org/10.1093/jn/129.3.758s>
24. Estrogen | Hormone Health Network [Internet]. Hormone.org. 2018 [cited 3 March 2021]. Available from: <https://www.hormone.org/your-health-and-hormones/glands-and-hormones-a-to-z/hormones/estrogen>
25. Kuiper, G. G. J. M., Lemmen, J. G., Carlsson, B., Corton, J. C., Safe, S. H., Van Der Saag, P. T., Van Der Burg, B., & Gustafsson, J. Å. (1998). Interaction of estrogenic chemicals and phytoestrogens with estrogen receptor β . *Endocrinology*, 139(10), 4252–4263. <https://doi.org/10.1210/endo.139.10.6216>
26. Bolander F. Molecular endocrinology. 3rd ed. Amsterdam: Elsevier Academic Press; 2004.
27. Barakat, R., Oakley, O., Kim, H., Jin, J., & Ko, C. M. J. (2016). Extra-gonadal sites of estrogen biosynthesis and function. *BMB Reports*, 49(9), 488–496. <https://doi.org/10.5483/BMBRep.2016.49.9.141>
28. Domingo E. Virus as populations. 2nd ed. Spain: Academic Press; 2019.
29. Moulds, P. (2002). Dietary flavonoids: bioavailability, metabolism effects and safety. *Preventing School Failure*, 51(3), 49–51. <https://search.proquest.com/docview/220297257?accountid=12834>
30. Moulds, P. (2002). Dietary flavonoids: bioavailability, metabolism effects and safety. *Preventing School Failure*, 51(3), 49–51. <https://search.proquest.com/docview/220297257?accountid=12834>

31. Xiao, J. X., Huang, G. Q., Geng, X., & Qiu, H. W. (2011). Soy-derived Isoflavones Inhibit HeLa Cell Growth by Inducing Apoptosis. *Plant Foods for Human Nutrition*, 66(2), 122–128. <https://doi.org/10.1007/s11130-011-0224-6>
32. Kuete V. Medicinal Spices and Vegetables from Africa. 1st ed. Cameroon: Academic press; 2017.
33. Abbasi, E., Aval, S. F., Akbarzadeh, A., Milani, M., Nasrabadi, H. T., Joo, S. W., Hanifehpour, Y., Nejati-Koshki, K., & Pashaei-Asl, R. (2014). Dendrimers: Synthesis, applications, and properties. *Nanoscale Research Letters*, 9(1), 1–10. <https://doi.org/10.1186/1556-276X-9-247>
34. Kukowska-latallo, A. J. F., Bielinska, A. U., Johnson, J., Tomalia, D. A., Baker, J. R., Tomaliat, D. A., & Baker, J. R. (2020). Efficient Transfer of Genetic Material into Mammalian Cells Using Starburst Polyamidoamine Dendrimers Source : Proceedings of the National Academy of Sciences of the United States of America, Published by National Academy of Sciences Stable. *Proceedings of the National Academy of Sciences of the United States of America*.
35. Baker J, Bielinska A, Kukowska-Latallo J. Dendrimer-Mediated Cell Transfection In Vitro. Gene Delivery to Mammalian Cells. 2004;;67-82.
36. Platt E, Bilaska M, Kozak S, Kabat D, Montefiori D. Evidence that Ecotropic Murine Leukemia Virus Contamination in TZM-bl Cells Does Not Affect the Outcome of Neutralizing Antibody Assays with Human Immunodeficiency Virus Type 1. Journal of Virology. 2009;83(16):8289-8292.
37. Lembert N. Firefly luciferase can use L-luciferin to produce light. Biochemical Journal. 1996;317(1):273-277.
38. Terminology: TCID50(Median Tissue Culture Infectious Dose) | Sinanen Zeomic Co., Ltd. [Internet]. Zeomic.co.jp. 2021 [cited 10 March 2021]. Available from: <https://www.zeomic.co.jp/en/glossary/virus/71>
39. Virus quantification / TCID50 assay [Internet]. 2021 [cited 10 March 2021]. Available from: <https://www.coriolis-pharma.com/analytical-services/biosafety-level-1-2/virus-quantification-tcid50-assay>
40. Cann A. Principles of molecular virology. 2nd ed. Amsterdam: Elsevier science and technology; 2005.
41. Ramakrishnan M. Determination of 50% endpoint titer using a simple formula. World Journal of Virology. 2016;5(2):85.
42. Sharp, P. M., & Hahn, B. H. (2011). Origins of HIV and the AIDS pandemic. *Cold Spring Harbor Perspectives in Medicine*, 1(1). <https://doi.org/10.1101/cshperspect.a006841>
43. Cunningham, A. L., Donaghy, H., Harman, A. N., Kim, M., & Turville, S. G. (2021). Manipulation of dendritic cell function by viruses. *Current Opinion in Microbiology*, 13(4), 524–529. <https://doi.org/10.1016/j.mib.2010.06.002>
44. Bhatti, A. B., Usman, M., & Kandi, V. (2016). Current Scenario of HIV/AIDS, Treatment Options, and Major Challenges with Compliance to Antiretroviral Therapy. *Cureus*, 8(3), 1–12. <https://doi.org/10.7759/cureus.515>
45. Szabo, R., & Short, R. V. (2000). *Education and debate How does male circumcision protect against HIV infection?* 320(June).
46. Dev, J., Park, D., Fu, Q., Chen, J., Ha, H. J., Ghantous, F., Herrmann, T., Chang, W., Liu, Z., Frey, G., Seaman, M. S., & Chen, B. (2016). Structural basis for membrane anchoring of HIV-1 envelope spike. *Science*, 353(6295), 22341–22345.
47. L. C. James, The HIV-1 capsid: More than just a delivery package. Adv. Exp. Med. Biol. 1215,69–83 (2019).

48. Blair, W. S., Pickford, C., Irving, S. L., Brown, D. G., Anderson, M., Bazin, R., Cao, J., Ciaramella, G., Isaacson, J., Jackson, L., Hunt, R., Kjerrstrom, A., Nieman, J. A., Patick, A. K., Perros, M., Scott, A. D., Whitby, K., Wu, H., & Butler, S. L. (2010). HIV capsid is a tractable target for small-molecule therapeutic intervention. *PLoS Pathogens*, *6*(12). <https://doi.org/10.1371/journal.ppat.1001220>
49. Lamorte, L., Titolo, S., Lemke, C. T., Goudreau, N., Mercier, J. F., Wardrop, E., Shah, V. B., Von Schwedler, U. K., Langelier, C., Banik, S. S. R., Aiken, C., Sundquist, W. I., & Mason, S. W. (2013). Discovery of novel small-molecule HIV-1 replication inhibitors that stabilize capsid complexes. *Antimicrobial Agents and Chemotherapy*, *57*(10), 4622–4631. <https://doi.org/10.1128/AAC.00985-13>.
50. Wynn, J. E., & Santos, L. W. (2016). HIV-1 Drug Discovery: Targeting Folded RNA Structures With Branched Peptides. *Org Biomol Chem*, *176*(1), 100–106. <https://doi.org/10.1039/c5ob00589b>.HIV-1
51. Hamy, F., Felder, E. R., Heizmann, G., Lazdins, J., Varani, G., Karn, J., Imkaitt, T. K. L. (2021). *An Inhibitor of the Tat / TAR RNA Interaction that Effectively Suppresses HIV-1 Replication*.
52. Naeim F. Hematopathology. Academic Press; 2008.
53. Sekaly, R., & Rooke, R. (1998). CD4. *Encyclopedia of Immunology*, *2*, 468. <http://journal.unair.ac.id/download-fullpapers-ln522cc87c61full.pdf>
54. Li, Y., Yin, Y., & Mariuzza, R. A. (2013). Structural and biophysical insights into the role of CD4 and CD8 in T cell activation. *Frontiers in Immunology*, *4*(JUL), 1–11. <https://doi.org/10.3389/fimmu.2013.00206>
55. Sattentau, Q. J., & Moore, J. P. (1993). The Role of CD4 in HIV Binding and Entry. *Philosophical Transactions: Biological Sciences*, *342*(1299), 59–66.
56. Sweet, R. W., Truneh, A., & Hendrickson, W. A. (1991). CD4: Its structure, role in immune function and AIDS pathogenesis, and potential as a pharmacological target. *Current Opinion in Biotechnology*, *2*(4), 622–633. [https://doi.org/10.1016/0958-1669\(91\)90089-N](https://doi.org/10.1016/0958-1669(91)90089-N)
57. Maestro | Schrödinger [Internet]. Schrodinger.com. 2021 [cited 22 March 2021]. Available from: <https://www.schrodinger.com/products/maestro>
58. Auld, D., Southall, N., & Jadhav, A. (2008). Characterization of chemical libraries for luciferase inhibition activity. *Assay and Drug Development Technologies*, *6*(3), 2372–2386. <https://doi.org/10.1089/adt.2008.9991>.
59. Gehm, B. D., McAndrews, J. M., Chien, P. Y., & Jameson, J. L. (1997). Resveratrol, a polyphenolic compound found in grapes and wine, is an agonist for the estrogen receptor. *Proceedings of the National Academy of Sciences of the United States of America*, *94*(25), 14138–14143. <https://doi.org/10.1073/pnas.94.25.14138>
60. Mousseau, G., Kessing, C. F., Fromentin, R., Trautmann, L., Chomont, N., & Valente, S. T. (2015). The tat inhibitor didehydro-cortistatin a prevents HIV-1 reactivation from latency. *MBio*, *6*(4), 1–14. <https://doi.org/10.1128/mBio.00465-15>.
61. Prokofjeva, M. M., Spirin, P. V., Yanvarev, D. V., Ivanov, A. V., Novikov, M. S., Stepanov, O. A., Gottikh, M. B., Kochetkov, S. N., Fehse, B., Stocking, C., & Prassolov, V. S. (2011). Screening of Potential HIV-1 Inhibitors/ Replication Blockers Using Secure Lentiviral in Vitro System. *Acta Naturae*, *3*(4), 55–65. <https://doi.org/10.32607/20758251-2011-3-4-55-65>
62. Mace, T. A., Ware, M. B., King, S. A., Loftus, S., Farren, M. R., McMichael, E., Scoville, S., Geraghty, C., Young, G., Carson, W. E., Clinton, S. K., & Lesinski, G. B. (2019). Soy isoflavones and their metabolites

- modulate cytokine-induced natural killer cell function. *Scientific Reports*, 9(1), 1–12. <https://doi.org/10.1038/s41598-019-41687-z>
63. Mediouni, S., Jablonski, J. A., Tsuda, S., Richard, A., Kessing, C., Andrade, M. V., Biswas, A., Even, Y., Tellinghuisen, T., Choe, H., Cameron, M., Stevenson, M., & Valente, S. T. (2018). Potent suppression of HIV-1 cell attachment by Kudzu root extract. *Retrovirology*, 15(1), 1–18. <https://doi.org/10.1186/s12977-018-0446-x>
 64. Keung W, Vallee B. Kudzu root: An ancient Chinese source of modern antidipsotropic agents. *Phytochemistry*. 1998;47(4):499-506.
 65. Qian, K. Morris-Natschke, S. L. Lee, K. H. (2009). HIV entry inhibitors and their potential in HIV therapy. *Medicinal Research Reviews*, 29(2), 369–393. <https://doi.org/10.1002/med.20138>
 66. Huang, L., & Chen, C. H. (2002). Molecular targets of anti-HIV-1 triterpenes. *Current Drug Targets - Infectious Disorders*, 2(1), 33–36. <https://doi.org/10.2174/1568005024605936>
 67. Ito, M., Sato, A., Hirabayashi, K., Tanabe, F., Shigeta, S., Baba, M., De Clercq, E., Nakashima, H., & Yamamoto, N. (1988). Mechanism of inhibitory effect of glycyrrhizin on replication of human immunodeficiency virus (HIV). *Antiviral Research*, 10(6), 289–298. [https://doi.org/10.1016/0166-3542\(88\)90047-2](https://doi.org/10.1016/0166-3542(88)90047-2)
 68. Pasetto, S. Pardi, V. Murata, R. M. (2014). Anti-HIV-1 activity of flavonoid myricetin on HIV-1 infection in a dual-chamber in vitro model. *PLoS ONE*, 9(12), 1–18. <https://doi.org/10.1371/journal.pone.0115323>
 69. Panche, A. N., Diwan, A. D., & Chandra, S. R. (2016). Flavonoids: An overview. *Journal of Nutritional Science*, 5. <https://doi.org/10.1017/jns.2016.41>
 70. Doitsh, G., & Greene, W. C. (2016). Dissecting How CD4 T Cells Are Lost during HIV Infection. *Cell Host and Microbe*, 19(3), 280–291. <https://doi.org/10.1016/j.chom.2016.02.012>
 71. HIV/AIDS-Related Cancer - Introduction [Internet]. Cancer.Net. 2021 [cited 31 March 2021]. Available from: <https://www.cancer.net/cancer-types/hiv-aids-related-cancer/introduction>
 72. Lewden, C., Salmon, D., Morlat, P., Bévilacqua, S., Jouglu, E., Bonnet, F., Héripert, L., Costagliola, D., May, T., & Chêne, G. (2005). Causes of death among human immunodeficiency virus (HIV)-infected adults in the era of potent antiretroviral therapy: Emerging role of hepatitis and cancers, persistent role of AIDS. *International Journal of Epidemiology*, 34(1), 121–130. <https://doi.org/10.1093/ije/dyh307>
 73. Kati, W. M., Johnson, K. A., Jerva, L. F., & Anderson, K. S. (1992). Mechanism and fidelity of HIV reverse transcriptase. *Journal of Biological Chemistry*, 267(36), 25988–25997. [https://doi.org/10.1016/s0021-9258\(18\)35706-5](https://doi.org/10.1016/s0021-9258(18)35706-5)
 74. Craigie, R. (2001). HIV Integrase, a Brief Overview from Chemistry to Therapeutics. *Journal of Biological Chemistry*, 276(26), 23213–23216. <https://doi.org/10.1074/jbc.R100027200>
 75. Yanagihara, K., Ito, A., Toge, T., & Numoto, M. (1993). Antiproliferative Effects of Isoflavones on Human Cancer Cell Lines Established from the Gastrointestinal Tract. *Cancer Research*, 53(23), 5815–5821.
 76. Varela-ramirez, A., Paso, E., & Aguilera, R. J. (2012). Cytotoxic effects of two organotin compounds and their mode of inflicting cell death on four mammalian cancer cells. *Cell Biol. Toxicology*, 27(3), 159–168. <https://doi.org/10.1007/s10565-010-9178-y>
 77. Callahan, L. N., Phelan, M., Mallinson, M., & Norcross, M. A. (1991). Dextran sulfate blocks antibody binding to the principal neutralizing domain of human immunodeficiency virus type 1 without interfering

- with gp120-CD4 interactions. *Journal of Virology*, 65(3), 1543–1550. <https://doi.org/10.1128/jvi.65.3.1543-1550.1991>
78. Kuritzkes, D. R., Jacobson, J., Powderly, W. G., Godofsky, E., DeJesus, E., Haas, F., Reimann, K. A., Larson, J. L., Yarbough, P. O., Curt, V., & Shanahan, W. R. (2004). Antiretroviral Activity of the Anti-CD4 Monoclonal Antibody TNX-355 in Patients Infected with HIV Type 1. *Journal of Infectious Diseases*, 189(2), 286–291. <https://doi.org/10.1086/380802>
 79. Kwong, P. D., Wyatt, R., Robinson, J., Sweet, R. W., Sodroski, J., & Hendrickson, W. A. (1998). Structure of an HIV gp 120 envelope glycoprotein in complex with the CD4 receptor and a neutralizing human antibody. *Nature*, 393(6686), 648–659. <https://doi.org/10.1038/31405>
 80. Chan, D. C., Fass, D., Berger, J. M., & Kim, P. S. (1997). Core Structure of gp41 from the HIV Envelope Glycoprotein. *Cell*, 89, 263–273.
 81. Koff WC. HIV vaccine development: Challenges and opportunities towards solving the HIV vaccine-neutralizing antibody problem. *Vaccine*. 2012;30(29):4310–5.
 82. Wiener, P., Wiener, D., Altshuler, G. B., Tuchin, V. V., Oblong, J. E., Millikin, C., Vejjabhinanta, V., Singh, A., Nouri, K. (2003). A Small Molecule HIV-1 Inhibitor That Targets the HIV-1 Envelope and Inhibits CD4 Receptor Binding. *PNAS*, 100(19), 11013–11018.
 83. Buzon V, Natrajan G, Schibli D, Campelo F, Kozlov MM. Crystal Structure of HIV-1 gp41 Including Both Fusion Peptide and Membrane Proximal External Regions. *PLoS Pathog*. 2010;6(5):1–7.
 84. Chan DC, Kim PS. HIV Entry and Its Inhibition. *Cell*. 1998; 93:681–4.
 85. Popovich, M., & van Loo, D. (2004). Enfuvirtide : A New Treatment Option for HIV. *Journal of Infectious Disease Pharmacotherapy*, 6(4), 1–16.
 86. Tan Q, Zhu Y, Li J, Chen Z. Structure of the CCR5 Chemokine Receptor-HIV Entry Inhibitor Maraviroc Complex. *Science*. 2013;341:1387–90.
 87. Labrecque J, Metz M, Lau G, Darkes MC, Wong RSY, Bogucki D, et al. HIV-1 entry inhibition by small-molecule CCR5 antagonists: A combined molecular modelling and mutant study using a high-throughput assay. *Virology*. 2011;413(2):231–43.
 88. Floden, A, Combs, C. (2009). The biology of CCR5 and CXCR4. *Curr Opin HIV AIDS*, 4(2), 1–7. <https://doi.org/10.1097/COH.0b013e328324bbec>.
 89. Pancera, M., Lai, Y., Bylund, T., Druz, A., Narpala, S., Dell, O., Schön, A., Bailer, R. T., Chuang, G., Geng, H., Louder, M. K., Rawi, R., Soumana, D. I., Finzi, A., Herschhorn, A., Madani, N., Freire, E., Langley, D. R., Mascola, J. R., ... Kwong, P. D. (2017). Crystal structures of trimeric HIV Env with entry inhibitors BMS-378806 and BMS-626529. *Nat Chem Biol*, 13(10), 1115–1122.
 90. Soderberg T. 7.5: Acid-base Properties of Phenols - Chemistry LibreTexts [Internet]. Chem.libretexts.org. 2021 [cited 29 March 2021]. Available from: [https://chem.libretexts.org/Bookshelves/Organic_Chemistry/Book%3A_Organic_Chemistry_with_a_Biological_Emphasis_v2.0_\(Soderberg\)/07%3A_Acid-base_Reactions/7.05%3A_Acid-base_Properties_of_Phenols](https://chem.libretexts.org/Bookshelves/Organic_Chemistry/Book%3A_Organic_Chemistry_with_a_Biological_Emphasis_v2.0_(Soderberg)/07%3A_Acid-base_Reactions/7.05%3A_Acid-base_Properties_of_Phenols)
 91. Al-Allaf F, Tolmachov O, Zambetti L, Tchetchelnitski V, Mehmet H. Remarkable stability of an instability-prone lentiviral vector plasmid in Escherichia coli Stbl3. *3 Biotech*. 2012;3(1):61–70.

92. GeneJET Plasmid Miniprep Kit [Internet]. ThermoFischer Scientific. 2021 [cited 4 April 2021]. Available from: <https://www.thermofisher.com/order/catalog/product/K0502#/K0502>
93. Constantinescu, T., Lungu, C. N., & Lung, I. (2019). Lipophilicity as a central component of drug-like properties of chalcones and flavonoid derivatives. *Molecules*, 24(8), 1–11. <https://doi.org/10.3390/molecules24081505>.
94. Chan DC, Kim PS. HIV Entry and Its Inhibition. *Cell*. 1998; 93:681–4.
95. Yee S. In Vitro Permeability Across Caco-2 Cells (Colonic) Can Predict In Vivo (Small Intestinal) Absorption in Man—Fact or Myth. *Pharm Res*. 1997;14(6):763–6.
96. Lea T. The impact of food bioactives on health. Springer Cham; 2015. 103–111.
97. Hong Yao, Junkai Liu, Shengtao Xu, Zheyang Zhu & Jinyi Xu (2017) The structural modification of natural products for novel drug discovery, *Expert Opinion on Drug Discovery*, 12:2, 121-140.
98. Day, A.J.; DuPont, M.S.; Ridley, S.; Rhodes, M.; Rhodes, M.J.; Morgan, M.R.; Williamson, G. Deglycosylation of flavonoid and isoflavonoid glycosides by human small intestine and liver β -glucosidase activity. *FEBS Lett*. 1998, 436, 71–75.
99. Jandacek RJ, Tso P. Factors affecting the storage and excretion of toxic lipophilic xenobiotics. *Lipids*. 2001 Dec;36(12):1289-305
100. Dextran sulfate sodium salt from *Leuconostoc* spp. Sigma-Aldrich. 2021 [cited 15 May 2021]. Available from: <https://www.sigmaaldrich.com/catalog/product/sigma/31404?lang=en®ion=ZA#productDetailSafetyRelatedDocs>
101. HEPES [Internet]. Sigma-Aldrich. 2021 [cited 15 May 2021]. Available from: https://www.sigmaaldrich.com/catalog/product/sigma/h4034?lang=en®ion=ZA&cm_sp=Insite--caContent_prodMerch_gruCrossEntropy--prodMerch10-2
102. DMEM, powder, high glucose [Internet]. ThermoFischer Scientific. 2021 [cited 15 May 2021]. Available from: <https://www.thermofisher.com/order/catalog/product/12100061#/12100061>
103. ThermoFischer [Internet]. Sodium Pyruvate. 2004 [cited 15 May 2021]. Available from: <https://www.thermofisher.com/order/catalog/product/11360070#/11360070>
104. Antibiotic Antimycotic Solution (100 \times), Stabilized [Internet]. Sigma-Aldrich. 2021 [cited 15 May 2021]. Available from: <https://www.sigmaaldrich.com/catalog/product/SIGMA/A5955?lang=en®ion=ZA>
105. Bright-Glo™ Luciferase Assay System [Internet]. Worldwide.promega.com. 2021 [cited 15 May 2021]. Available from: <https://worldwide.promega.com/Products/luciferase-assays/Reporter-Assays/Bright-Glo-Luciferase-Assay-System/?catNum=E2620>
106. Cis-Diammineplatinum(II) dichloride [Internet]. Sigma-Aldrich. 2021 [cited 15 May 2021]. Available from: https://www.sigmaaldrich.com/catalog/product/sigma/p4394?lang=en®ion=ZA&cm_sp=Insite--caContent_prodMerch_gruCrossEntropy--prodMerch10-4
107. MTT Formazan [Internet]. Sigma-Aldrich. 2021 [cited 15 May 2021]. Available from: <https://www.sigmaaldrich.com/catalog/product/sigma/m2003?lang=en®ion=ZA>
108. Polyfect transfection reagent [Internet]. Labettor. 2021 [cited 15 May 2021]. Available from: <https://labettor.com/forward?type=product&id=515>

109. Schutte C. Analysis of HIV-related mortality data in a tertiary South African neurology unit, 2006- 2012 [Internet]. Sajahivmed.org.za. 2021 [cited 13 May 2021]. Available from: [https://sajahivmed.org.za/index.php/hivmed/article/view/64/95#:~:text=In%20the%20HIV%2Dpositive%20group%2C%20meningitis%20was%20the%20most%20common,cause%20of%20death%20\(14%25\)](https://sajahivmed.org.za/index.php/hivmed/article/view/64/95#:~:text=In%20the%20HIV%2Dpositive%20group%2C%20meningitis%20was%20the%20most%20common,cause%20of%20death%20(14%25).).
110. Gulnik, S., & Erickson, J. W. (2000). HIV Protease: Enzyme Function and Drug Resistance *. *Vitamins and Hormones*, 58, 213–214.
111. Points to Consider in Drug Development of Biologics and Small Molecules [Internet]. Nuventra.com. 2021 [cited 10 May 2021]. Available from: <https://www.nuventra.com/resources/blog/small-molecules-versus-biologics/>
112. Hodgson, J. (2001). ADMET - Turning chemicals into drugs. *Nature Biotechnology*, 19(8), 722–726. <https://doi.org/10.1038/90761>
113. Meanwell, N. A., Krystal, M. R., Nowicka-sans, B., Langley, D. R., Conlon, D. A., Eastgate, M. D., Grasela, D. M., Timmins, P., Wang, T., & Kadow, J. F. (2018). Inhibitors of HIV - 1 Attachment: The Discovery and Development of Temsavir and its Prodrug Fostemsavir. *Journal of Medical Chemistry*, 61, 62–80. <https://doi.org/10.1021/acs.jmedchem.7b01337>.
114. aidsmap.com. 2021. *Fostemsavir (Rukobia)*. [online] Available at: <<https://www.aidsmap.com/about-hiv/arv-background-information/fostemsavir-rukobia>> [Accessed 4 November 2021].
115. Rukobiahcp. 2021. *Rukobia: Risks and side effects*. [online] Available at: <<https://www.rukobiahcp.com/risks-and-side-effects/>> [Accessed 4 November 2021].
116. Takechi, C. Uno, Y. T. (1994). Inhibitory activity of Flavonoids and Tannins against HIV-1 Protease. *Chemical Pharmaceutical Bulletin*, 17(11), 1460–1462. https://www.jstage.jst.go.jp/article/bpb1993/17/11/17_11_1460/pdf/-char/ja.
117. Yu, Y. B., Nakamura, N., Miyashiro, H., Hattori, M., & Jong, C. P. (2007). Effects of Triterpenoids and Flavonoids isolated from *Alnus firma* on HIV-1 viral enzymes. *Korean Journal of Pharmacognosy*, 38(1), 76–83.
118. Pasetto, S., Pardi, V., & Murata, R. M. (2014). Anti-HIV-1 activity of flavonoid myricetin on HIV-1 infection in a dual-chamber in vitro model. *PLoS ONE*, 9(12), 1–18. <https://doi.org/10.1371/journal.pone.0115323>
119. Varela-ramirez, A., Paso, E., & Aguilera, R. J. (2012). Cytotoxic effects of two organotin compounds and their mode of inflicting cell death on four mammalian cancer cells. *Cell Biol. Toxicology*, 27(3), 159–168. <https://doi.org/10.1007/s10565-010-9178-y>.
120. Yang, P. M., Hsieh, Y. Y., Du, J. L., Yen, S. C., & Hung, C. F. (2020). Sequential interferon β -cisplatin treatment enhances the surface exposure of calreticulin in cancer cells via an interferon regulatory factor 1-dependent manner. *Biomolecules*, 10(4), 1–17. <https://doi.org/10.3390/biom10040643>.
121. Hirudkar, J. R., Parmar, K. M., Prasad, R. S., Sinha, S. K., Jogi, M. S., Itankar, P. R., & Prasad, S. K. (2020). Quercetin a major biomarker of *Psidium guajava* L. inhibits SepA protease activity of *Shigella flexneri* in treatment of infectious diarrhoea. *Microbial Pathogenesis*, 138(July 2019), 103807. <https://doi.org/10.1016/j.micpath.2019.103807>.
122. Abian, O., Ortega-alarcon, D., Jimenez-alesanco, A., & Ceballos-laita, L. (2020). Structural stability of SARS-CoV-2 3CLpro and identification of quercetin as an inhibitor by experimental screening. *International Journal of Biological Macromolecules*, 164, 1693–1703.

123. Rai, M. A., & Pannek, S. (2016). Emerging reverse transcriptase inhibitors for HIV-1 infection. *Physiology & Behavior*, 176(1), 100–106. <https://doi.org/10.1080/14728214.2018.1474202>.
124. Reed LJ, Muench H (1938) A simple method of estimating fifty percent endpoints. *Am J Hyg* 27:493–497
125. Johnson, V. A., Byington, R. E. (1990) Infectivity assay (virus yield assay), in (Aldovani, A., and Walker, B. D., eds.), *Techniques in HIV Research*, pp71–76. Stockton Press, New York, N.Y.
126. Forman, S., & Ka, J. (1999). The Effect of Different Solvents on the ATP / ADP Content and Growth Properties of HeLa Cells. *J Biochem Molecular Toxicology*, 13(1), 11–16.
127. Campbell TB, Young RK, Eron JJ, D'Aquila RT, Tarpley WG, Kuritzkes DR. Inhibition of human immunodeficiency virus type 1 replication in vitro by the bisheteroarylpiperazine atevirdine (U-87201E) in combination with zidovudine or didanosine. *J Infect Dis*. 1993 Aug;168(2):318-26.
128. Ochsenbauer-Jambor C, Jones J, Heil M, Zammit KP, Kutsch O (2006) T-cell line for HIV drug screening using EGFP as a quantitative marker of HIV-1 replication. *Biotechniques* 40: 91–100.
129. Li, B. Q., Fu, T., Dongyan, Y., Mikovits, J. A., Ruscetti, F. W., & Wang, J. M. (2000). Flavonoid baicalin inhibits HIV-1 infection at the level of viral entry. *Biochemical and Biophysical Research Communications*, 276(2), 534–538.
130. Nihon Seikagakkai., K., & Nakane, H. (1990). Mechanisms Polymerases of Inhibition by Several of Various Flavonoids Cellular DNA and RNA Katsuhiko. *The Journal of Biochemistry*, 108(4), 609–613.
131. Fesen, M. R., Pommier, Y., Leteurtre, F., Hiroguchi, S., Yung, J., & Kohn, K. W. (1994). Inhibition of HIV-1 integrase by flavones, caffeic acid phenethyl ester (CAPE) and related compounds. *Biochemical Pharmacology*, 48(3), 595–608.
132. Daelemans, D., Pauwels, R., De Clercq, E., & Pannecouque, C. (2011). A time-of-drug addition approach to target identification of antiviral compounds. *Nature Protocols*, 6(6), 925–933. <https://doi.org/10.1038/nprot.2011.330>.
133. Gombos, R. B., Kolodkin-Gal, D., Eslamizar, L., Owuor, J. O., Mazzola, E., Gonzalez, A. M., Koriouth-Schmitz, B., Gelman, R. S., Montefiori, D. C., Haynes, B. F., & Schmitz, J. E. (2015). Inhibitory Effect of Individual or Combinations of Broadly Neutralizing Antibodies and Antiviral Reagents against Cell-Free and Cell-to-Cell HIV-1 Transmission. *Journal of Virology*, 89(15), 7813–7828. <https://doi.org/10.1128/jvi.00783-15>.
134. Martinez, J. P., Hinkelmann, B., Fleta-Soriano, E., Steinmetz, H., Jansen, R., Diez, J., Frank, R., Sasse, F., & Meyerhans, A. (2013). Identification of myxobacteria-derived HIV inhibitors by a high-throughput two-step infectivity assay. *Microbial Cell Factories*, 12(1)
135. Pancera, M., Lai, Y., Bylund, T., Druz, A., Narpala, S., Dell, O., Schön, A., Bailer, (2017). Crystal structures of trimeric HIV Env with entry inhibitors BMS-378806 and BMS-626529. *Nat Chem Biol*, 13(10), 1115–1122. <https://doi.org/10.1038/nchembio.2460>.
136. Daina, A., Michielin, O., & Zoete, V. (2017). SwissADME: A free web tool to evaluate pharmacokinetics, drug-likeness and medicinal chemistry friendliness of small molecules. *Scientific Reports*, 1–13.
137. Joseph A. DiMasias, Henry G. Grabowski, Ronald W. Hansenc (2016). Innovation in the pharmaceutical industry: New estimates of R&D costs. *Journal of Health Economics*. 47, 20-33.

138. Thomas J Moore, James Heyward, Gerard Anderson, Caleb Alexander (2020). Variation in the estimated costs of pivotal clinical benefit trials supporting the US approval of new therapeutic agents, 2015–2017: a cross-sectional study. *BMJ Open*. 10.
139. Asher Mullard (2016). Parsing Clinical Success Rates. *Nature Reviews*. 15.
140. Linda Martin, Melissa Hutchens & Conrad Hawkins (2017). Clinical trial cycle times continue to increase despite industry efforts. *Nature Reviews and Drug Discovery*. 16.
141. Hay, M., Thomas, D. Clinical development success rates for investigational drugs. *Nature Biotechnol.* 32, 40-41.
142. Gu, W., Zhang, X., & Yuan, J. (2014). Review Article Anti-HIV Drug Development Through Computational Methods. *The AAPS Journal*, 16(4), 674–680. <https://doi.org/10.1208/s12248-014-9604-9>
143. Mahmood, N., Pizza, C., & Aquino, R. (1993). Inhibition of HIV infection by flavonoids. *Antiviral Research*, 22, 189–199.
144. Shattock, R. J., & Rosenberg, Z. (2012). Microbicides: Topical prevention against HIV. *Cold Spring Harbor Perspectives in Medicine*, 2(2), 1–17. <https://doi.org/10.1101/cshperspect.a007385>.
145. Niaid.nih.gov. 2022. *Microbicides To Block Transmission of HIV*. [online] Available at: <https://www.niaid.nih.gov/diseases-conditions/microbicides>.
146. Shattock, R., & Solomon, S. (2004). Microbicides - Aids to safer sex. *Lancet*, 363(9414), 1002–1003. [https://doi.org/10.1016/S0140-6736\(04\)15876-5](https://doi.org/10.1016/S0140-6736(04)15876-5).
147. Who.int. 2022. *WHO recommends the dapivirine vaginal ring as a new choice for HIV prevention for women at substantial risk of HIV infection*. [online] Available at: <https://www.who.int/news/item/26-01-2021-who-recommends-the-dapivirine-vaginal-ring-as-a-new-choice-for-hiv-prevention-for-women-at-substantial-risk-of-hiv-infection>.
148. Hay, A. J. (1993). Inhibition of HIV infection by flavonoids. *Antiviral Research*, 22, 189–199.
149. Hay, A. J. (1993). Inhibition of HIV infection by flavonoids. *Antiviral Research*, 22, 189–199.
150. Okesola, M. A., Adegboyega, A. E., Lasisi, A. J., Bello, F. A., Ogunlana, O. O., & Afolabi, I. S. (2022). Elucidating the interactions of bioactive compounds identified from *Camellia Sinensis* plant as promising candidates for the management of fibroids - A computational approach. *Informatics in Medicine Unlocked*, 31(April), 101002. <https://doi.org/10.1016/j.imu.2022.101002>.
151. Forli S, Huey, R. (2016). Computational protein-ligand docking and virtual drug screening with the AutoDock suite. *Nature Protocols*, 11(5), 905.
152. Vangala, R., Sivan, S. K., Peddi, S. R., & Manga, V. (2020). Computational design, synthesis and evaluation of new sulphonamide derivatives targeting HIV-1 gp120. *Journal of Computer-Aided Molecular Design*, 34(1), 39–54.
153. Sivan, S. K., Vangala, R., & Manga, V. (2013). Molecular docking guided structure-based design of symmetrical N,N'-disubstituted urea/thiourea as HIV-1 gp120-CD4 binding inhibitors. *Bioorganic and Medicinal Chemistry*, 21(15), 4591–4599.
154. Schrodinger.com. 2010. *What is considered a good GlideScore?* | Schrödinger. [online] Available at: <<https://www.schrodinger.com/kb/639>> [Accessed 8 September 2022].
155. Courter, J. R., Madani, N., Sodroski, J., Schön, A., Freire, E., Kwong, P. D., Hendrickson, W. A., Chaiken, I. M., Lalonde, J. M., & Smith, A. B. (2014). Structure-based design, synthesis and validation of CD4-mimetic

- small molecule inhibitors of HIV-1 entry: Conversion of a viral entry agonist to an antagonist. *Accounts of Chemical Research*, 47(4), 1228–1237. <https://doi.org/10.1021/ar4002735>.
156. Xie, H., Ng, D., Savinov, S. N., Dey, B., Kwong, P. D., Wyatt, R., Smith, A. B., & Hendrickson, W. A. (2007). Structure-activity relationships in the binding of chemically derivatized CD4 to gp120 from human immunodeficiency virus. *Journal of Medicinal Chemistry*, 50(20), 4898–4908. <https://doi.org/10.1021/jm070564e>.
157. Matume, N. D., Tebit, D. M., & Bessong, P. O. (2020). HIV - 1 subtype C predicted co-receptor tropism in Africa: an individual sequence level meta-analysis. *AIDS Research and Therapy*, 1–16. <https://doi.org/10.1186/s12981-020-0263-x>.
158. Han, Y. S., Xiao, W. L., Xu, H., Kramer, V. G., Quan, Y., Mesplède, T., Oliveira, M., Colby-Germinario, S. P., Sun, H. D., & Wainberg, M. A. (2015). Identification of a dibenzo cyclooctadiene lignan as an HIV-1 non-nucleoside reverse transcriptase inhibitor. *Antiviral Chemistry & Chemotherapy*, 24(1), 28–38. <https://doi.org/10.1177/2040206614566580>.
159. Schrodinger.com. 2022. *What are the main differences between HTVS, SP, and XP docking?* | Schrödinger. [online] Available at: <https://www.schrodinger.com/kb/1013>.
160. Sundaram, M. K., Raina, R., Afroze, N., Bajbouj, K., Hamad, M., Haque, S., & Hussain, A. (2019). Quercetin modulates signaling pathways and induces apoptosis in cervical cancer cells. *Bioscience Reports*, 39(8), 1–17. <https://doi.org/10.1042/BSR20190720>.
161. RAINA, R., PRAMODH, S., RAIS, N., HAQUE, S., SHAFARIN, J., BAJBOUJ, K., HAMAD, M., & HUSSAIN, A. (2021). Luteolin inhibits proliferation, triggers apoptosis and modulates Akt/mTOR and MAP kinase pathways in HeLa cells. *Oncology Letters*, 21(3), 1–15. <https://doi.org/10.3892/ol.2021.12452>
162. Ozdener, H. (2005). Molecular mechanisms of HIV-1 associated neurodegeneration. *Journal of Biosciences*, 30(3), 391–405. <https://doi.org/10.1007/BF02703676>.
163. Monroe, K. M., Yang, Z., Johnson, J. R., Geng, X., Doitsh, G., Krogan, N. J., & Greene, W. C. (2014). IFI16 DNA Sensor Is Required for Death of Lymphoid CD4 T Cells Abortively Infected with HIV. *Science (New York, N.Y.)*, 343(January), 428–432. <https://doi.org/10.1126/science.1243640>.
164. Fesen, M. R., Pommier, Y., Leteurtre, F., Hiroguchi, S., Yung, J., & Kohn, K. W. (1994). Inhibition of HIV-1 integrase by flavones, caffeic acid phenethyl ester (CAPE) and related compounds. *Biochemical Pharmacology*, 48(3), 595–608. [https://doi.org/10.1016/0006-2952\(94\)90291-7](https://doi.org/10.1016/0006-2952(94)90291-7).
165. Youdim, K. A., Qaiser, M. Z., Begley, D. J., Rice-Evans, C. A., & Abbott, N. J. (2004). Flavonoid permeability across an in situ model of the blood-brain barrier. *Free Radical Biology and Medicine*, 36(5), 592–604. <https://doi.org/10.1016/j.freeradbiomed.2003.11.023>.
166. Zhang, Z., Wang, C. Z., Du, G. J., Qi, L. W., Calway, T., He, T. C., Du, W., & Yuan, C. S. (2013). Genistein induces G2/M cell cycle arrest and apoptosis via ATM/p53-dependent pathway in human colon cancer cells. *International Journal of Oncology*, 43(1), 289–296. <https://doi.org/10.3892/ijo.2013.1946>.
167. Chen, H. H., Chen, S. P., Zheng, Q. L., Nie, S. P., Li, W. J., Hu, X. J., & Xie, M. Y. (2018). Genistein promotes proliferation of human cervical cancer cells through estrogen receptor-mediated PI3K/Akt-NF-κB pathway. *Journal of Cancer*, 9(2), 288–295. <https://doi.org/10.7150/jca.20499>.

168. Kenda, M., Vegelj, J., Herlah, B., Perdih, A., Mladěnka, P., & Sollner Dolenc, M. (2021). Evaluation of firefly and Renilla Luciferase inhibition in reporter-gene assays: A case of isoflavonoids. *International Journal of Molecular Sciences*, 22(13). <https://doi.org/10.3390/ijms22136927>.
169. Lai, R. P. J., Yan, J., Heeney, J., McClure, M. O., Göttinger, H., Luban, J., & Pizzato, M. (2011). Nef decreases HIV-1 sensitivity to neutralizing antibodies that target the membrane-proximal external region of TMGP41. *PLoS Pathogens*, 7(12), 1–15. <https://doi.org/10.1371/journal.ppat.1002442>
170. Kunyane, P., Sonopo, M. S., & Selepe, M. A. (2019). Synthesis of Isoflavones by Tandem Demethylation and Ring-Opening/Cyclization of Methoxybenzoylbenzofurans. *Journal of Natural Products*, 82(11), 3074–3082. <https://doi.org/10.1021/acs.jnatprod.9b00681>
171. Stantchev, T. S., Markovic, I., Telford, W. G., Clouse, K. A., & Broder, C. C. (2007). The tyrosine kinase inhibitor genistein blocks HIV-1 infection in primary human macrophages. *Virus Research*, 123(2), 178–189. <https://doi.org/10.1016/j.virusres.2006.09.004>.
172. Huggins, D. J., Sherman, W., & Tidor, B. (2012). Rational approaches to improving selectivity in drug design. *Journal of Medicinal Chemistry*, 55(4), 1424–1444. <https://doi.org/10.1021/jm2010332>.
173. Collier, R. (2009). Rapidly rising clinical trial costs worry researchers. *CMAJ: Canadian Medical Association Journal = Journal de l'Association Médicale Canadienne*, 180(3), 277–278. <https://doi.org/10.1503/cmaj.082041>.
174. Gong, Y., Chowdhury, P., Nagesh, P. K. B., Rahman, M. A., Zhi, K., Yallapu, M. M., & Kumar, S. (2020). Novel elvitegravir nanoformulation for drug delivery across the blood-brain barrier to achieve HIV-1 suppression in the CNS macrophages. *Scientific Reports*, 10(1), 1–16. <https://doi.org/10.1038/s41598-020-60684-1>.
175. Lun, T., & Chin-Ho, C. (2012). Blocking HIV-1 entry by a gp120 surface binding inhibitor Lun. *Bioorg Med Chem Lett*, 22(9), 3358–3361. <https://doi.org/10.1016/j.bmcl.2012.02.079>.
176. Moyo, S., Hunt, G., Zuma, K., Zungu, M., Marinda, E., Mabaso, M., Kana, V., Kalimashe, M., Ledwaba, J., Naidoo, I., Takatshana, S., Matjokotja, T., Dietrich, C., Raizes, E., Diallo, K., Kindra, G., Mugore, L., & Rehle, T. (2020). HIV drug resistance profile in South Africa: Findings and implications from the 2017 national HIV household survey. *PLoS ONE*, 15(11 November), 1–13. <https://doi.org/10.1371/journal.pone.0241071>
177. Rossi, E., Meuser, M. E., Cunanan, C. J., & Cocklin, S. (2021). Structure, function, and interactions of the hiv-1 capsid protein. *Life*, 11, 1–25.
178. Bhatt, H., Patel, P., & Pannecouque, C. (2014). Discovery of HIV-1 integrase inhibitors: Pharmacophore mapping, virtual screening, molecular docking, synthesis, and biological evaluation. *Chemical Biology and Drug Design*, 83(2), 154–166. <https://doi.org/10.1111/cbdd.12207>
179. Brown, D. G., & Shotton, E. J. (2015). Diamond : shedding light on structure-based drug discovery Subject Areas : Author for correspondence : *The Royal Society*.
180. Montefiori, D. C. (2009). Measuring HIV neutralization in a luciferase reporter gene assay. *HIV Protocols*, 485, 395–405. https://doi.org/10.1007/978-1-59745-170-3_26
181. Murray, C. W., & Rees, D. C. (2009). The rise of fragment-based drug discovery. *Nature Chemistry*, 1(3), 187–192. <https://doi.org/10.1038/nchem.217>

182. Vangala, R., Sivan, S. K., Peddi, S. R., & Manga, V. (2020). Computational design, synthesis and evaluation of new sulphonamide derivatives targeting HIV-1 gp120. *Journal of Computer-Aided Molecular Design*, 34(1), 39–54. <https://doi.org/10.1007/s10822-019-00258-0>
183. Li, Q. (2020). Application of Fragment-Based Drug Discovery to Versatile Targets. *Frontiers in Molecular Biosciences*, 7(August), 1–13. <https://doi.org/10.3389/fmolb.2020.00180>
184. Tian, S., Wang, J., Li, Y., Li, D., Xu, L., & Hou, T. (2015). The application of in silico drug-likeness predictions in pharmaceutical research. *Advanced Drug Delivery Reviews*, 86, 2–10. <https://doi.org/10.1016/j.addr.2015.01.009>.
185. C.A. Lipinski, F. Lombardo, B.W. Dominy, P.J. Feeney, Experimental and computational approaches to estimate solubility and permeability in drug discovery and development settings, *Adv. Drug Deliv. Rev.* 23 (1997) 3–25
186. Daina, A., & Zoete, V. (2016). A BOILED-Egg To Predict Gastrointestinal Absorption and Brain Penetration of Small Molecules. *ChemMedChem*, 11. <https://doi.org/10.1002/cmdc.201600182>.
187. Lei, C., Yang, J., Hu, J., & Sun, X. (2020). On the Calculation of TCID₅₀ for Quantitation of Virus Infectivity. *Virologica Sinica*, 36. <https://doi.org/10.1007/s12250-020-00230-5>
188. Lin, J., Sklar, G. E., Oh, V. M. Sen, & Li, S. C. (2008). Factors affecting therapeutic compliance: A review from the patient's perspective. *Therapeutics and Clinical Risk Management*, 4(1), 269–286. <https://doi.org/10.2147/tcrm.s1458>.
189. Alabsi, A. M., Lim, K. L., Paterson, I. C., Ali-Saeed, R., & Muharram, B. A. (2016). Cell Cycle Arrest and Apoptosis Induction via Modulation of Mitochondrial Integrity by Bcl-2 Family Members and Caspase Dependence in *Dracaena cinnabari* -Treated H400 Human Oral Squamous Cell Carcinoma. *BioMed Research International*. <https://doi.org/10.1155/2016/4904016>
190. Shaker, B., Ahmad, S., Lee, J., Jung, C., & Na, D. (2021). In silico methods and tools for drug discovery. *Computers in Biology and Medicine*, 137(July 2021), 104851. <https://doi.org/10.1016/j.compbiomed.2021.104851>.
191. Anthanasiou, C. Cournia, Z. From Computers to Bedside: Computational Chemistry Contributing to FDA Approval (2018). *Methods and Principles in Med Chem.* 7. <https://doi.org/10.1002/9783527806836.ch7>.
192. H. Jhoti, A.R. Leach, *Structure-based Drug Discovery*, Springer, 2007.
193. D.B. Kitchen, H. Decornez, J.R. Furr, J. Bajorath, Docking and scoring in virtual screening for drug discovery: methods and applications (2004). *Nat. Rev. Drug Discov.* 935–949.
194. Indrayanto, G. *et al* (2021). Validation *in-vitro* bioassay methods: Application in herbal drug research. *Profiles of drug substances*,. 273-307.
195. de Castro, S. & Camarasa, M. J. (2018). Polypharmacology in HIV inhibition: can a drug with simultaneous action against two relevant targets be an alternative to combination therapy? *European Journal of Medicinal Chemistry*, 150, 206–227. <https://doi.org/10.1016/j.ejmech.2018.03.007>.
196. Sivan, S. K., Vangala, R., & Manga, V. (2013). Molecular docking guided structure based design of symmetrical N,N'-disubstituted urea/thiourea as HIV-1 gp120-CD4 binding inhibitors. *Bioorganic and Medicinal Chemistry*, 21(15), 4591–4599. <https://doi.org/10.1016/j.bmc.2013.05.038>.

197. Cole, A. L., Hossain, S., Cole, A. M., & Phanstiel, O. (2016). Synthesis and bioevaluation of substituted chalcones, coumaranones and other flavonoids as anti-HIV agents. *Bioorganic and Medicinal Chemistry*, 24(12), 2768–2776. <https://doi.org/10.1016/j.bmc.2016.04.045>.
198. Ghose, A. K., Viswanadhan, V. N., & Wendoloski, J. J. (1999). A knowledge-based approach in designing combinatorial or medicinal chemistry libraries for drug discovery. 1. A qualitative and quantitative characterization of known drug databases. *Journal of Combinatorial Chemistry*, 1(1), 55–68. <https://doi.org/10.1021/cc9800071>.
199. Putterill, B., Rono, C., Makhubela, B., Meyer, D., & Gama, N. (2022). Triazolyl Ru(II), Os(II), and Ir(III) complexes as potential HIV-1 inhibitors. *BioMetals*, 35(4), 771–784. <https://doi.org/10.1007/s10534-022-00400-w>